CYPRUS INTERNATION UNIVERSITY

Institute of Graduate Studies and Research

Electrical & Electronics Engineering

Design and Fabrication of Organic High Efficiency Flexible Supercapacitor for Renewable Energy Applications

Electrical & Electronics Engineering Thesis

Muhammad Asif Rabbani

SUPERVISOR
Prof.Dr. Mehmet Kusaf

Nicosia

May 2023

JURY PAGE

ABSTRACT

In recent years, the energy consumption has greatly grown due to the rapid expansion of human civilisation. The demand for using renewable energy sources to replace conventional fossil fuels like coal, natural gas, and crude oil is considerable. Due to its viability as a backup power source and their uses in portable electronics and electric vehicles, the development of low-cost and high-performance energy storage devices (ESDs) and systems has received a lot of attention. Due to their many charging-discharging cycles, huge power capacity, and wide operating temperature range, supercapacitors are among the most significant ESDs. In this thesis high performance supercapacitor electrodes are made using carbon from water melon rind and later the performance of fabricated supercapacitor device is observed.

In comparison to N-doped and P-doped carbons, N, P dual-doped watermelon peel-derived carbon (NPW) showed superior hierarchically linked pores and a bigger specific surface area of 1809 m^2 g^{-1}. In a three-electrode configuration with 1 M H_2SO_4, 6 M KOH, and 1 M Na_2SO_4 electrolytes, the NPW electrode displays excellent electrochemical activity, with high specific capacitance (498.8, 397.6, and 378.6 F g^{-1} at 1 A g^{-1}, respectively), and an average capacitance retention of 96.9% after 10,000 charge-discharge cycles at 10 A g^{-1}. With 1 M H_2SO_4-PVA-electrolyte, the NPW/NPW-based symmetric cell offered a high energy density of 71.84 Wh kg^{-1} at 1 A g^{-1} and a specific capacitance of 263.9 F g^{-1}. With no detectable anodic current and a broader working voltage range of up to 2.0 V in the neutral electrolyte, NPW produced 97.11 Wh kg^{-1} of energy density.

ACKNOWLEDGEMENTS

TABLE OF CONTENTS

LIST OF TABLES

LIST OF FIGURES

CHAPTER 1

INTRODUCTION

1.1 Background

The electronics play a very important rule in everyday life of the people. The development of electronics revolutionized the way people live their daily lives. The use of electrical appliances and electronic devices is so much common that we cannot even imagine to live without these. The more the innovation and technological advancement in the electronics the more is the increase in demand of these by the humanity. As the production of the electronics and electrical devices is increased that is risking the environment at an enormous scale. We all want to get the best from the electronics but we never think that what would be the future of the world with so much of electronic hazardous waste being dumped every second everywhere in the world. According to global e-waste monitor (Forti, Baldé, Kuehr, & Bel, 2020) the worldwide electronic waste generation has been approximately fifty four million metric tons in the year 2019.The advanced and rich countries produce more electronic toxic wastes than the developing and poor countries. In order to get rid of the toxic wastes produced by electronics, these countries export the waste to the developing and poor countries which don't have proper recycling structure and government regulations to control the release of toxic materials, volatile organic chemicals and heavy metals from the e-waste.

As per (Sinnaduraiand & Charles, 2009), the following substances are present in electronic waste:

Table 1 Substances Contained in Electronics Waste

Bulk Substances
- Plastic(thermosetting), epoxy resins, fibre glass polychlorinated biphenyls (PCBs) and poly vinyl chloride (PVC)
Bulk Elements
- Lead, tin, copper, silicon, beryllium, carbon, iron and aluminium
Elements in small amounts
- Cadmium, mercury, thallium
Trace Elements
- Americum, antimony, arsenic"', barium, bismuth, baron, cobalt, auropium, gallium"', germanium", gold, molium, lithium, manganese, nickel, niobium, palladium, platinum, rhodium, ruthenium, selenium, silver, tantalum, terbium, thorium, titanium, vanadium and yttrium

The advancement in electronic technology and mass production of electronic devices without keeping in mind sustainability and green future of the world would result in the increase in non-environmentally friendly toxic electronic waste like mercury, arsenic and chromium which can have a great impact on the environment besides affecting the health and wellness of the people. Therefore, in case proper recycling is not possible it is very important to minimize the electronic waste by producing the electronic devices with environmentally friendly materials such as non-hazardous and biodegradable. According to (European Commission, 2014), the European directive on Waste Electrical and Electronics Equipment (WEEE) 2012/19/EU the main purpose is to reduce the negative environmental effects produced because of the electronic waste. The directives and Registration of Hazardous Substances (RoHS) provide the guidelines to the manufacturer to use the environmentally friendly materials for electronic devices.

1.2 The Green Electronics and Energy Storage in Devices

The most electronics are still using inorganic semiconductors keeping silicon and gallium arsenide as the fundamental materials. By locating the natural chemicals that can be utilised in ecologically friendly (biodegradable) or/and biocompatible technologies, synthetic materials may now be produced. This is the concept of "Green" electronics that will not only make use of organic materials for electronics more common but will also help in providing the low cost and energy efficient materials and devices for sustainable future (Irimia-Vladu, 2014).

Thus, the green electronics concept in the design process of the electronic device should be encouraged from the very initial stage of the product development. In every device there is always a need of energy storage. In order to fulfil the concept of "Green Electronics" the batteries used in the electronic devices should also be environmentally friendly and sustainable. In most of the device's rechargeable lithium-ion (Li-ion) and lithium-polymer (Li-poly) batteries are used. The main reason of widely using these is their high energy density and long life. These batteries used widely in portable devices can be considered highly hazardous for the environment as they have a significant amount of metal pollutants such as Co, Cu, Ni, and Pb which can exceed the regulatory limits defined by the U.S federal and state laws under simulated landfill conditions and effect not only environment but also the human health (Kang, Chen, & Ogunseitan, 2013). Also, the commonly used devices such mobile phones, tablets and digital TV sets are mostly using Multi-layer ceramic capacitors (MLCCs) which are used in large quantities during manufacturing and are later discarded as electronic waste. The electrodes are made up of three layers of Ag, Ni and Sn and the concentration of these metals

is very high (Niu & Xu, 2019). The batteries production and recycling both have an impact on greenhouse generations (GHG) and environment. The material used to make the electrodes of the batteries besides the utilization of energy-intensive manufacturing processes determine the CO2 footprints and climate impact (Hans, Melin, & Storage, 2019). So it is very essential to produce the batteries which are environment friendly.

In portable devices there is a huge demand for rechargeable batteries. The rechargeable batteries are usually Ni-Cd ,Ni-MH, Pb-acid,Li-ion and ZA/MnO_2 types. The worst and most toxic of them is Ni-Cd and now hardly used. The selection of rechargeable battery is based on properties such as average of specific energy (Wh/kg), energy density (Wh/L), average of specific power (W/Kg), power density (W/L), low temperature operation, discharge profile, shelf life and efficiency (Gianfranco Pistoia, 2005). The batteries overall impact on health and the environment during their useful life can be determined by the selection of raw material, the process used during the manufacturing besides the way the rechargeable batteries are used, distributed and recycling is processed.

Table 2 Materials of Batteries and their Health Impact

Material	Health Impact Score	Material	Health Impact Score
Arsenic	65	Florine	22
Cadmium	57	Zinc	21
Lead	56	Aluminium	20
Antinomy	51	Carbon Black	20
Nickel	45	Vanadium	18
Cobalt	35	Tin	13
Manganese	33	Sulphuric Acid	11
Phosphorous	33	Sulphur	9
Copper	31	Iron	8
Lithium	25	Zirconium	7
Chlorine	23	KOH	5
Sodium	23	Titanium	4
		Plastic	3

Note: A higher value denotes a stronger impact.

The use of rechargeable batteries which are considered as primary energy source in portable devices besides the stabilizing the required performances of the devices are on increase with the technical improvements are part and parcel of our daily life specially for medical and fitness purposes. Rechargeable batteries are used in wearable electronic devices such as smart glasses, smart watches, smart T-shirts, and smart shoes. (Y. Liang et al., 2019)

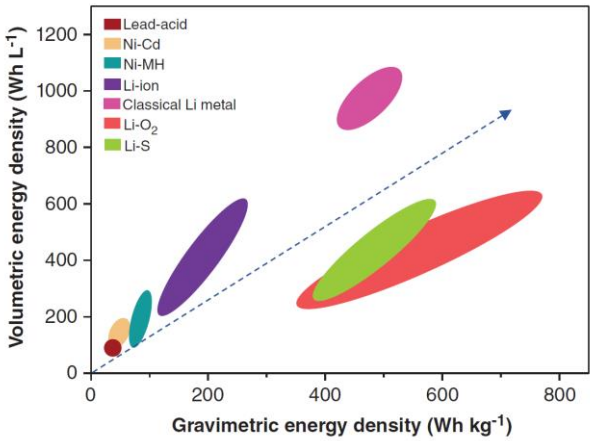

Figure 1 Gravimetric energy density vs volumetric energy plot of several rechargeable battery types

The main focus in development of energy storage technologies is to provide high power charging and discharging with long cycle life whether it is for use in power plants with distributed microgrids in smart grid scenario or for portable and wearable devices. The biosensor devices for medical purposes utilize lightweight flexible materials for fabrication. The flexible and wearable vital sign devices use biosignals to measure the heart rates, temperatures, blood pressure, respiration rates and glucose levels. All these health monitoring devices require power requirements for their operations and these requirements can be fulfilled by using supercapacitors as well. Flexible supercapacitors can be considered as the future of power supplies for flexible wearable devices for medical purposes. The power requirements for wearable medical sensing system components is provided in (Khan, Ostfeld, Lochner, Pierre, & Arias, 2016) and (Hartono, Sanjaya, & Ramli, 2018).

The ideal option to select between electrolytic capacitors and a rechargeable battery to be used in wearable devices is super capacitor as it has a high capacity with capacitance values much greater than others. Supercapacitors are broadly used as “energy reservoirs" that level out

power supplies to electrical and electronic equipment. Supercapacitors can also be connected to batteries to standardise the power they supply. They are also known as electric double layer capacitors (EDLCs), and they are made up of two electrodes separated by a separator and submerged in electrolyte. They have a large energy capacity and can manage the charging and discharging speeds to meet the needs of the devices. Since the characteristics remain constant even after being subjected to pressures from daily living, skin-comfortable printed supercapacitors are regarded as trustworthy and safe (Railanmaa et al., 2020) and (Chandra, Roberts, Yee, & Slade, 2009).

We know from past experiences that the increase in use of batteries as a primary energy storage and source also had a great impact on the environment but now as the transition is taking place from conventional battery usage to the supercapacitors so it is very vital to take into consideration the materials which are to be used for future supercapacitors so they are in the line of UN's sustainable environmental goals. The conventional supercapacitors although are considered more environmentally friendly as they are low toxic, maintenance free but still have significant amount of hazardous conventional electrolytes disseminated in carbon electrodes.

The electrolytes such as aqueous, organic solvent based and ILs are mostly used in supercapacitors but the selection of the right electrolytes used in the manufacturing determines future environmental effects. Electrolytes such as H_2SO_4, KOH and AN are hazardous to the human skin, IL are considered very expensive and can add to water pollution. Also the use of electrolytes with liquid nature can result in leakage in device resulting in high risks for the user besides also being problematic during packaging and portability (Dutta, Mahanta, & Banerjee, 2020). Therefore, novel solid and/or quasi-solid electrolytes are under studies for use in supercapacitors and other electrochemical devices. A quasi-solid-state SC equipped with gel polymer electrolyte (GPE) showed more 13% more capacitance and exceptional flexibility than SC containing liquid electrolyte. Moreover quasi solid electrolyte showed good chemical properties in terms of cycle life, energy density and energy power as compared to the supercapacitors using liquid electrolytes (Chae, Kwon, Yoon, & Roh, 2018) and (Yong, Park, & Jung, 2020). The use of the green electrolyte DES (deep eutectic solvent) has gain attention to be a potential electrolyte for green supercapacitors as they are low in toxicity and are highly biodegradable. The deep eutectic solvents (DES) are liquids that are prepared by mixing two to three chemical substances that are low in price and chemically safe to use. The resulting mixture is in liquid form at temperatures below 100C (Anshupriya Si, Anup Kumar Misra, 2020).

The performance of supercapacitors is determined by the electrochemical characteristics of the electrode material, as well as the choice of electrolyte and voltage range. The properties like superior power density, long life span, rapid charge/discharge rate and wide operational temperature range have introduced supercapacitors globally as a powerful energy storage devices (Iro, Subramani, & Dash, 2016).

Mostly supercapacitors use carbonaceous materials considered suitable for electrodes but different materials can also be used such as composite materials which are the arrangement of carbon-based materials and other components in order to have better performances in terms of energy density and power density. The active materials such as nanocarbons, metal oxides, and organic compounds combined with carbons were examined, as well as how composite materials solve the primary challenges associated with traditional electrode design while providing improved performance(Borenstein et al., 2017).

In (Fallah, Oladipo, & Gazi, 2020), the production and usage of multiparous boric acid-doped sucrose (Bx-pC) electrodes for supercapacitors showed remarkable energy density of ~ 56 Wh kg^{-1}, a high power density of 1300 W kg^{-1} and superior capacitance of 239 F g^{-1} at 1 A g^{-1} in 1 M H_2SO_4 electrolyte.

The supercapacitors performance has also been optimized using artificial neural network (ANN) model by establishing the relation between the performance and the constraints such as electrode material and operating conditions. The researchers are putting all efforts in developing an electrode material with sufficient pore size distribution and large specific surface area in order to have high electrochemical performance.

1.3 Latest Advances of Biomass-based activated carbon supercapacitors

The use of biodegradable and environmentally friendly electrode material which can be recycled as well is to be used as electrode material in supercapacitors fabrication for sustainable future. Pine cone biomass was converted into porous carbon using KOH activation as an electrode material, demonstrating a variety of structural and morphological analyses, the substance has three-dimensional porous cavities with a particular surface area of 1515 m^2 g^{-1}. When the active carbon material was tested in electrolyte of 1 M Na_2SO_4, a high voltage of 2.0V was witnessed for balanced carbon/carbon electrode cell providing 137 F g^{-1} and 19 W h Kg^{-1} capacitance and energy density respectively. Considering these outcomes in neutral 1 M Na_2SO_4 electrolyte are very interesting, progressive and have shown the usefulness of carbons obtained from pine cones, demonstrating the intriguing potential for a cheap porous carbon that can be employed on an industrial scale in applications like energy storage, as an absorbent, and

for catalysis. (Bello et al., 2016). The bicarbon derived from chicken bones doped in nitrogen and sulphur ($CB_{0.5}$-N, S) was prepared for supercapacitors application and the material used in symmetric supercapacitor delivered a high energy power output and 80.8 Wh kg^{-1} and 59.7 W h kg^{-1} energy densities were delivered at power density of 2.5 and 1.3 KW kg^{-1} in 2 M $TEABF_4$/AN and 1 M H_2SO_4 at 1 A g^{-1}, respectively. The performance of the supercapacitor was also optimized using artificial neural network model (ANN) and the predicted performance results were found very close to the actual performance of the supercapacitor. The surface area chicken bone derived $CB_{0.5}$-N,S is 1615.6 m^2 g^{-1} and provided capacitance of 493.9 F g^{-1} (in 1 M H_2SO_4) and 266.3 F g^{-1} (in 2 M $TEABF_4$/AN) at 1 A g^{-1} thus can be considered as an outstanding material for supercapacitor electrodes with high performance and efficiency (Oladipo, 2021). The biomass wastes can be transformed into renewable source of carbon which can be used in production of supercapacitors. The onion husk which are found in large quantities as By using a direct carbonization and activation procedure, biomass wastes were employed to create three-dimensional, interconnected porous carbon frameworks (OHCFs) with additional value. The supercapacitors utilizing OHCFs demonstrated high energy densities of 35.4–47.6 Wh/kg at power densities of 675–20250 W/kg and high capacitance of 188 f g^{-1} at 1 A g^{-1} in addition to cycle stability (D. Wang, Liu, Fang, Geng, & Ma, 2016). The renewable bioresource materials such as lignocellulosic feed stocks which are found in abundance can be utilized to produce hierarchically porous carbon materials using carbonization/activation approach to be used in supercapacitors which showed excellent energy storage and high capacitance along with stability and use of biochar provides a cost effective and efficient approach towards environmentally acceptable supercapacitor material (Gao, Wang, Zheng, Zhao, & Yu, 2020). Also, the biomass carbon obtained from water hyacinths (WHs) and sensitive plan (SP) which are known for their fast growth might be utilized as a cheap source for the electrode material for supercapacitors. It was described that the highest capacitance obtained for WH and SP used as raw material is 38 and 16 F g^{-1} at 2 mV s^{-1} using cyclic voltammetry (CV) respectively (Kasian, Nilmoung, & Pukird, 2019). Also, corncob residue which is a main waste and by product in furfural industry can be utilized to obtain high porous carbon material for electrodes synthesis of supercapacitors at low cost and with environmentally friendly impact. The carbon electrodes provided very high capacitance of 314 F g^{-1} in 6 M KOH electrolyte and can be considered a promising material for commercial supercapacitor production (Qu, Xu, Lu, Zhang, & Li, 2015).

Carbon materials obtained from natural biomass would be more significant, appealing, and useful than carbon materials derived from non-renewable and unsustainable fossil energy because of their low cost, renewability, and ease of supply.

1.4 Statement of the Problem

Energy storage technologies with high energy and power densities that are effective, sustainable, and ecologically compassionate are urgently needed. Therefore, our intention is to produce a high-performance activated carbon-based supercapacitor by using bio waste from watermelon rind (WR) to prepare carbonized material for supercapacitor electrodes which can easily be recycled and reused.

The main aim is to fabricate a highly effective, robust, flexible supercapacitor using bio-waste as precursor for fabrication of the electrode materials and polymeric gel electrolyte.

1.5 Objective of Study

The following are the key objective of this research: -

a) To synthesize high-performance carbon-based electrode material for supercapacitor from biomass.
b) To do the structural study of electrode materials of the SCs made from biomass
c) To explore and investigate the electrochemical performance of the SCs made from biomass

1.6 Importance and Significance

The major purpose of this development is to use carbon from biomass to create an energy storage system that is sustainable and kind to the environment. The biomass from agricultural residues is the material derived from growing plants or from animal manure and is a term used to describe biologically produced matters. In our research we are using left over water melon rind as biomass to produce our carbon-based electrode material. The demand of lithium which is widely used in rechargeable batteries has increased considerably as it is used in industries and specifically for batteries in electronic devices and electric vehicles and according to (Lithium South Development Corp. and Emerging Markets Consulting, 2021), the lithium could runout by 2025 due to high demand. Also, the lithium batteries are not considered as

environmentally friendly and to dispose or recycle these batteries is not a feasible and green task. The Lithium mining is under criticism as it is causing droughts and threatening livestock farming and finishing the green vegetation as well.

Therefore, here in this research we are trying to develop supercapacitors as an energy storage device using electrodes materials derived from the biomass which can be used in many applications related to power, electronics and electric automobile industry.

CHAPTER 2
LITERATURE REVIEW

2.1. Energy Storage Devices

An apparatus that can be used for storing electrical energy when needed and release the energy when required is known as energy storage device. There are many types of energy storage devices being used in the world according to the required storage demands. The batteries, fuel cells, capacitors and supercapacitors are nowadays more generally commercialized energy storage devices.

As the demand of energy storage is increasing around the world so improvement and technical advancement in technologies related to energy storage is very important for sustainable future as well. The energy storage devices are used in portable devices, transport vehicles and as stationary energy storage resources.

The energy storage can be achieved technically using chemical, mechanical, electrical, thermal and electrochemical means.

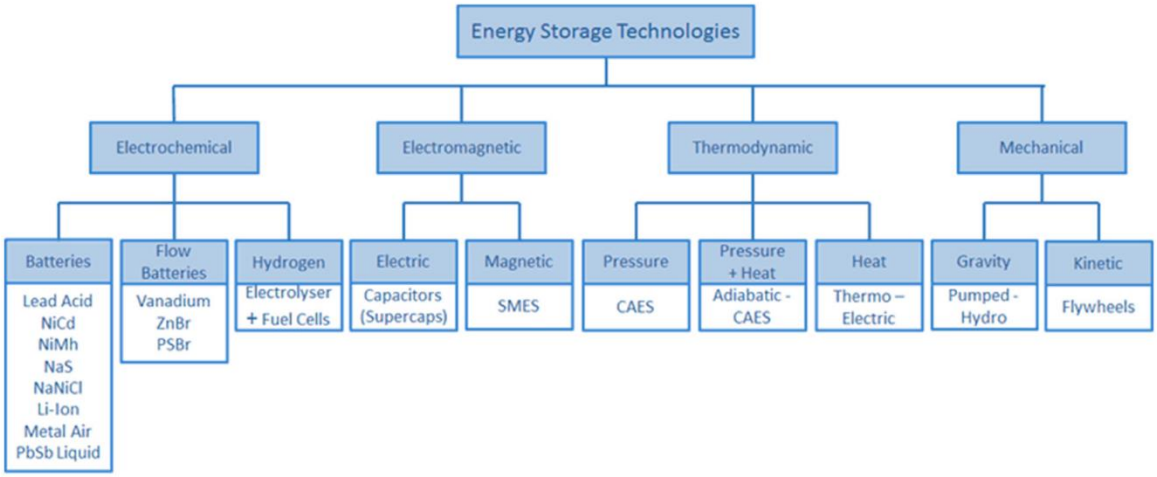

Figure 2 Classification of Energy Storage technologies

2.1.1.1 Batteries

The batteries are energy storage devices which converts chemical energy into electrical energy by using a galvanic cell which is made up of two electrodes an anode and cathode with electrolyte solution between them. Batteries are made up of several galvanic cells connected in

series or in parallel according to the need. The electrochemical energy storage is the most traditional way of storing energy and mostly used by the batteries.

The electrodes are made up of two different materials and when wires from electrodes are connected to the electric load the negatively charged electrons and positively charged metal ions are released as a result of oxidation of the electrodes. The electrons travel through the wire towards the cathode which is positively charged and combine with the material. This process is known as the reduction process which produces negative metal oxide ions which react with the electrolyte and decompose water into hydrogen ion and hydroxide ion. The cathode is deposited by the hydrogen molecules from electrolyte whereas metal ions from anode dissolve in water. The battery becomes fully discharged when the anode is completely oxidized or the cathode is fully reduced thus halting the chemical reaction in the battery(Ingram, 1998).

That's why the external voltage is applied in the plates of rechargeable batteries in order to reverse the chemical process. The type of material of the electrodes in batteries determine the amount of voltage and current that can be produced. The batteries are further characterized as primary batteries and secondary batteries. The primary batteries can be completely discharged once and then can be discarded like zinc carbon and alkaline batteries etc. whereas as rechargeable batteries can be recharged and discharged 100 to 1000 times. The batteries are Lithium-ion cells, nickel-zinc, lead acid, Nickle metal hydride etc.

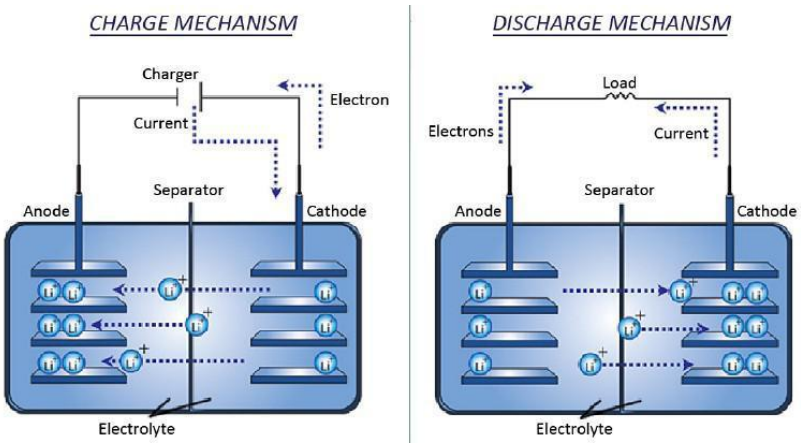

Figure 3 Battery

Lead Acid batteries were developed 150 years ago and can be used in different temperature ranges from extremely low and very high temperature with great output performance. Also, the

recycling technologies for lead acid batteries have is already been adopted and being used in order to minimize the environmental effect due to battery wastes and the development and improvements in lead acid batteries are still going on and they are still in demand. The Lithium ion secondary batteries(LIB) and lithium ion capacitor(LIC) are considered as the new generation of battery storage(Ishii, 2013).

The mostly used rechargeable battery is Lithium-Ion battery as it has a very high density of 120-170 Wh/Kg. They are considered as the power houses of digital electronics and energy storage. Also the self-discharge rate of these batteries is very low i.e. <5% per month as compared to the 20-30% of Ni-based batteries (Deng, 2015).

In portable devices there is a huge demand for rechargeable batteries. The rechargeable batteries are usually Ni-Cd, Ni-MH, Pb-acid, Li-ion and ZA/MnO_2 types. The worst and most toxic of them is Ni-Cd and now hardly used. The selection of rechargeable battery is based on properties such as standard average of specific energy (Wh/kg), energy density (Wh/L), average of specific power (W/Kg), power density (W/L), low temperature operation, discharge profile, shelf life and efficiency (Holze, 2012). The batteries overall impact on health and the environment during their useful life can be determined by the selection of raw material, the process used during the manufacturing besides the way the rechargeable batteries are used, distributed and recycling is processed.

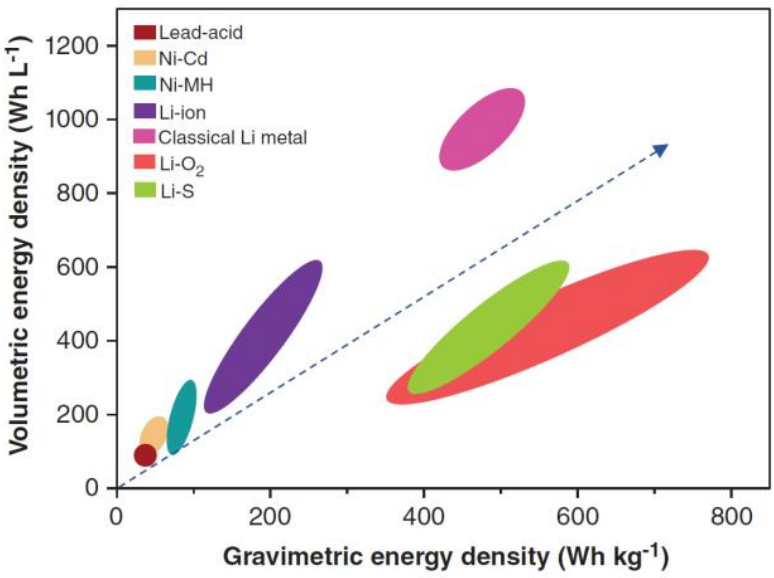

Figure 4 Plot of several types of rechargeable batteries' gravimetric energy density vs volumetric energy

In electrochemical chemical energy storage besides using sodium Sulphur batteries (Na-S) and Lithium-Ion batteries, Redox flow batteries are also widely applied for different storage purposes. In flow batteries ions move from negative and positive electrodes upon charging and discharging just like conventional batteries but through a selective polymer membrane which allows passage of ions. In Redox flow batteries there are two electrolyte solutions in two different tanks and circulation is done using two independent loops. Amongst numerous flow batteries, vanadium redox flow battery is considered as the most advanced one. These batteries are considered as safest options for large scale applications besides being less in price and having quick response as compared to lithium ion and lead acid batteries. The pricing, high energy density, and high power densities will determine the viability of batteries as a sustainable storage option in the future (Chen, Kim, & Chang, 2017).

2.1.1.2 Hydrogen Energy Storage

A type of chemical energy storage, hydrogen energy storage uses power to create a chemical that may be used as fuel. This fuel may be used to sustain the thermal load, the production of power, and transportation. Converting electricity into hydrogen is the process of hydrogen energy storage. A water electrolyzer, compressed hydrogen gas storage tanks, and a fuel cell make up a regenerative fuel cell. In an electrolyzer, water is used to create hydrogen using electrical energy. The created hydrogen is kept in the high-pressure tanks until it is needed and then sent to hydrogen fuel cells to make energy.

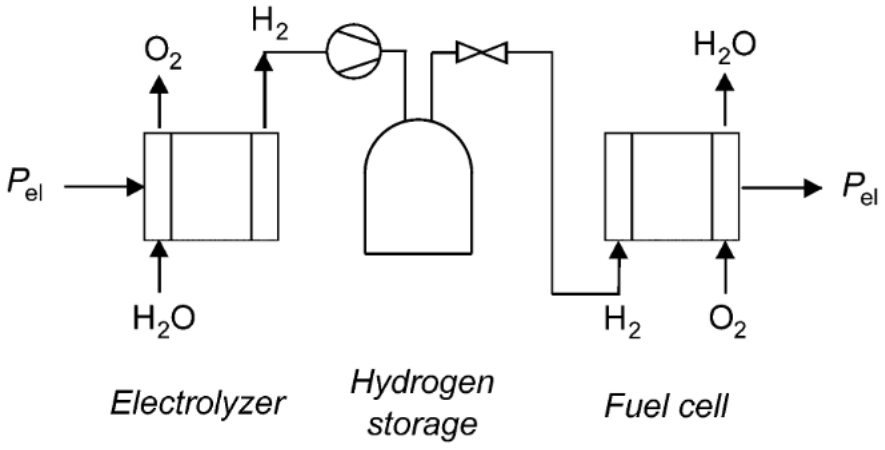

Figure 5 Schematic of a regenerative hydrogen fuel cell system

Hydrogen is a practical solution for grid-scale energy storage. and has advantages like high energy density and low discharge rates. Also, when hydrogen storage is used of storing excess of energy by wind farms it provided back the energy similar to the batteries although it has lower round-trip efficiency which is for batteries is between 70% to 95% whereas for hydrogen system using 350bar compressed gas storage is about only 47%. The by-product of the fuel cell is also very environmentally friendly when compared with batteries. The hydrogen energy storage is more than “electricity in , electricity out”(Melaina & Eichman, 2015).

There are many different types of fuel cells, but the most popular is the polymer electrolyte membrane fuel cell (PEMFC). The PEM is designed to allow positive particles to flow on the opposite side, allowing electrons to accumulate on the anode side. When a charge is applied, the electrons go over the external circuit to the cathode and combine with the anode's protons in the presence of oxygen (Hamilton & Pollet, 2010).

2.1.1.3 Pumped Hydrogen Storage (PHS)

This is a mechanical energy storage type and energy is deposited in the form of gravitational potential energy. The two vertically separated water reservoirs are used at different heights. When there is less demand in electricity during off-peak hours low-cost electricity is utilized to pump water to higher reservoir from the lower one using a pump and turbine unit and during peak hours when there is increase in demand for electricity the power is generated by the flow of water from higher reservoir to the lower reservoir running the turbines. This power is then fed to the grid to overcome the shortages.

Pumped hydrogen storage (PHS) is providing 95% of global energy storages and is a cost-effective way to provide large scale storage solutions. The other mechanical storage types include compressed air and fly wheel energy systems(World Energy Council, 2020) .

2.1.1.4 Molten Salt Energy Storage (MSES)

The thermal energy is stored using by heating or cooling a molten salt, water and phase change materials (PCMs). In molten salt energy storage (MSES) the concentrated solar power plants are used to heat the molten salt by using concentration and reflection of the solar energy. The molten slat which is a combination of 60% sodium nitrate and 40% potassium nitrate are non-flammable and environmentally friendly. The solar thermal plants use MSES as heat transfer and energy storage medium as it can be used at high temperature up to 550-570 degree C

instead of oil which can only be heated up to 400 degree C(Breidenbach, Martin, Jockenhöfer, & Bauer, 2016). The molten salt is capable of storing energy for up to 20 hours and that make it a good choice for solar plants as the storage will be provided a7 days a week even if there is a bad weather and no sun. The main purpose of using MSES in solar thermal power plants is to reduce the cost of operation. The two-tank molten salt energy storage (MSES) is used in parabolic trough solar power plants where the heat transfer fluid (HTF) which is molten salt also serving as the storage medium. Nitrate salt inventory, nitrate salt storage tanks, oil to salt heat exchangers, and nitrate salt circulation pumps are the elements of thermal storage (Herrmann, Kelly, & Price, 2004) .

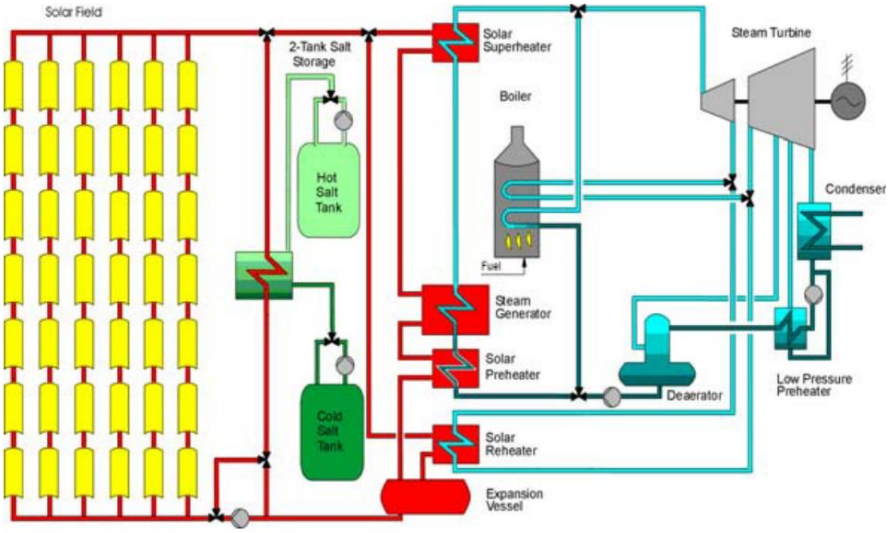

Figure 6 Demonstration flow diagram of a parabolic trough power plant with 2-tank molten salt storage

2.2. Overview of Capacitors

The capacitors were developed before the invention of batteries. The battery was invented in 1800, by Alessandro Volta whereas even before the use of batteries, in mid 1700s Leyden jar was invented by the university of Leyden in Holland. Leyden jar is considered as an early capacitor made up of glass jar coated by the silver foil from inside and outside. The static electricity was used to charge the inner side of the jar while keeping the outer foil grounded thus producing a high electrical discharge. The capacitors are classified into different types depending upon the dielectric and the physical state of the capacitor. Each type of capacitor has its own features and can be applied for different purposes (Tony Pandolfo, Vanessa Ruiz, Seepalakottai Sivakkumar, 2013).

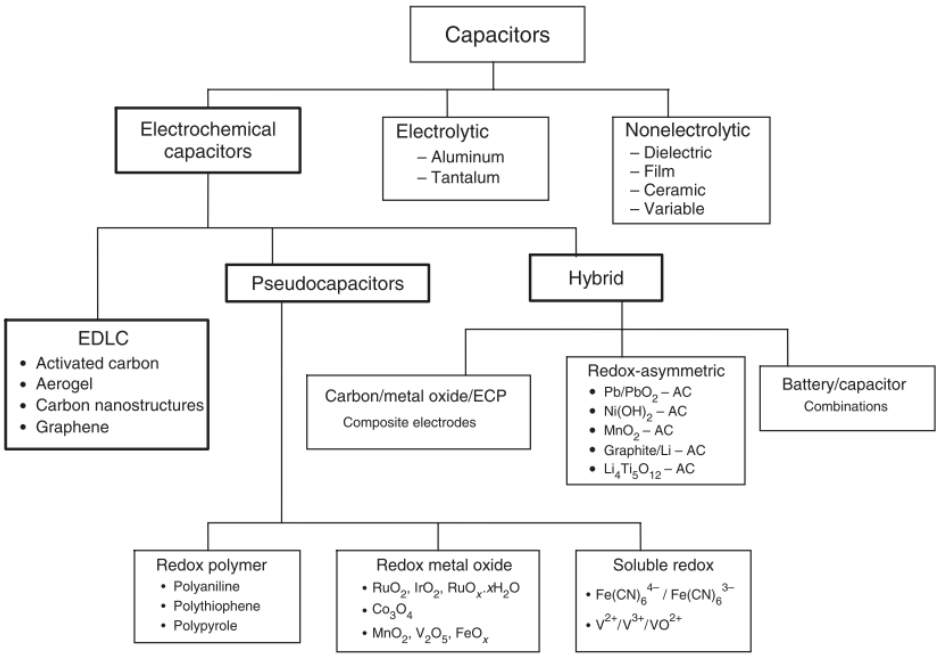

Figure 7 Classification of common types of capacitors

2.2.1 The progress of capacitors and electrochemical supercapacitors

The capacitors are the energy storage devices using two conductive plates in presence of an electric field. They are the basic electrical circuit elements and their main function is to charge and discharge electricity. In electric circuit they are used as filters to eliminate unwanted frequencies, for smoothing of the power supplies and also in microcomputers and time circuits that make use of charging and discharging property of the capacitors. Generally, the electrostatic capacitor is constructed using electrodes which are separated by the dielectric material acting as an insulator between them. When an external voltage is applied an electric field is produced by storing the charges on the surface of the electrodes. The positive and negative charges are accumulated on electrodes when a dc voltage is applied across the capacitor. The number of protons a positive charge accumulated is same as number of negative charge electrons on the plates. This makes the plates neutral and there remains a potential difference between them. A stage comes when there is no charge flowing through the capacitor due to the properties of the dielectric material used between the plates to separate them. At this state the capacitor is said to be “Fully Charged”. When this stored energy is released the potential difference among the plates start to decrease with the charge flowing from one plate to other and the stage comes when it is “Completely Discharged” and the current and potential difference becomes zero. The next generation of capacitors are electrolytic capacitors, which have a cell structure similar to batteries but a higher capacitance per unit volume than previous varieties due to the use of an ionic conducting liquid as one of its plates.

The selection of the large aluminium electrolytic capacitors is based on factors such cost, space and performances.(Stevens, Shaffer, & Vandenham, 2002). As electrolyte is the second plate of the capacitor so that's why we call such capacitors as "Electrolyte Capacitors".(Primavesi, 1997)The first patent for electrolytic capacitor was granted for borax electrolyte aluminium (AL) to Charles Pollak in 1897. It was used in radios during 1920s .(Ho, Jow, & Boggs, 2010).

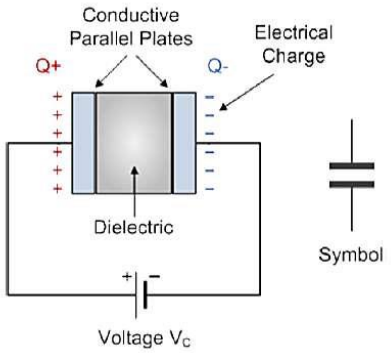

Figure 8 Basic structure of a parallel plate capacitor.

In capacitors the shape of the conducting surface can be varying according to the need but is has two conducting surfaces known as capacitor plates, in between is the insulating material called "dielectric" which can be air, mica, glass, waxed paper, ceramic etc. The capacitors fundamentals and technology is discussed by (W. J. Sarjeant, 1990) and review is provided regarding how different capacitors perform in both high and low power electronics. The mode of operation of capacitor and its impact on the capacitor's life, discharging and charging, reliability, high and low frequency filtering in ac and dc systems, inverters and switching of power supply mode is provided. It is very significant to select a capacitor design which is according to the available capacitor characteristics and according to the required application.

The supercapacitor (SC), also known as the Electric/electrochemical double layer capacitor (EDLC), is the next generation of capacitors that can store significantly more energy than normal capacitors while simultaneously having far greater power densities than batteries. This is the reason that they fill up the gap between the batteries and capacitors and thus increase the scope of use of these in various applications where there are power and energy requirements (Jayalakshmi & Balasubramanian, 2008).

The working principle of the supercapacitor is same as both have the electrodes and dielectric materials but in case of supercapacitor high surface area of electrode is produced using carbon black or any other material coating on electrodes. Also, the selection of the dielectric which is present between the two electrodes is kept thin for non-resistive flow of charges between plates.

This increases the energy and capacitance of the capacitor and make it a supercapacitor. In supercapacitors the equivalent series resistance is also very small that results in high power densities. The double layer capacitors are now widely used because of their capacitor and battery like properties. As the world is becoming more electrified so there is always a need to improve the capacitor technology (Ho et al., 2010).

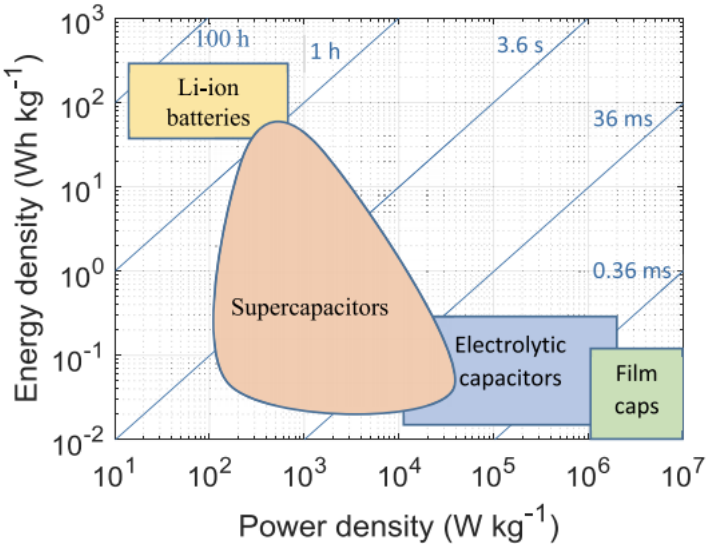

Figure 9 Ragone Plot of electrical energy storage systems (Berrueta, Ursua, Martin, Eftekhari, & Sanchis, 2019).

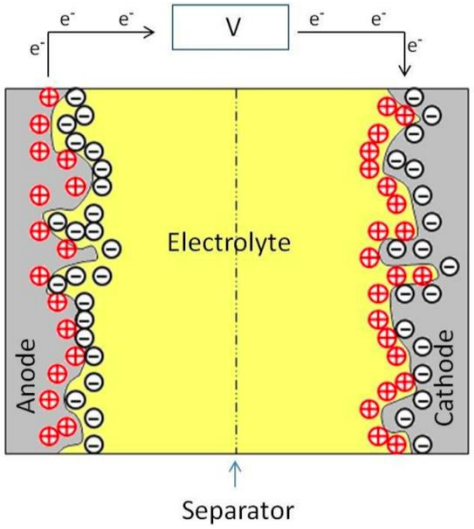

Figure 10 Schematic of a supercapacitor

In supercapacitors the energy is stored either by using an electrochemical double layer or reversible redox reaction at the electrode/electrolyte interface. Also compared to the batteries they have excellent cycle stability meaning that throughout charge and discharge cycles they the electrodes of the supercapacitors remain unchanged.

2.2.2 Charge Storage Mechanism

In supercapacitors, electrons move from the negative electrode to the positive electrode when an external voltage is provided during the charging process. Additionally, the positive and negative ions in the electrolyte diffuse to the surfaces of the positive and negative electrodes simultaneously. When a load is connected to the supercapacitor and the discharging process begins, electrons instantly flow from the positive electrode to power the external load before concurrently building up on the negative electrode.

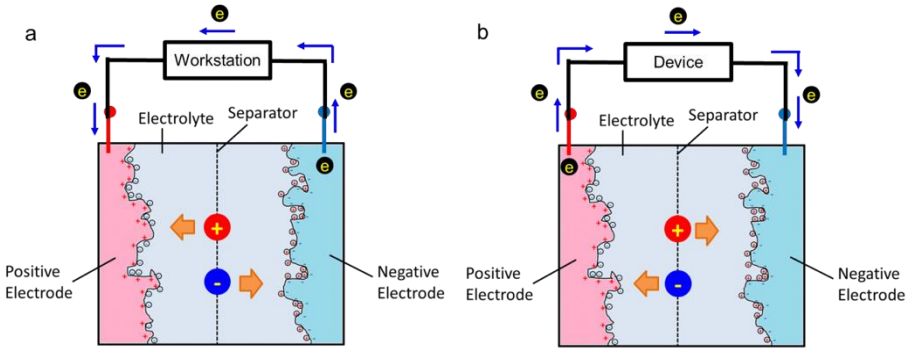

Figure 11 supercapacitor a) charging process b) discharging process

When compared to other typical capacitors, supercapacitors are notable for being able to store a significant quantity of energy in a relatively small space. It has been shown that the total charge held in supercapacitors is proportional to the square of the voltage at the electrodes. The capacitance of supercapacitors is voltage dependant. Additionally, it was discovered that once charges from the electrolyte diffused to the electrodes, the voltage of SC increased following the discharge. The charge grows linearly as the voltage across the electrodes increases (Szewczyk et al., 2016) .

The capacitance, which is a measurement of the charge in capacitors, determines the amount of charge that a supercapacitor can store. The ratio of the charge q on each conductor to the potential difference V between the conductors may be used to determine capacitance C i.e.

$$C = q/v \quad (2.1)$$

Where C is capacitance in Farads (F), q is the surface charge measured in coulomb C and v is potential at the surface in volts, V.

Porous carbon is commonly used as an electrode material in super capacitors because it has a larger surface area for ion build-up. The Helmholtz double layer capacitance model may be used to compute capacitance when charges are polarized between electrodes and electrolytes.

$$C = \varepsilon_r \varepsilon_o A/d. \quad (2.2)$$

Where ε_r is the permittivity of the electrolyte, ε_o is the vacuum permittivity, d is the charge separation distance (thickness of the double layer) and surface area is A. The thickness of the electrical double layer capacitance depends on the electrode surface charge density, concentration of the electrolyte and size of ions (Salanne et al., 2016).

Specific power is measured in watts per kilogram (W Kg-1), whereas specific energy is measured in watt-hours (Wh kg-1) and defines how much energy can be stored and we can determine the energy by combining the following equation with eq 1:

$$W = \int_0^Q V dq = \int_0^Q \frac{q}{C} dq = \frac{1}{2}\frac{Q^2}{C} = \frac{1}{2} UQ = \frac{1}{2} CU^2 \quad (2.3)$$

Where C is the specific capacitance and U is the operating potential. The maximum power is determined by the equation

$$P = W/t = \tfrac{1}{2}\, UI = \tfrac{1}{4}\, U^2/R \quad (2.4)$$

Where R is the series resistance. The values obtained for energy and power of the supercapacitors is regulated by the weight or volume of the electrode.

2.2.3 Models and Structures

It is very important for the researches to have a common mathematical framework in order to do the analysis of supercapacitors as by mathematical modelling one can study and predict the design, working conditions and control synthesis. As the models are the first step towards the implementation in the real world so to make them more accurate different assumptions are considered to check models for specific purpose. The performance characteristics can be predicted by the quantitative models which can help to decrease time and cost of fabrication and physical testing. There are many diverse models to explain the physical characteristics of the supercapacitors and a single model is not enough for all characteristics. Electrical models can be used to describe the behaviour of supercapacitors in terms of voltage, temperature and frequency. Some of the fundamental models are (Gautham Prasad, Shetty, Thakur, Rakshitha, & Bommegowda, 2019):

1- Electric double layer model
2- Porous electrode model
3- Equivalent circuit model

4- Intelligent model

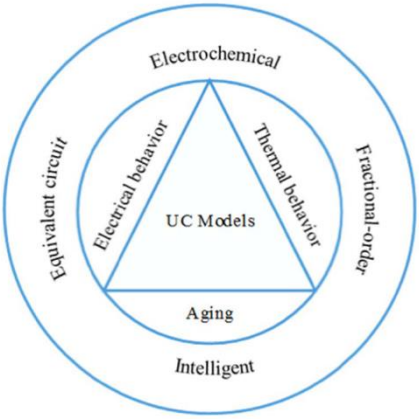

Figure 12 SC models

In 19th century Helmholtz pioneered the first concept and model of the double layer ultra-capacitor after investigating the distribution of negative and positive charges at the interface of colliding particles. In his model, two layers of opposite charge from the electrode/electrolyte interface make double layer of the electrode interface which are separated by an atomic distance. Also, he assumed that no electron transfer reaction occur at the electrode and the solution is only compromised of electrolyte. As the electrodes hold the charge density which is due to the excess or deficiency of electrons at the electrode surfaces so it can be stated that the interfaces between the ions in solution and the electrode surface is of electrostatic nature. The redeployment of ions closes to the electrode exterior make the interface neutral by balancing the charge held on the electrodes. Helmholtz's view is shown below

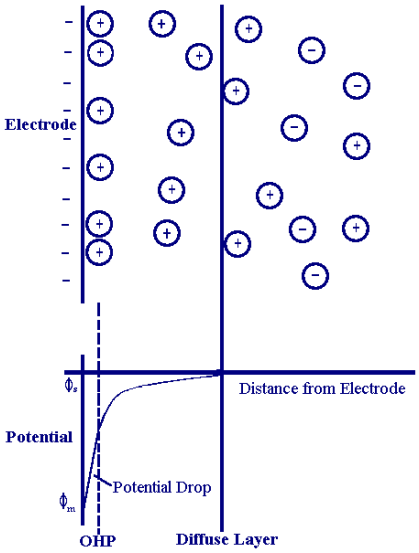

Figure 13 Helmholtz Model

If we assume that the electrode is negatively charged then the positive ions are attracted by the negative charged electrons near the electrode surface due to the electrostatic attraction. So, these first attracted cations align with each other to form an inner layer which is ordered and compact to be called as inner Helmholtz layer (IHL). The second layer is built up with the opposite ions that are attracted by the IHL is called the outer Helmholtz layer (OHL). The IHL and the OHL are together called "electric double layer(Panda, Grigoriev, Mishra, & Ahuja, 2020).

When two layers of charge are created because of attracted ions that accumulate at the surface of the electrode in order to balance the charge on the surface of the electrode, forming two layers of charge (Double Layers), the potential drop is constrained in the area known as the outer Helmholtz Plane (OHP).

The model does not provide details regarding other factors such as diffusion/mixing in solution, the chances of absorption on to the surface of the electrodes and also regarding any details like the interaction between the solvent dipole movements and their relation with the electrodes. This basic model was altered by Gouy and Chapman by introducing a concept of the diffuse layer with distance d due to thermal instability defining the continuous distribution of the of the ions in the electrolyte solution. Later a model by Stern which is a combination of Helmholtz and Gouy and chapman model was developed so that the non-neutral surfaces charges can also be neutralized by the diffused layer.

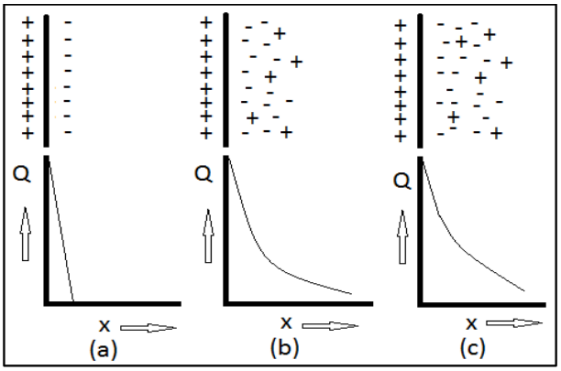

Figure 14 Schematic of electric Double layer (a) Helmholtz model; (b) Gouy Chapman model; (c) Stern model. (Q: electric potential over the thickness of the double layer; x: distance from the electrode surface)

In stern model there is an inner region prepared up of inner Helmholtz plane (IHP) and outer Helmholtz plane (OHP) is called as the compact layer and diffuse region. The specifically adsorbed ions are nearest to the IHP whereas OHS refers to the non-specifically adsorbed ions. It is also notable that the diffuse layer starts from the OHP plane. The characteristic layers for the stern model are also known as Stern layer (Helmholtz layer) and the diffuse layer (Gouy-

Chapman layer). Therefore, in the electric double layer (EDL), the overall capacitance is by Stern layer and diffuse layer capacitance connected in series. Other models like Poisson-Boltzmann (PB) are used to treats the ions as point charges by not taking into account their sizes and Bikerman model that includes the finite ion size under balanced conditions where the positive and negative ions in electrolyte have same valences but different sizes. Also, Verbrugge and Liu introduced one dimensional one domain mathematical model and later expanded it to the three-domain model based on constant formulation of electrode electrolyte system. In There dimensional(3D) model developed by Wang and Pilon Stern layer behaviour was described by using a set of boundary conditions (L. Zhang, Hu, Wang, Sun, & Dorrell, 2018).

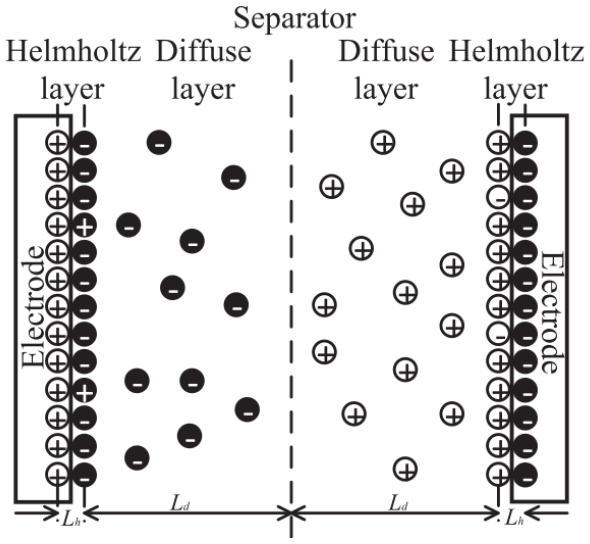

Figure 15 The Gouy-Chapman-Stern Model

2.2.4 Equivalent Circuit Representation

We can represent the electrode interphases by equivalent circuits. In case of double layer the capacitances is a sum of capacitances of the regions i.e. the compact layer and diffusion region capacitances in stern model. The simple equivalent circuit of the stern model is

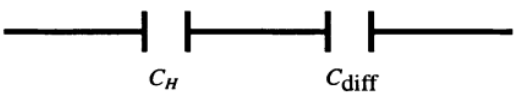

Figure 16 Simple equivalent circuit depiction of the Stern model of the electrical double-layer

The C_H represents the adsorption of ions in compact layers whereas the C_{diff} is a capacitance of double layer representing the remaining ionic charges in diffuse region. The total capacitance of double layer (Cdl) is summation of C_H and C_{diff} connected in series is given as:

$$1/Cdl = 1/ C_H + 1/ C_{diff.} \qquad (2.5)$$

The change in potential across the capacitor in response to the charging current can have an effect on the capacitance of the capacitor. We can characterize the capacitance by the analysing the time dependent changes of potential as the response functions of currents. Therefore, using alternating current (ac) impedance measurement is considered as a basis for calculating the capacitance of individual electrode. The interface of double layer is capacitive in nature when there is a potential variance between the electrode and the electrolyte
without any external applied potential or established in absence of Faradic charge. When the external voltage is applied the stored charge also increases linearly and faradic process may result at the boundary of the electrode and we include Faradic resistance Rf in parallel with double layer capacitance which is exponentially dependent on the potential of electrode (Mastragostino, Soavi, & Arbizzani, 2002).

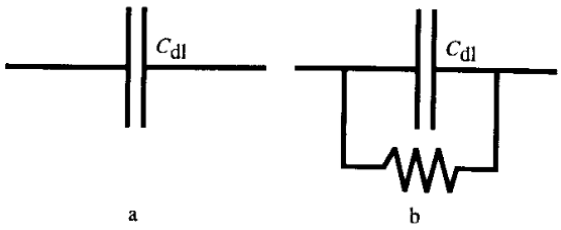

Figure 17 The behaviours of equivalent circuits (a) is purely capacitive (b) has a maximum capacitive impedance for a given value of Cdl and Rf at a certain frequency

(Sedlakova et al., 2015) proposed equivalent circuit model of supercapacitor made up of two perfect capacitors, two ideal resistors, and one resistor with time reliant resistor. This time dependent is able to characterize the movement of charges by diffusion from the electrolyte to the electrode material. The resistance values increase with square root of time which shows that the transportation of additional charge carriers by diffusion is minimized and decreased to a greater extend.

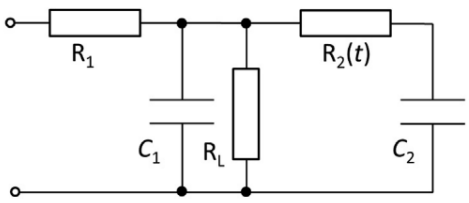

Figure 18 Two branch equivalent electrical circuit with time dependent diffuse resistance

In above figure 18 the five parameters are:

C1 relates to Helmholtz capacitance $C_{H,}$

C_2 relates to diffuse capacitance $C_{D,}$

R_1 denotes the equivalent series resistance (ESR)

R_L denotes the leakage resistance.

R_2(t) is the resistance between the Helmholtz and diffuse capacitances.

Different correspondent circuit models use RC(Capacitor-resistor) circuits to simulate the electrical behaviour of the Supercapacitors. The most common equivalent circuit models for SC are shown in figure 18. In figure 18(a) is the classical equivalent circuit model of SC and by adding a parallel resistor helps to minimize the self-discharge of the capacitor. The figure 18(b) shows a three-branch model using of variable resistor to further characterize the self-discharge in SC. In figure 18(c) two parallel RC networks are connected with a series resistor and a bulk capacitor and is a vibrant model using electrochemical spectroscopy (EIS) in the frequency domain. The figure 18(d) uses transmission line models by considering the long-term and transitional behaviour of the capacitor in order to simulate electrolyte resistance and the distributed capacitance(L. Zhang et al., 2018).

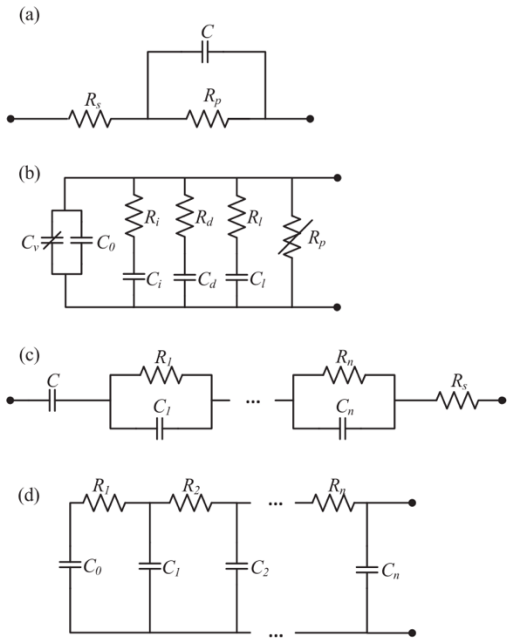

Figure 19 different equivalent circuit models for SC(L. Zhang et al., 2018)

In SC modelling applications where there is more accuracy is required the fractional order mathematical models are used instead of integral models. The model consists of a constant phase element (CPE), Walberg-like element a series and a parallel resistor. Also in (Freeborn, Maundy, & Elwakil, 2015) it is found that using fractional-order capacitors gives better accuracy and also do the simulations according to the physical electrochemical properties of the device. The fractional models of super capacitors are used to model impedance, high performance, transient characteristics and control.

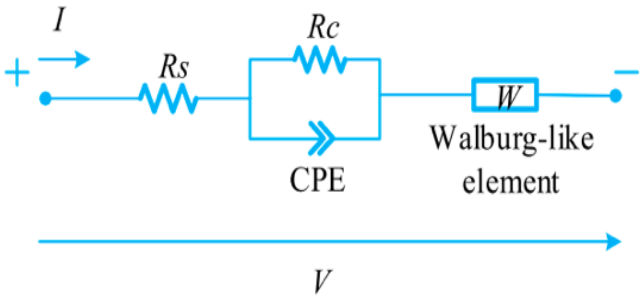

Figure 20 Example of SC fractional-order model.

2.3 Energy Storing Applications of Supercapacitors

Hybrid Energy Storage Systems (HESS) integrate two or more energy storage system (ESS) technologies to maximize their strengths and minimize their weaknesses in order to deliver the combined power outputs from them. The HESS are used where there is a need of high-power supply and at the same time high storage is also required. Hence according to (Hemmati & Saboori, 2016) the supercapacitors are widely used for different hybrid energy storage systems as a combination of battery-supercapacitor , compresses air energy storage(CAES)-supercapacitor and fuel cell –supercapacitor. The supercapacitors have high specific power and low specific energy besides having a high life cycle whereas the rechargeable batteries are used as the secondary storage devices and have high specific energy and low specific power beside much lower life cycles as compared to the supercapacitors. In (Jiya, Gurusinghe, & Gouws, 2018), hybridizing of three energy storages battery, supercapacitors and hybrid capacitor is proposed using three different techniques mainly using direct hand wiring of the three energy storages, individual power controllers as DC-DC converters and also using the parallel configuration of Hybrid capacitor with the Supercapacitor by connection of battery pack with DC-DC converter and sharing power controller. In general, there are two types of battery and supercapacitor hybridization: exterior and internal. The HESS combination can be internal serial, internal parallel, external series and external parallel.

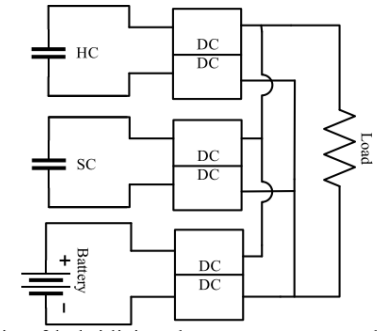

Figure 21 Schematic of hybridizing the energy storage through individual DC-DC converters in order to achieve maximum control of the energy storage devices

An off-peak electric energy system called a compressed air energy storage system (CAES) uses air pressure to compress it in surface vessels and subsurface cavities. During the peak demand hours when there is more demand of energy generation this stored energy in form of compressed air is then used with the combination of conventional fuels to run the turbine generator in order to fulfil the demanded electric energy. When the supercapacitor is combined

with the CAES energy storage system as shown below it performs as a filter and smooth the output power. The use of supercapacitor with CAES improves the overall performance of the storage system and this HESS is considered suitable for low power stand alone and grid connected applications specifically in renewable energy systems where good power quality is required for sensitive appliances(Lemofouet & Rufer, 2006).

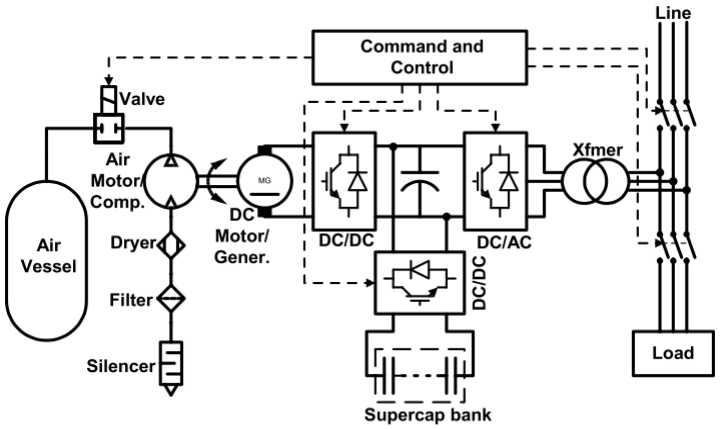

Figure 22 Principle of Compressed Air and Supercapacitor Energy Storage System

According to (Guerrero, Romero, Barrero, Milanes, & Gonzalez, 2009) they have fast charging and discharging without any degradation in their efficiencies which makes them suitable for using in energy storage systems. Also, supercapacitors have high energy and power densities with efficiencies greater than 95% and high life expectancy. The supercapacitors can be used in renewable energy system storages and also in active power filters, for power quality improvement of distributed and transport systems, locomotives, in electronic devices and in any medium level power application where low maintenance cost is required for energy storage of high response times and small energy storage capacity. In (Rabbani, 2021), energy storage devices can be categorized on the basis of energy stored and also the time it takes for the discharging. Depending on the application, these storage devices might be short-term, medium-term, or long-term.

The supercapacitors can be used in several applications commercially and the most sectors which can be considered as mostly relaying on their advancements ranges from transportations, wireless sensor network, stationary storage, renewable integration, railway, consumer electronics, industrial vehicles and many more. Here will discuss some of the usage of supercapacitors as energy storage systems for the following sectors.

2.3.1 Supercapacitors in Transportation

As most of the harm to the environment is caused by the emission of greenhouse gases released mainly by the conventional means of the transportation so now there is awareness among the people regarding using environmentally friendly transportations and electric vehicles are getting a lot of good responses not only by the governments but also by the citizens for the sustainable and clean future. Hence the hybrid vehicles, battery electric vehicles (BEV) and fuel cell electric vehicles (FCEVs) are now considered as an ideal option for low carbon emissions. The vehicle to grid technology is advancing now and in smart grid scenario the electric vehicles can be used as mobile energy storage devices as the excess energy needs to be stored instead of being wasted. In order to achieve V2G for electric vehicles (EV) bi directional intelligent chargers are required to bridge the grids and the vehicles(Y. Zhou & Li, 2015). Integrating the EV with the grid is crucial to minimizing battery degradation during charging and discharging cycles. In (Pay & Baghzouz, 2003) batter-supercapacitor combination is proposed where supercapacitor bank is connected directly in parallel with the battery and also using DC-DC converter. Here the supercapacitor bank is used as a power buffer to smooth in and out the fast fluctuations caused by the electric or hybrid vehicle battery. Thus, using supercapacitor bank with the battery or fuel cell driven vehicle reduce battery stress by assisting with transient currents during acceleration and deceleration.

In (Benaouadj, Aboubou, Becherif, Ayad, & Bahri, 2012) battery electrical vehicle recharging topologies are provided along with the fact that hybridization of battery with the supercapacitor (SC) in battery electric vehicles (BEV) helps to reduce the volume, weight and cost of the batteries used in vehicle. Also, SC can recover energy during the braking of the vehicle as they have high number of cycles and the fast recharging. The renewable energy resources like wind and solar can be used to charge the batteries and Li-Ion batteries along with the SC battery pack can be charged fully in minimum time as compared to the lead acid batteries.

The supercapacitors are preferred to be used in electric vehicles as they have better performances in terms of overcharging, over discharging, safety and stability. In order to deliver energy without needing a complex power supply circuit, wireless energy is used to charge electric cars while supercapacitor energy storage is used. In comparison to Li-Ion batteries, wireless charging of a car using a supercapacitor is faster and is used as an additional power source to give the car enough start-up energy in addition to cutting down on the charging time, whereas Lithium batteries are used as the primary driving energy to enable vehicles to travel farther on the same amount of electric power(Lan et al., 2019).

In (Yaici, Kouchachvili, Entchev, & Longo, 2019) , the simulation of hybrid energy storage system (HESS) using supercapacitors with parallel batteries for Electric Vehicles (EV) is done using MATLAB-Simulink. In this study dynamic simulations were performed for Tesla S70 electric car and it was found that the supercapacitors hybridization helped in increasing the power contribution by 21.5% and the range was also extended to 80 KM for USC06 driving cycle. Also, the battery stress in vehicle can be significantly reduced by deploying transient currents during accelerations and decelerations, battery life is increased as number of cycles/years is reduced besides improving the vehicle's driving range. Also, the use of supercapacitors helps to reduce the size of battery in EV.

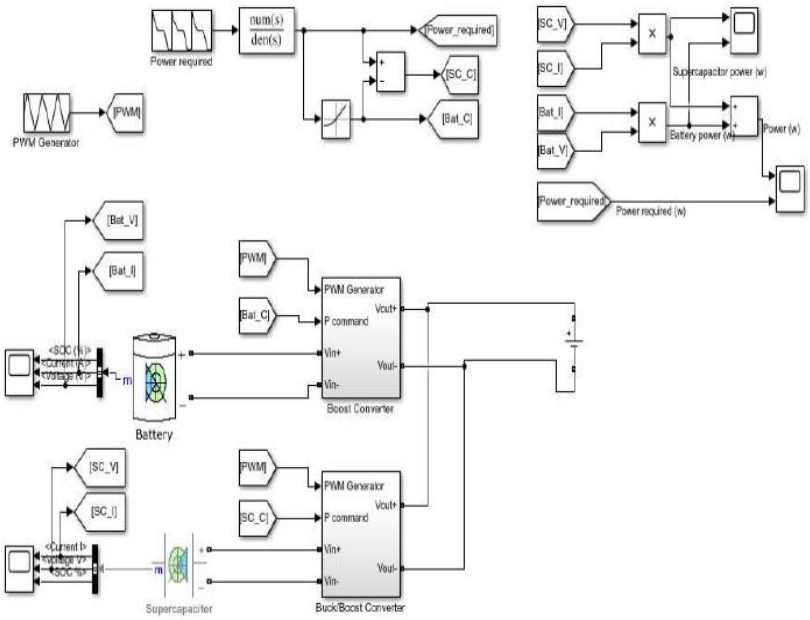

Figure 23 Simulation model in Matlab-Simulink of the battery/SC HESS for the EV((Yaici et al., 2019)

The supercapacitors lack in specific energy density and this is a disadvantage for them as the full energy cannot be utilized during the discharge which is required when we are using them for transportation purposes. In order to overcome this (Dasari, Ronanki, & Williamson, 2020) designed switching circuit made up of primary and secondary supercapacitor(SC) banks to make transition series and parallel combinations of SC cells as per load requirements. This switching enhances the energy utilization and power delivery time for an electrified transportation. This switching enables SC bank to regulate voltage for lengthier duration during the discharging and hence energy utilization of SC is increased.

The supercapacitor system to drive the urban transportation like trams and hybrid vehicles in (Goia, Popa, Popescu, & Popescu, 2011) describes that as overhead power transmission lines are not required or encouraged by the city councils in order to preserve culture and heritage so an ecological, low cost and no electrical wire net system using supercapacitor traction system is required. Supercapacitor system for tram consists of two systems mainly suburban and mobile system. As the supercapacitor battery needs to be recharged when the tram is at the stations so during this time a secondary battery is used to stabilize the overall power system. The supercapacitors for tram systems are hybridized using static power converters or choppers which provide high energy efficiencies. The integration of supercapacitors is done in traction system using static power converters.

The French railway company has implemented energy storage system based on supercapacitors for a 750 V DC railway power supply which is used to stabilize the voltage and power supply and various tests have been performed on trains before their commissioning, the aim of tests was to determine the compliance with the signalling. (Castaings, Caron, Kharrat, Ovalle, & Vulturescu, 2019). It was found that the ESS behaviour shows that current limitations have limited the voltage increase and secondly there was not enough energy to avoid the second significant voltage drop which shows the limitation of the supercapacitor technology as energy density is low.

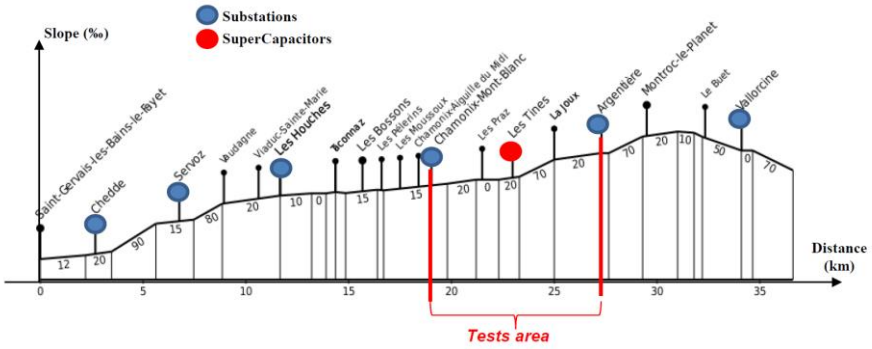

Figure 24 Saint-Gervais / VAllorcine Line slopes, train stations, substations and the Supercapacitors ESS (Castaings et al., 2019)

The supercapacitors are used in energy storage systems of high speed railway by connecting it on to the dc link of railway power static conditioning (RPC) via bi directional dc-dc converter that aids in the increase of the regenerative braking energy (RBE) besides improving the quality of traction power supply system and reduction in the overall operational cost of the railway substation by dropping the peak power demand (Cui et al., 2019).

Supercapacitors are now thought to be used in electric cars (HEVs), metro trains, and tramways as the transportation of the future. The advancement in supercapacitor technology provides more option for the electric vehicle designer for the powertrain design and to figure out the best control strategies for on/off operation of the engines. Also the fuel economies based on supercapacitors vehicles is much better than the for the vehicles using the batteries only (Burke, Liu, & Zhao, 2014).

2.3.2 Supercapacitors in Grid Applications (Stationary power)

In old times the power was generated by the power plants and was utilized by the consumers. The generation was unidirectional meaning that the power delivered that was not consumed by the consumers was considered wasted but now the consumers are also generating their own power using renewable energy resources like wind and solar and the excess power they produce is fed back to the grids in smart grid scenario. This bi directional flow of energy between the grids and the consumers is controlled using the inverters and net metering is used to buy excess energy produced by the consumers. Energy storage devices made of supercapacitors are thought to be useful in ensuring the stability of the grid by absorbing the energy and releasing it when it is needed. When solar power systems at the users' ends are connected with the grid, there is a chance that a lot of swings can take place due to weather conditions (Rabbani, 2018). In renewable energy integration specifically for solar and wind systems control algorithms are developed for the supercapacitors to enhance the stability of the power system besides utilization of them in energy storage for voltage and power flow stabilization as well. When there is an increase in energy flow reversal frequency the effective capacitance is decreased and normalized derating coefficient of the state of charge (SOC) increases. The energy rating of supercapacitor energy storage system is also higher as compared to the discharging of the system. The use of supercapacitor in energy storage acts as a low pass filter and smooths the high frequency power fluctuations. If SOC is not close to its limit, a supercapacitor energy storage system (SESS) can be utilized to restrict the bigger ramps (Bostrom, Von Jouanne, Brekken, & Yokochi, 2013).

The super capacitors are also used to bridge the gap during the power failures and this avoids complete shut of the equipment before the back power is available. The supercapacitors are very useful in stabilizing the power systems in order to meet the power needs with the changing loads.

The supercapacitors play a vital role in future smart grids as energy storages. They are used as a backup power banks which can be stored to full capacity when excess energy is sent back to the grid from the consumers producing their own energy using the renewable energy resources like wind and solar. So, in this way this excess stored energy can be distributed to the places where there is shortage of power during peak hours. This reduces the production cost of the power plants as well as they would not need to start up their peak generators to overcome the demand shortages. Supercapacitors in smart grids help to provide the two-way effective power transfers with efficiency. Also, these banks are used in to provide the integration between the grid and the renewable energy resources by compensating the voltage sag and smoothing the fluctuations. The supercapacitors used in hybrid energy storages systems for grid applications helps to suppress fluctuations, oscillation damping i.e. ability to absorb and discharging energy during sudden un predicable power decrement in very short durations to avoid complete shut downs, Frequency regulation that helps to maintain the frequency within the electricity network required standards, provide reactive support thus compensating active and reactive powers through the storage systems, Fault ride through when integration in done at the external grid which makes sure that grid remains online during the faults and reduces the risks of a network collapse are some to mention (Nikolaidis & Poullikkas, 2011). Also, the energy storages with supercapacitors can be used as the voltage regulation, peak shaving and to avoid transmission and distribution congestion.

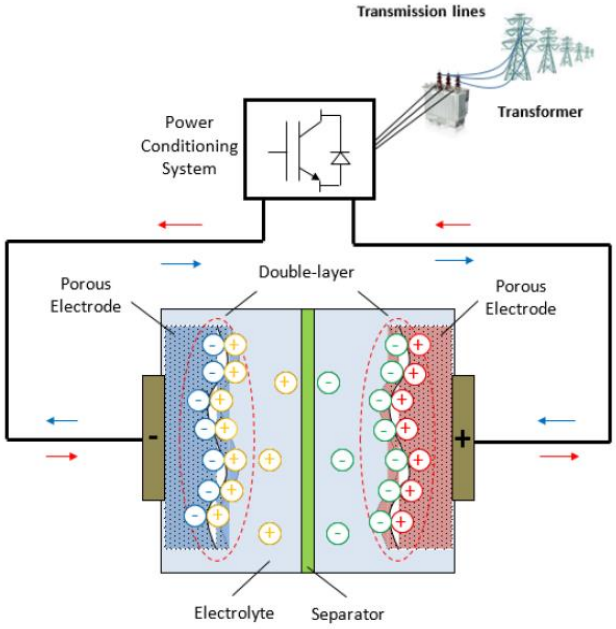

Figure 25 Schematic diagram of supercapacitor

The microgrids are considered as an effective system now a days and distributed networks are encouraged as this helps the governments to reduce the costs and supply of interrupted power to the communities. As power system has both AC and DC components so energy storage systems are always required for a stabilized system which can compensate the power disturbances. In (J. Li, Cornelusse, Vanderbemden, & Ernst, 2017) supercapacitor(SC) and battery hybrid energy storage system has been used to compensate the unbalanced power between the generation and the load demand. The results showed that using supercapacitor with battery in hybrid energy storage system helped to guard the battery from intense power changes and relieved the battery charge/discharge intensity and thus helps in improving the battery life time as well.

Power converters are required for the integration of the grid with the solar power system and more the number of converters the less efficient the system becomes so when a direct connection is used between the supercapacitor and the battery hybrid energy storage system is used with the grid connected photovoltaic system it reduces the number of power converters and results in increment in the system efficiency besides increasing the life time of energy storage system (Perdana, Muyeen, Al-Durra, Morales-Paredes, & Simoes, 2019).

The combination of supercapacitors with the batteries as energy storage devices is very logical as these two technologies complement one another as batteries are used where long-term energy discharges are required as they have higher energy density whereas the supercapacitors having higher power density are considered as ideal for applications where rapid response to sudden changes in power are expected and thus helps in improving electrical networks in case of microgrids. The integration of supercapacitors in microgrids ensures the better and efficient operations (Perez, Hoffmann, Dos S Pereira, Küster, & Durce, 2019).

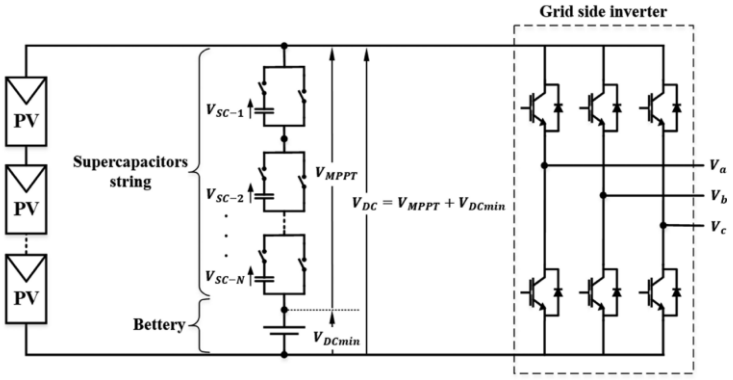

Figure 26 Direct connection scheme of supercapacitor-battery hybrid system (Perdana et al., 2019)

In (Reddy, Mishra, & Srinivas, 2015), energy management scheme for microgrid is discussed using the supercapacitors where reference current generated by the supercapacitors and fast acting current control loop is used. It has been discovered that supercapacitors play a vital role in establishing rapid DC link voltage dynamics because they respond extremely quickly to unexpected changes in DC link voltages. In addition, during rectifier mode of operation, a single-phase grid interactive voltage source converter (GIVSC) is employed to charge the battery and supercapacitor packs by acting as a bridge for actual power supply between the utility grid and the DC connection. In the event of a rapid shift in GIVSC, the supercapacitor bank absorbs and supplies reference current, and the battery pack controls average current, resulting in little stress on the battery bank and extending its life.

As discussed earlier that like solar energy, wind energy usage is also on rise and for wind energy integration again we prefer using supercapacitor energy storages. In (Naswali et al., 2011), supercapacitor storage system (SCSS) is designed and integration with the grid is studied aimed to optimize energy creation while increasing the wind farm outputs in order to improve wind energy integration. The sizing of the supercapacitor storage bank is discussed and using the control algorithm designed for fast response of supercapacitors it can be found that energy storing meets the forecasted power with less than +/- 4% per unit fault.

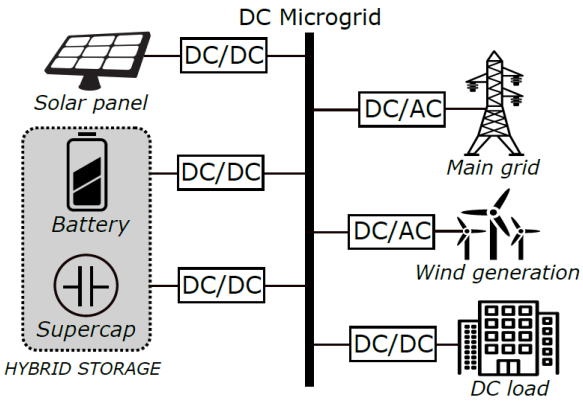

Figure 27 Basic configuration of HESS applied in microgrid

2.3.3 Supercapacitors in Electronics (Portable Power)

The world is more concerned about the climate change and the use of environment friendly materials so the performance of supercapacitor is considered as more environmentally friendly as it is sensitive to energy consumption. In most of the electronic devices lithium rechargeable batteries are used but now the trend suggest that supercapacitors can take the market share from these batteries in electronics. The supercapacitors are preferred as storage devices over lithium rechargeable as they highest specific power and appropriate energy density.

The use of portable devices in daily life routine which are multipurpose and multifunctional is getting more common. The portable devices like smart phones and smart watches use WIFI-connectivity for different applications. This increase in portable devices has also increased trend in power demand in terms of peak power requirements from lithium and other types of batteries. This power demand increase also applies to the wireless sensors as well. The figure below shows different power profiles for different smart phone uses ("Supercapacitors can take market share from lithium batteries | IDTechEx Research Article," 2012)

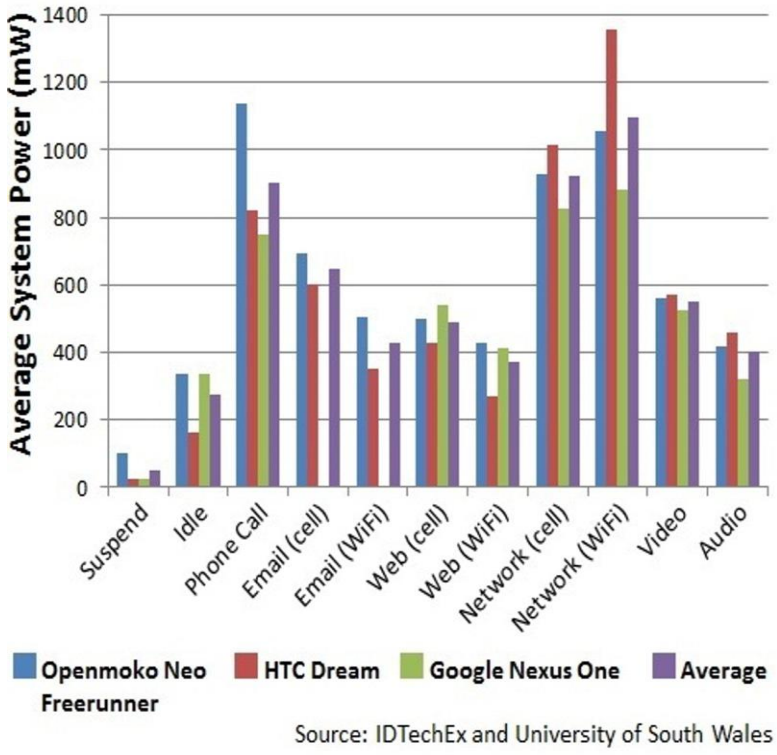

Figure 28 Different power profiles for different smartphone uses

As the super capacitors can deliver significant amount of energy at high power so they can be used in portable devices where high power is required by portable multifunctional device which

cannot be provided by the current batteries as their energy capacity reduces with the power supplied. Also, as it is required to produce more compact and small sized devices so supercapacitors can be used to revolutionized the sizes of portable devices with increased number of web-based software applications and communication involved. The growth of portable electronic devices has increased exponentially in recent years and further growth is expected as well. The devices including the Laptops PCs and Tablet Pcs all need environment friendly energy storage solution to power them while making them light weight and smaller in sizes. As the demand of using supercapacitors has increased in portable electronic device sector so there is requirement for supercapacitors to be integrated in device for different functionalities.

There has been a lot of current research regarding the fabrication of smart components of supercapacitors and to configure them as a novel device configuration. The recent advances in smart supercapacitors includes integration of functions of self-healing, shape memory, electrochromic and photodetection. Also the material for the electrodes and optimization of the configuration of smart supercapacitors along with in depth study of working mechanism is still ongoing (R. Wang, Yao, & Niu, 2020).

The progress of portable and wearable devices such as bendable smart phones, flexible wireless sensors and wearable biomedical devices have paved way for use of flexible energy storage equipment and stretchy all solid state supercapacitor(SC) is considered as the best option due to their extra ordinary flexibility, small size, light weight and easy to operate properties (Zheng, Yang, Chen, & Yuan, 2016). These flexible supercapacitors can also be used in micro electronic devices as well. As all solid flexible supercapacitors are considered as a better option than the liquid ones as there are no chances of leakage of harmful electrolytes and dislocation of electrodes while extensive stretching and thus are consider safer for sensitive wearable device applications. In medical sciences, the regular hear beat is controlled by using supercapacitors by supplying electric current to the chest wall. The supercapacitors can provide stable and reliable outputs and therefore can also be used as wearable displays, on body sensors, artificial electronic skin(e-skin) and as sensors, it was reported by (J. Wang et al., 2015) that fibre supercapacitors (FSCs) integrated with fibre based triboelectric nanogenerator(FTENG) which can convert mechanical energy produced due to motion into electrical can make a reliable flexible self-charging power system to be considered in wearable electronics.

The textile-based supercapacitors are now in production for the smart garments and the e-textile industry is developing fast. The portable and wearable electronic devices need energy storages which are small in sizes and are flexible. The yarn supercapacitors have these properties and

the main drawback is their low-energy densities and cannot be used where device requirements are high energy densities. A cloth supercapacitor using the combination of scalable coaxial wet-spinning technology is considered very safe for wearable electronics (Kou et al., 2014). The smart garments can be used as wearable devices and in the health sector for monitoring of the vital signs of the patients. In defence sector these garments can be used to track the location and health status of the soldiers in the field as well. There are now waterproof stretchable supercapacitors for smart textiles that can be developed in just three minutes using the laser base process("Waterproof supercapacitor fabrics to be laser printed in minutes," 2019). The wearable devices in e-textile and e-skin require safe, flexible and sustainable energy storage devices and as Li cannot be used so the most preferred in flexible supercapacitors. The flexible supercapacitors with high-power density ($\leq 10^3$ Wkg-^{1}), long life cycle (>10^6 charging discharging cycles) and low recharge time(~1minute) make them ideal option to be used to power various wearable devices lying in this domain. An asymmetric supercapacitor(ASC) in (Pullanchiyodan, Manjakkal, & Dahiya, 2021) provided the metal coated fabric based ASC with ability to self-charge by flexible solar cells have long term cyclic stability and can be considered suitable and sustainable for usage in wearable applications.

The supercapacitors are also used in wireless power transmissions (WPT) and radio frequency energy harvesting (RFEH). A rectenna is a type of receiving antenna that transforms electromagnetic waves into direct current (DC) electricity in electronic textile (e-textile), which then powers a wearable device continuously. The textile-integrated rectenna in (Wagih, Hillier, Yong, Weddell, & Beeby, 2021) This technique of charging is said to be the most dependable and effective way to power the wearable devices since it charges the supercapacitor to 1.5V(8.4mJ) in 4 minutes at 4.2 m from a license-free source. The radio frequency (RF) dielectric characteristics of the textile substrate are not necessary for the integration of the rectenna and textile supercapacitor on the same textile substrate.

Figure 29 Integrated e-textile RF harvester and storage module

As the internet of things (IOT) is becoming a reality so Wireless Sensor Network (WSN) usage is now a part and parcel of the digitalized new world order to get the environmental data and send it to specified location for storage. So, it is very important for a WSN device to operate in remote locations continuously without any disturbance and break. As these devices are powered by the battery so it is always a difficult job to replace the battery on time for uninterrupted operation. So as the transfer of energy in an intelligent way to the microprocessor of the device is done using the buffers. The energy buffers collect and stores the source energy and supply it in time of need to ensure the continuous operation of the device. The supercapacitors are used as the primary buffers as it has a long-life cycle and a good storage. The larger primary buffer increases the life of the secondary buffer which is made up of mostly rechargeable batteries(Kaushal & Prakash, 2019).

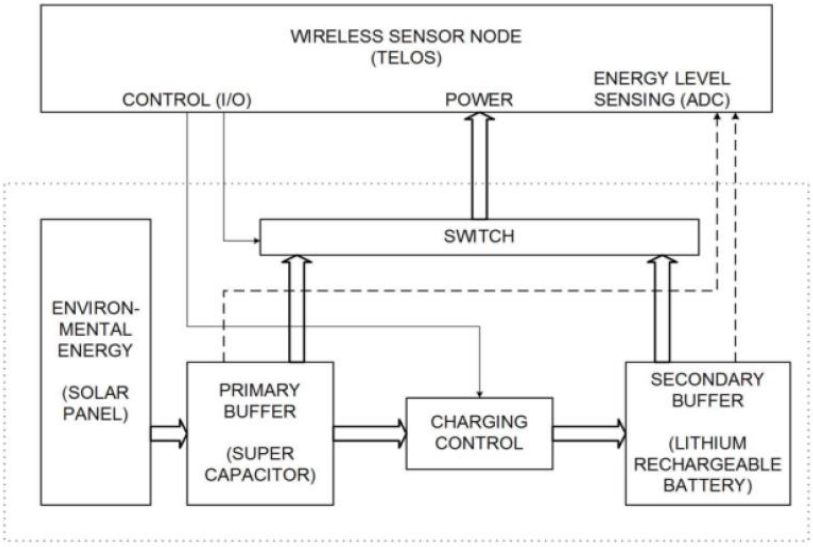

Figure 30 Prometheus Implementation and System Architecture

The on-chip micro supercapacitors are used as a solution to self-power the microelectronics like wireless sensor networks (WSN), implantable medical devices and for radio frequency identification (RFID) systems. The micro supercapacitor future depends on building 3-D electrodes with usage of high-performance materials and keeping the fabrication cost minimum (Shen et al., 2017).

2.4 Types of Supercapacitors based on Working Principals

There are different working principles of Supercapacitors which distinguish different supercapacitors from one another. The supercapacitors can mainly be classified in to following three types:

- Doble layer Capacitors
- Pseudo-capacitors
- Hybrid capacitors

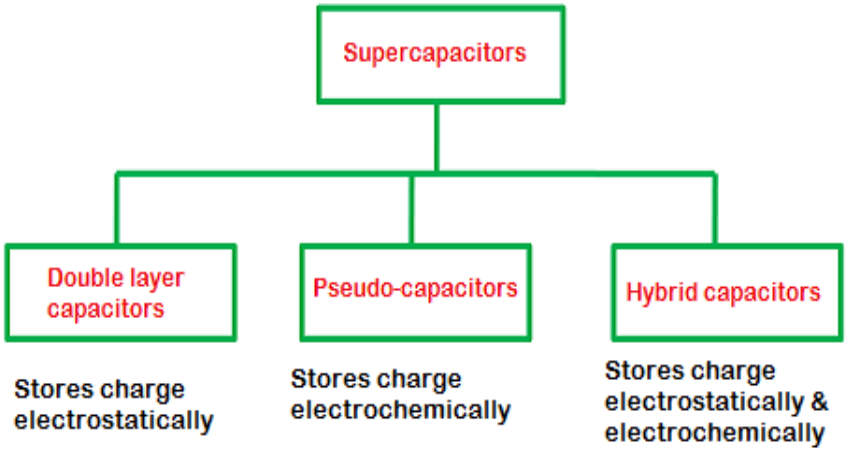

Figure 31 Types of supercapacitors

2.4.2 Electrochemical Double Layer

The supercapacitor also known as electric double layer capacitor (EDCL) is made up of two electrodes, separator, and an electrolyte. The electrodes of these capacitors are made up of carbon-based materials that have a high surface area so a charge of up to 10^6 Farads can be stored. Usually activated carbon, carbon aerogel, carbon fibre-cloth and carbon nanotubes are used as material. The electrolyte is made up of positive and negative ions dissolved in water and a separator is used to keep two electrodes apart. A common boundary is formed where the respective electrodes make contact with the electrolyte. These results in the formation of two electric charge layers which are opposite to each other are separated by a monolayer of solvent or water molecule. The dielectric is formed because of the solvent molecules and prevents the electric charge flow between the electrode and electrolyte. When external voltage is applied

double layer, capacitor starts to attain the charge and this builds up positive charge on one electrode and negative charge on the opposite electrode. As opposite charges attract each so the negative ions in electrolyte are attracted towards the positive charged electrode and vice versa but when the negative ion or positive ions move closer to the electrode, they experience a strong opposition from the dielectric (solvent molecules) and thus no charge is transferred. As the opposite charges apply electrostatic force on each other that results in a build-up of a large amount of charge at the common boundary of electrode and electrolyte. At the positive electrode and the negative electrode, respectively, there are two electric double layers. The equivalent circuits of a single capacitor are given below (Mastragostino et al., 2002). EDCL capacitance requires large electrode surface area and conductivity.

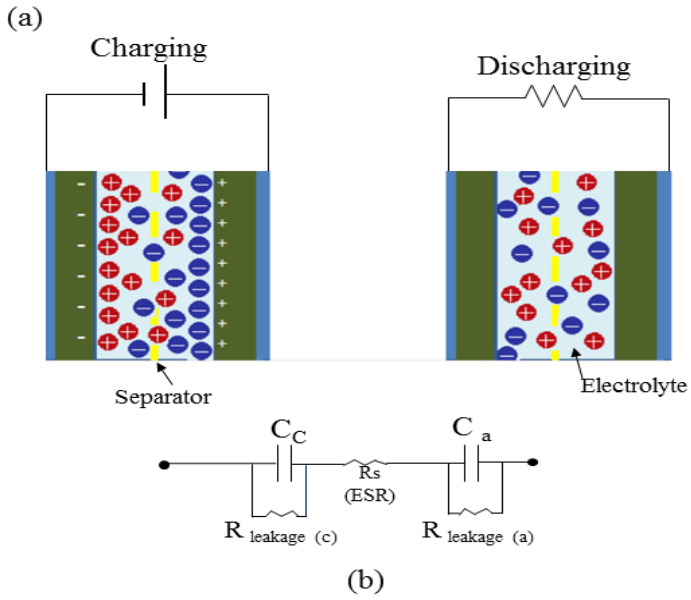

Figure 32 a) Charging and discharging of EDLC b) equivalent circuit for a single capacitor

2.4.3 Pseudocapacitance

In the 1970s, the pseudo-capacitance concept of storing the capacitive charge was established and there are three types of different methods related with charge transfer in this kind of capacitors. The metal oxides such as RuO_2 and MnO_2 besides electronically conducting polymers such as polyamilines, polyprroles and polythiopheses are most commonly used as pseudocapacitive materials(LeiZhou, ChunyangLi, XiangLiu, YusongZhu, YupingWu, 2018). When a charge is transmitted across a double layer under specific thermodynamic conditions and electrode potential (V) is seen as a continuous function of the charge (q) that passes through the electrode, a pseudocapacitance is created. Pseudocapacitance is the word used to describe the presence of dq/dV when expressed in terms of capacitance.

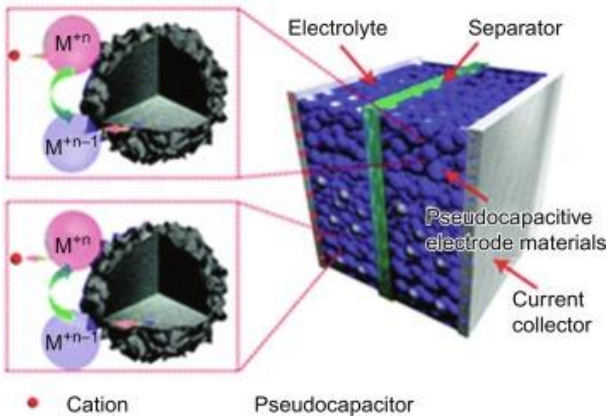

Figure 33 Schematic representation of Pseudocapacitors (LeiZhou, ChunyangLi, XiangLiu, YusongZhu, YupingWu, 2018)

In these capacitors reduction oxidation reaction (Redox) is used to transfer electrons charges between the electrode and electrolyte. In these capacitors faradic charge transfer is seen in the electrode porous layer through thermodynamically and kinetically produced electrochemical reduction-oxidation (redox) reaction. The faradic is electrochemical process in which faradic current is produced through the supercapacitor cell when the charges pass through the double layer. Also, it is important for Redox reaction to be reversible so it can ensure charge and discharge of the supercapacitor.

In electrochemical supercapacitors (ESs) the electrostatic charge accumulation and separation at the electrode-electrolyte interface results in development of double-layer capacitance but the capacitance is limited as relatively low as materials having large surface areas such as active carbon are needed to have a porous electrode. The carbon particle on the porous electrode can store the charges and electrolyte ion approachability of the porous structure is not large and up to certain level. To enhance the capacitance of the ESS, electrochemically active materials are employed to provide a higher capacitance known as pseudo capacitance, which is dependent on the change in charge quantity resulting from the Redox reaction and its relationship to the change in electrode potential. The redox reaction resembles the electrochemical reaction that occurs in a rechargeable battery.

The term "underpotential deposition" (UPD) refers to the first approach, which is a two-dimensional process and takes place at the electrode surface. The charge is stored via this method, which involves the electrochemical adsorption of hydrogen or metals such as lead, bivalent chromium, and copper onto the surface of a platinum or gold electrode. The second kind, on the other hand, involves Faradic redox processes as well as doping and dedoping at the surfaces and inside the interlayer spacing of metal oxides or conducting polymers

(CPs).The first two types are two dimensional and in the three-dimensional third type, is intercalation pseudo capacitance where Lithium intercalation occurs when Li^+ ion electroporation occurs into a layer-lattice of the materials such as TiS_2, MoS_2. (Aiping Yu, 2013). In this form of redox active electrode, ions intercalate into the layers of the electrode, which is followed by a faradaic charge transfer but does not involve any crystallographic phase separation (Chodankar et al., 2020).

Because they have a far greater specific capacitance than high surface area carbon-based double layer type capacitors, the use of metal oxide materials is the most popular method for producing pseudo capacitance. This is due to the fact that these materials display pseudo capacitance. Classic examples of metal oxides are ruthenium oxide (RuO2) and hydrous ruthenium oxide (RuO2. xH2O), both of which may acquire a specific capacitance in the range of 750-2000/F/g and show pseudocapacitive features, such as reversible redox processes (Mohd Abdah, Azman, Kulandaivalu, & Sulaiman, 2020). In (Xia, Shirley Meng, Yuan, Cui, & Lu, 2012), a novel symmetric RuO_2 / RuO_2 supercapacitor have energy density of 18.77 Wh kg^{-1} and a power density of 500 W kg^{-1} shows the potential of using RuO_2 as negative electrode for supercapacitor with high energy density.

The temperature and electrode voltage both affect the pseudo capacitance. Electrostatic double layer capacitance is included in pseudo-capacitors since they all contain double layers. Hence the total capacitance is the sum of the double layer capacitance (C_{dl}) and the pseudo capacitance (C_{ps}) as shown below:

$$C^T = C_{dl} + C_{pc}(E). \qquad (2.6)$$

We can find Cpc by using the following formula:

$$C_{pc}(E) = n^2F^2/RT\ C_{ox}^0 \quad \exp\left(nF/RT(E_{ox}^0/_{Rd} - E)/[1+\exp(nF/RT(E_{ox/Rd} - E)\right]^2 \qquad (2.7)$$

Here E is the adjustable electrode potential induced due to thermodynamic reasons in the Redox process and is defined by the Nernst equation. $E_{ox}^0/_{Rd}$ is the standard electrode potential of reaction, C_{ox}^0 is concentration of O_x (mol.cm^{-3}), R is the universal gas constant (8.314 J/K.mol), and T is the temperature (K)(Aiping Yu, 2013).

2.4.4 Hybrid Capacitors

Both electrostatic and electrochemical mechanisms contribute to the storage of charge in hybrid capacitors. Pseudo-capacitors lack strong power density and cyclic stability but have high specific capacitances, while EDLCs have the opposite characteristics and are characterized by their low specific capacitances and high-power density. Hybrid supercapacitors mitigate the drawbacks of limited cyclability in both EDCLs and pseudo capacitors by combining faradic and non-faradic methods to store energy. High power and energy densities can be achieved with hybrid supercapacitors, which also have a longer lifespan and greater stability (Y. Zhang et al., 2009).

Table 3 Comparison between EDLCs, pseudocapacistance and Hybrid Supercapacitors (Y. Zhang et al., 2009)

Parameters	EDLC	Pseudo capacitor	Capacitor hybrid
Storage device	Charge stored at the metal-electrolyte interface that is not faradic or electrostatic.	Faradic, reversible redox reaction	Both faradic and non-faradic
Particular Specific capacitance	Lower	Higher	Higher
Energy density	Low	High	High
Cycle Stability/Lifespan	High	Low	High
Material	Materials composed of carbon, such as activated carbon and carbon nanotubes	Metal oxides, conducting polymers, e.g., NiO, MgO, PANI	Metal oxide/carbon-based materials, conducting polymer/carbon-based materials, e.g., Ni(OH)2/rGO, PANI/rGO

The anode of hybrid supercapacitor is composed of electrolytic capacitor and cathode is made up of electrochemical capacitor(battery) and an electrolyte solution. When $Ni(OH)_2$ is used as a positive electrode material, electrolysis occurs and the negative electrode is made up of active carbon using KOH as an aqueous electrolyte, the hybrid supercapacitor is unit is shown in figure 33 below:

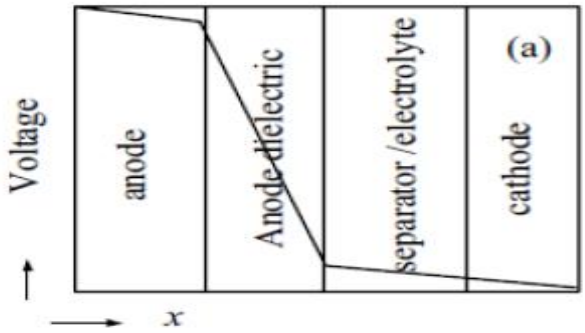

Figure 34 Internal structure and voltage distribution of hybrid super-capacitor

During the process of charging and discharging, a chemical reaction will take place between the positive electrode and the electrolyte. At the positive electrode, there is a chemical reaction taking place, so its equivalent circuit is a resistor and a capacitor connected in parallel. On the other hand, at the negative electrode, there is no chemical reaction taking place, so its equivalent circuit is a capacitor only. Because of this, the asymmetric hybrid super capacitor's two electrodes are linked in series (Denge, 2016).

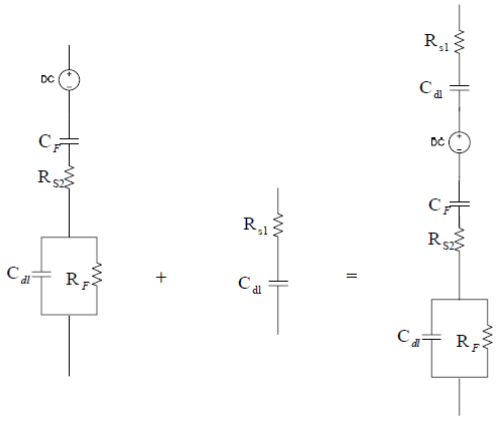

Figure 35 Forming of equivalent circuit model of hybrid supercapacitor

In (El-Kady et al., 2015), 3D extraordinary performance hybrid supercapacitors and micro-supercapacitors are demonstrated to overcome the energy density limitations of the carbon based supercapacitors. The hybrid supercapacitor LSG-MnO_2 have an energy density between 22 and 42 Wh/l, power densities upto ~10 kW/l and the energy storage are 6 times the capacity of commercially available EDCLs carbon supercapacitors. The novel hybrid capacitors can be recharged in seconds, in contrast to the hours it takes to recharge ordinary batteries.

Because hybrid supercapacitors are capable of producing high voltage, they are an excellent option for high voltage applications like those seen in electric cars.

In addition, hybrid supercapacitors may be differentiated from other types of supercapacitors depending on the arrangement of their electrodes, which can be composite, asymmetric, or battery type. The composite type combines carbon-based materials with conducting polymers or metal oxide materials in a single electrode, which enables the physical and chemical charge storage mechanisms to be combined. On the other hand, asymmetric hybrids combine non-Faradic and Faradic processes by combining an EDCL electrode with a pseudo capacitor electrode in order to achieve this combination. When it comes to hybrids that use batteries, the coupling happens between the battery electrode and the supercapacitor electrode. This combination makes it possible to make high energy and high power available for use in a variety of applications. In battery-type hybrid supercapacitors, the energy properties of batteries and the power, cycle life, and recharging capabilities of supercapacitors are combined together. These forms of the bridge the gap between the supercapacitors and the batteries (Ellenbogen, 2006).

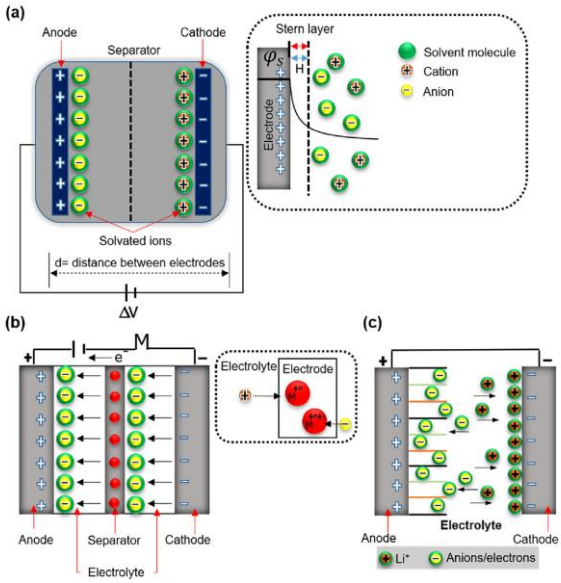

Figure 36 Schematics of working mechanism for supercapacitors showing reactions: a) EDCL b) Pseudo capacitors c) Asymmetric/hybrid Supercapacitor

CHAPTER 3

CONSTRUCTION OF SUPERCAPACITOR CELL

Electrode, electrolyte, separator, and current collector make up the supercapacitor. The performance of the supercapacitor as a whole is determined by all of these parts. The capacitance, power, and energy density of a supercapacitor are determined by the size of the pores and how they are distributed in the electrode material, the electrodes' specific surface area, and their conductivity.

The performance of the supercapacitor is known to be largely influenced by the electrolytes. Aqueous, organic, ionic liquids, solid state or quasi-solid state, and redox-active electrolytes are the subcategories of electrolytes. When choosing an electrolyte for the best supercapacitor performance, factors like ion concentration, size, type, and interaction with the electrode material are given priority. This is because improved electrolyte materials improve the electrochemical performance of supercapacitors (Iqbal, Zakar, & Haider, 2020).

The separators are used to separate the anode and cathode and have a very important role in electrochemical devices such as supercapacitors for efficient, reliable, flexible and environmentally friendly operations. The material for separator should bear a very good porosity, ionic conductivity, electrolyte wettability and low price. The separator in supercapacitors is ion-permeable membrane that permits only the ionic charge from the electrolyte but not from the electron. The separator of the supercapacitors must has excessive electrical resistance, swift ionic transfer and a very low thickness (A.Amin Izazi, Chin-Wei Lai, Joon-Ching Juan, Siew-Moie Phang, 2019). The separator also prevents short circuiting between the anode and cathode.

Anode and cathode components of supercapacitors are separated from one another using separators and submerged in an electrolyte. Active substance, conductive filler, binder, and current collector make up the cathode and anodes. The current collector serves as a power conduit between the external components and the active material. In order to create a strong electrical connection with the active material when electrochemical processes take place on its surface, supercapacitors need high performance current collectors. The active material-electrolyte interfaces may be expanded thanks to the greater surface areas of current collectors, which also reduce contact resistance and promote excellent conductivity of ions and all charge

carriers. Supercapacitors most frequently employ copper (Cu), stainless steel, aluminium (Al), and nickel (Ni) as current collectors (Salleh, Kheawhom, & Mohamad, 2020).
In this section a comprehensive and detailed discussion of the components of the supercapacitor is provided.

3.1 Electrode Materials for supercapacitors

It is necessary to have excellent power and energy performances in supercapacitors in order to reduce the size of the power gap that exists between capacitors and batteries and to make it possible to use supercapacitors in a greater variety of power and energy-related applications. Either by expanding the voltage window of the electrolyte or by raising the capacitance, the energy density of the battery may be raised.
It is possible to raise the capacitance of supercapacitors by employing electrode materials that have a high capacitance. Because of this, the door has been opened for the discovery of novel materials that, when used as electrode material, may give a larger capacitance. In EDCLs, the anode and cathode electrodes are both formed of the same material; therefore this fact is another thing that needs to be taken into consideration. The following is a list of the most significant parameters that must be satisfied for the optimization of electrode materials (Forouzandeh, Kumaravel, & Pillai, 2020):

• Lifelong cycle stability
• Irreversible redox reactions should be reduced to a minimal level in order to avoid a deterioration in stability and performance
• Specific surface area should be High
• In case of large potential applied it should be stable under high temperatures.
• Controlled pore size, particle size, and distribution of material
• Surface wettability
• High electrical conductivity
• Good thermal conductivity reduces cell heat.
• Electrochemical stability

Carbon-based materials, metal oxides, conducting polymers, and nanocomposite materials made from the aforementioned three types of materials in various combinations can all be used as electrode materials. Depending on how they perform, several types of supercapacitors utilise these materials. The following diagram illustrates the typical materials used as electrodes for various types of supercapacitors (Bokhari et al., 2020):

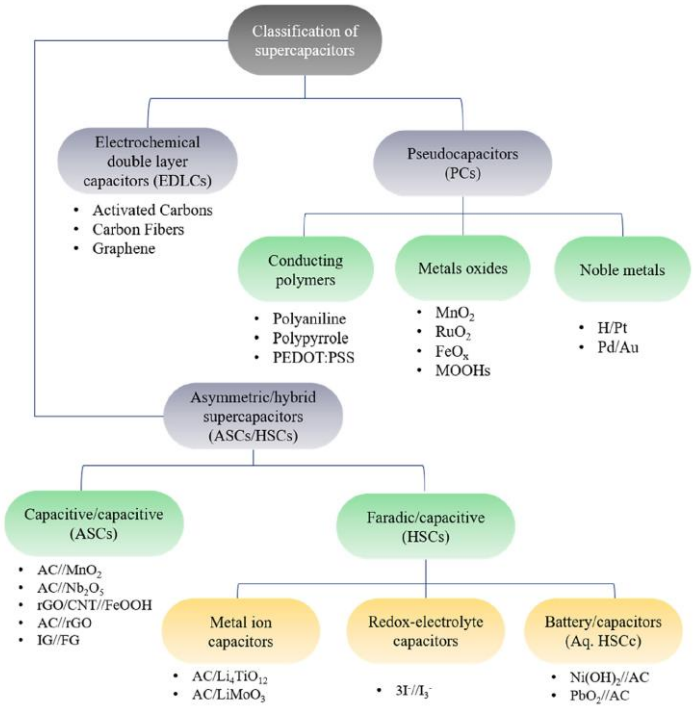

Figure 37 Classification of different types of supercapacitors and their representative electrode materials based on the charge storage mechanism that takes place in each class of SC

3.1.1 Carbon Based Materials

The electrodes are said to be the most crucial part of supercapacitors and are often made utilizing porous materials with high specific areas and a lot of carbon-based compounds. This section discusses several carbon-based materials that can be used to make supercapacitor electrodes.

3.1.1.1 Activated Carbon (AC), Aerogel and other Carbon Structures

There has been a long going research on supercapacitor carbons although carbon-carbon supercapacitors do provide higher power, better life cycle and are much reliable than the batteries but they still lack behind in the energy density. The recent developments show that that the supercapacitor carbon energy density is increased using premium supercapacitor carbons but that increases the cost as well. So, in order to keep the cost low most supercapacitor manufacturer is using activated carbon from coconut shell as an active material. Activated carbon is produced by carbonising a material and then oxidizing the charred material using agents like stream or carbon dioxide to produce nanoscopic pores. Thus the in order to increase the cycling the supercapacitor carbon is purified to decrease the ash below 1% and to minimize

the halogen and iron impurities to levels below 100ppm (Weinstein & Dash, 2013).This active carbons reduces the manufacturing costs as well.

Carbons with a large surface area are used, which enhances capacitance. To create large surface area and three-dimensional porous electrodes, activation is applied. The pore sizes are classified as micropores(<2nm), mesopores (2-50nm) and macroporoes(>50nm) and carbon produced by the combination of these different pore combinations results in achievement of good capacitive performances. In (Abbas, Raza, Shabbir, & Olabi, 2019), it has been reviewed that the heteroatom doping can be used to increase the capacitive performance of carbon based electrodes. In addition to using nitrogen to dope carbon, functional materials such as sulphur, phosphorous, and boron can also be used as electrodes to enhance the performance of supercapacitors. These functional materials increase capacitance, energy density, and while maintaining power density, as well as electronic reactivity, which increases pseudo-capacitance and enhances wettability.

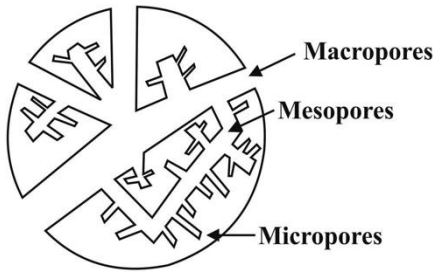

Figure 38 Schematic diagram of the pore size network of an activated carbon (Patel, 2018)

When it comes to supercapacitors, the degree to which the electrolyte allows access to the pores in the material is a critical factor in determining the device's overall performance. Because the accessible surface area of the holes increases in proportion to the particle size, the mobility of the ions within the pores is strongly influenced by the electrode's pore size. Capacitance is raised at the electrodes because tiny pores bear a short distance of ionic charge at the electrode surfaces. This results in an increase in capacitance at the electrodes. If, on the other hand, the pore sizes are exceedingly small, then they are not going to permit the flow of electrolyte ions and, as a result, they would not contribute to the functioning of a double-layer supercapacitor. Because of this, it is of the utmost importance to select the pore size for the electrode that is appropriate for the electrolyte and to make certain that the pore size distribution is as ideal as possible depending on the size of the ions (Equilibria, 2006).

The carbon aerogels are very light and porous with low thermal conductivity. In supercapacitors a high specific surface area, well inner connected three-dimensional (3-D)

texture and high specific capacitance of carbon aerogels is desired. In (Xu, Ren, Wang, Zhang, & Liu, 2018), Hummers oxidation is used to prepare aerogel with increased specific surface area and electrochemical performance.

3.1.1.2 Carbon Nanotubes (CNTs)

The carbon nano tubes (CNTs) have high surface area, strong chemical stability, excellent conductivity and are also light weight which makes them a good choice for use in energy generation and storage applications. The nanotechnology is used to develop more powerful supercapacitors. A graphene is rolled to form a carbon nano tube of 1/50,000 diameter of human hair. The structure of CNTs is one-dimensional and when carbon nanotubes are aligned to form a more organized structure the capacity for a provided space is optimized for maximum results. When a matrix of CNTs is arranged vertically the electrode structure formed has a very high capacitance.

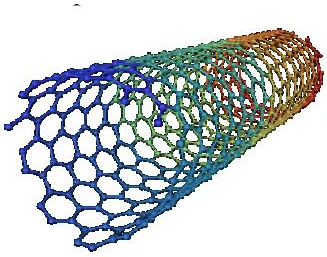

Figure 39 Carbon Nanotube

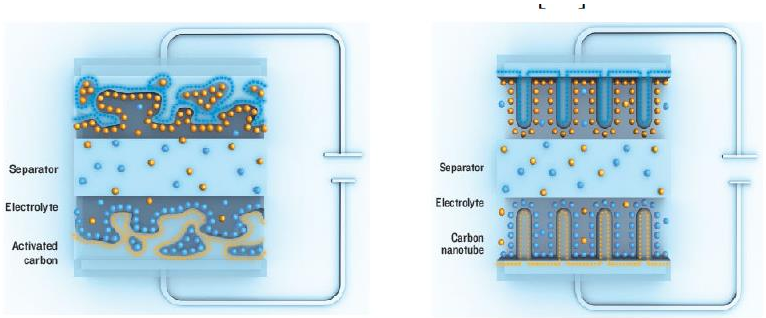

Figure 40 Supercapacitors made of porous carbon and with carbon nanotubes (Dixon, 2010)

The expected life cycle of supercapacitors with nanotube can be more than 300,000 with very high specific energy and specific power (Dixon, 2010). As opposed to the 2000 square centimeters for a normal carbon-based supercapacitor, the new generation of supercapacitors employing CNTs can feature conductive plates that are one square centimeter in size and have a surface area of around 50,000 square centimeters (Donnellan, Vowles, & Soong, 2015). Single-walled carbon nanotubes (SWCNTs) and multiwalled carbon nanotubes (MWCNTS)

are two types of CNTs that can be used as electrode materials for supercapacitors. However, SWCNTs have been reported to have higher capacitance than MWCNTs due to their larger surface area and higher conductivity (Rajendran & Balakumar, 2019).

3.1.1.3 Graphene

The carbon allotrope graphene is thought to provide an excellent electrode material for supercapacitors because it has a large specific surface area (2630 m^2/g), is extremely stable, and conducts electricity well. The unique structural characteristic of graphene, a one-atomic thick sheet of 2-D single layer sp2-bonded carbon, has exceptional mechanical strength and extraordinarily high electrical and thermal conductivity (Huang, Liang, & Chen, 2012). In (Rout, 2008), the performance characteristics of graphene, which depend on the quality, number of layers, and surface area, are much better than those of single-walled and multi-walled carbon nanotubes, according to research that used graphene as an electrode material for supercapacitors.

In a study (Y. Wang et al., 2009), graphene material as supercapacitor has been investigated and multilayer graphene based supercapacitors have shown 205 F/g specific capacitance in aqueous H_2SO_4, 1 V operating voltage, 28.5 Wh/kg energy density and 10 KW/kg of power density.

The type of graphene-based materials used in supercapacitor electrodes depends on the macrostructural complexity of the material, such as whether it is zero-dimensional (OD), which are free-standing graphene particles and dots, two-dimensional (2D), which includes graphene and graphene-based nanocomposite films, or three-dimensional (3D), which can be graphene foam and hydrogel-based nanocomposites (Ke & Wang, 2016). In (L. Wang et al., 2019), Electric field-assisted assembly of graphene oxide sheets is used to create 3D graphene networks, which result in supercapacitors with high specific capacitance (238 Fg^{-1} at 0.5 A g^{-1}) and retention of 60% at 10 A g^{-1}. Performance is enhanced by the substantial electrolyte accessible surface (257 $m^2\ g^{-1}$) and strong electrical conductivity (12.58 S cm^{-1}). In comparison to techniques like chemical vapor deposition, freeze drying, etc., the electric field aided assembly approach also lowers manufacturing costs, which can support industrial production.

In (H. Zhang et al., 2015), a symmetrical SC was produced using numerous electrode materials made of nano structured graphene oxide (GO), polyvinylidene fluoride (PVDF), and KOH with a different ratio. It was found that G1p4K6-2, and G1p9K6-4 showed better electrochemical performance, in which, for the sample G1p9K6-4, the maximum E_d

of 78 $Wh.kg^{-1}$ at P_d of 875 Wkg^{-1} and high specific capacitance of 185 Fg^{-1} at 0.5 Ag^{-1} was obtained. Furthermore, graphene nano sheets (GNSs) can also be utilized as an electrode material for the supercapacitors in 2D. The graphene nanosheets are also known as graphene paper which is flexible and it's electrochemical properties are improved because of the open structure resulting in easy storage of charge and ion transfer (Forouzandeh et al., 2020).

In general, we can say that carbon materials which have high surface area and a suitable porous structure are a reasonable choice for electrode material for good specific power and long-life cycle requirements.

3.1.2 Metal Oxide

Transitional metal oxides, such as RuO_2, Co_3O_4, MnO_2, ZnO, XCo_2O (where X=Mn, Cu, Ni), and $AmoO_4$ (where A=Co,Mn,Ni,Zn), can be used to provide higher energy density and better electrochemical stability as compared to carbon material and conducting polymers CPs because the electrochemical performance of supercapacitors is greatly dependent on the electrode material (R. Liang et al., 2021).

RuO_2 as an electrode material has a wide potential window, highly reversable redox reactions besides having high thermal stability, metallic type conductivity, high-rate capability and a very high specific capacitance of 900 F/g. It's not preferable to use RuO_2 on commercial scale as it is not environmentally friendly and toxic in nature with high production costs. Therefore, MnO2 is frequently employed in place of RuO2 and has a steady cyclic stability, low production cost, while having a lower specific capacitance of around 110-260 F/g. Low capacitance and poor columbic efficiency are caused by the active material's low conductivity and poor proton transport in MnO2. The utilization of biomass resources to extract carbon is a significant step towards sustainability since it lowers manufacturing costs and takes environmental implications of the material for supercapacitor electrodes into consideration. Because of its multistage pore structure and carbon stability, biomass carbons are an excellent choice to be used as an electrochemical material. Therefore in (Yang & Park, 2018), carbon source for electrodes was obtained from the banana peels to synthesize MnO_2/biomass based porous carbon (BPC) composites by hydrothermal method. The specific capacitance of 139.6 $F\ g^{-1}$, current density of 300 $mA\ g^{-1}$ and 70 $F\ g^{-1}$ at 10 $A\ g^{-1}$ was obtained using MnO_2/ BPC electrodes in supercapacitor.

The process of charge storage of MnO_2 based electrode in neutral solution is shown below:

$$MnO_2 + H+ + e- \Leftrightarrow MnOOH$$

In process of charge storage, the intercalation/de-intercalation reaction of H^+ and the adsorption/desorption of cations of electrolyte (H^+) during the redox reaction process takes places. The space for growth of the MnO_2 particles is provided by the carbon structure substrate which avoids the aggregation of MnO_2 particles therefore resulting in more sites for rapid, faradic redox reactions which in returns improves the electrochemical performance. Therefore, the charge storage process is based on the surface adsorption of cations in the electrolyte and the incorporation of protons.

3.1.3 Conducting Polymers

Polymers are macromolecules that are formed when smaller molecules, known as monomers, are bonded together in a variety of different ways over and over again. Initially polymers were used as an insulating material in electronic devices unless it was discovered that polyacetylene (PAc) which is a polymer of acetylene can conduct 10^8 times when doped in iodine. Hence the conducting polymers are those which can possess values almost near to be an insulator but when doped can be considered as conductors. CPs can be used in various applications such as in development of organic solar cells, sensors, organic light emitting diodes (OLED), displays, and in printing of electronic circuits. The most frequently used conducting polymers are polypyrrole (PPy), polyaniline (PANI) and polythiophenes (PTh). Even in the presence of oxygen and water, conducting polymers can exhibit metal- and plastic-like characteristics because to their unique conduction mechanism and high environmental resilience. The CPs can be classified as electron conducting, proton conducting and ion conducting polymers(Choudhary, Ansari, & Majumder, 2021).

The CPs are created using the methods of photochemical polymerization, emulsion polymerization, inclusion polymerization, plasma polymerization, and pyrolysis. CPs are used as an electrode material as they are known to be environmentally friendly, low in cost with high conductivity and for high capacitance in supercapacitors.

The main disadvantage of using CPs as electrode material in supercapacitors is their limited life cycle and instability, which means that the working potential range of the CP electrodes cannot exceed certain levels and can cause swelling, shrinkage, cracks, or even breakage during long-term charge-discharge processes, thereby reducing their conductivity.

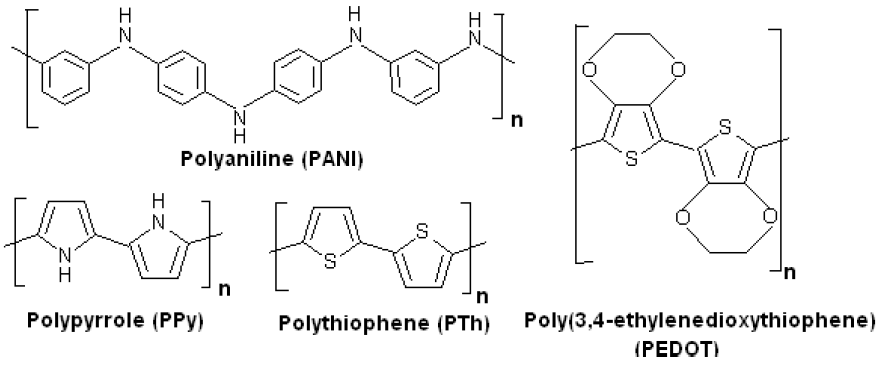

Figure 41 Chemical structure of Some CPs

3.1.3.1 Conductivity of CPs

The three conductivity classes in terms of band gaps are metal, semiconductors and insulators. In the conduction band there are unfilled energy levels which can be filled in response to an electric field giving rise to conduction. In case of CPs their semiconductor band structure allows electronic excitation or electron removal/addition from the valence band to the conduction band. When there is no doping of CP, electrons do not flow in polymer structure and thus there is no conductivity but when the CPs are doped it is can be oxidized by removal of electrons and form radical cation(hole polaron) or can form radical anion(electron polaron) by addition of electrons to the conjugated backbone of the polymer(Chandrasekhar, 2018). When the potential is applied across the polymer the charges which are due to the removal of electrons from valence band are in general strongly delocalized occurring along the backbone of the polaron and provide the free movement of electrons and increases the conductivity of the CP many folds. The oxidation process produces positively charged CP whereas reduction process results in the negatively charged CP. The following table shows the conductivity comparison different metals and polymers:

Table 4 Comparison of conductivity and specific gravity of metals and polymers (Joel R.Fried, 2nd ed.,2003)

Material	Conductivity [a] (S cm^{-1})	Specific gravity
Silver	10^6	10.5
Copper	6 × 105	8.9
Aluminium	4 ×105	2.7
Platinum	10 ×104	21.4
Mercury	1 × 104	13.5
Carbon fiber	0.05 × 104	1.7–2
Carbon black-filled polyethylene	0.001 ×104	1
PTFE (Teflon)	10–8	2.1–2.3
Polyacetylene (non-doped)	1 × 104	1
Polyacetylene (doped)	15 × 104	1
Polythiophene (doped)	1 × 104	1

[a] Unit of siemens (S) per cm.

3.2 Electrolytes

Either a solute that has been dissolved in the solvent or a pure salt makes up the electrolyte. Because the high power and energy density of the supercapacitors are mostly dependent on the type of electrolyte that is being used, making a good selection of electrolyte is seen as being just as crucial as the material that is used for the electrodes in the supercapacitor cell. The electrolytes have a role in the construction of an electronic double layer (EDL) in electrical double layer capacitors (EDLCs), charge compensation on each electrode, and also participate in the process of charge storage, which involves reversible redox processes. The performance of the supercapacitor is heavily influenced by the magnitude of the ion, the kind of ion, and the concentration of the ion in the solvent that is produced as a result of the interaction between the electrolyte and the electrode material. The highest voltage that may be supplied to the electrolyte in order to get the supercapacitor to work is determined by the electrochemical stability of the electrolyte. As a result, the energy and power densities of an electrochemical

supercapacitor are determined by the kind of electrolyte. The equivalent series resistance (ESR) of the supercapacitor is also affected by the ionic conductivity of the electrolytes. It is very important to select the right electrolyte for the supercapacitor and the general requirement for the electrolyte include the electrochemical stability, high ionic conductivity, operational temperature ranges, a low viscosity and volatility. It is also very important to have electrolyte which is environmental friendly , low in cost and found in abundance in high purity form(Zhong et al., 2016).

When it comes to stabilizing the parameters that affect the performance of the supercapacitors, the function that electrolytes play is quite significant. The following figure 42 illustrates the impact that the electrolyte has on the various performance metrics of the supercapacitor:

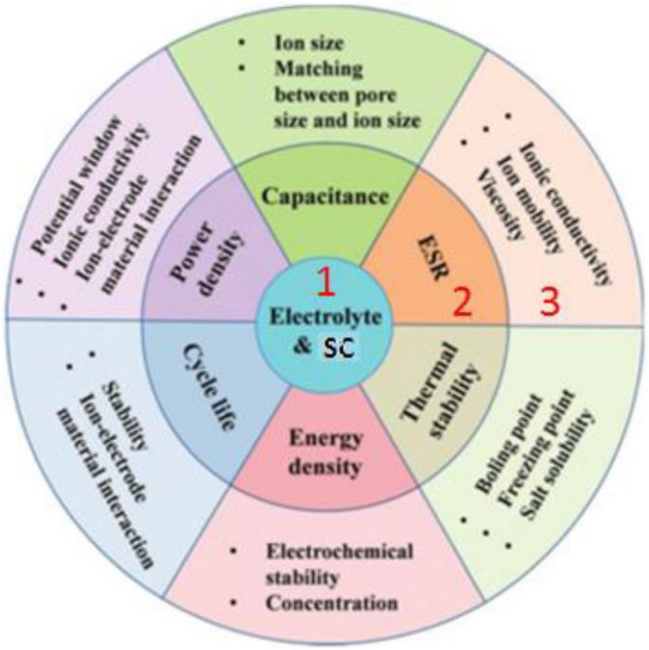

Figure 42 Effect of electrolyte properties on different parameters affecting the performance of SC (Zhong et al., 2015a)

Three concentric circles are depicted in the above figure: circle 1, which represents electrolytes and supercapacitors, circle 2, which displays supercapacitor performance metrics, and circle 3, which shows the electrolytes that influence circle 2's performance parameters. We can see from the above picture that ionic conductivity, ion mobility, and electrolyte viscosity all have an impact on the equivalent series resistance (ESR) of supercapacitors.

The electrolytes are classified as liquid electrolytes and solid/quasi-solid-state electrolytes. The liquid electrolytes are further grouped as aqueous electrolyte, organic electrolyte and ionic

liquids (ILs). Organic and inorganic electrolytes fall under the category of solid or quasi solid state of electrolytes.

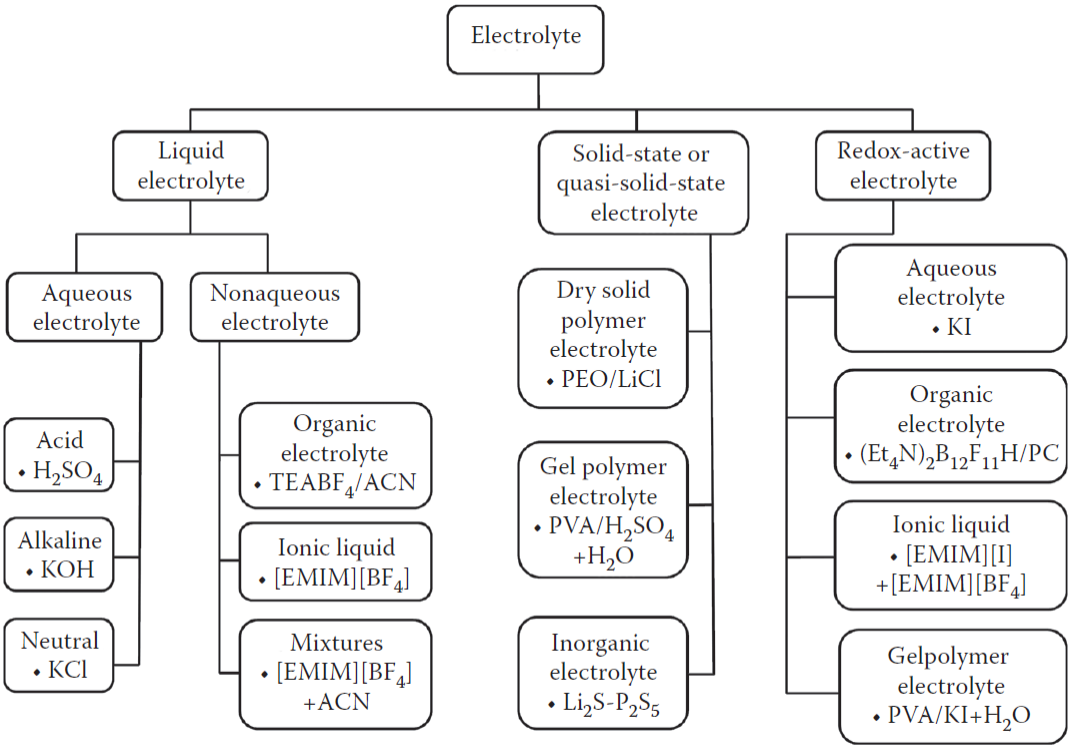

Figure 43Classification of electrolytes for Supercapacitors (Zhong et al., 2016)

Since each electrolyte has benefits and drawbacks, no one has yet created the optimum electrolyte that can be utilized in supercapacitors. Although aqueous electrolytes-based electrochemical supercapacitors have excellent capacitance and conductivity, their operational voltage is constrained. Similar to this, the operating voltage increases when organic and ionic liquids (ILs) are used as the electrolyte, but their ionic conductivity decreases. Solid state electrolytes allow us to avoid any possible leakage issues that may arise from liquid electrolytes, but they also have lesser conductivity(Zhong et al., 2015b).

In this section, we will have a brief discussion on the many types of electrolytes that are often used in supercapacitors, such as aqueous, organic, ionic liquids, and solid or quasi-solid-state electrolytes. For example, aqueous electrolytes are the most popular form of electrolyte.

3.2.1 Aqueous Electrolytes

Aqueous electrolytes are low cost, highly conductible, environmentally friendly and have results in high capacitance in supercapacitors. They can be acidic, alkaline or neutral in nature

and most commonly used are KOH, H_2SO_4 and NA_2SO_4. The aqueous electrolytes cannot exceed certain level of voltages and that's the main reason that commercially produced supercapacitors manufacturers prefer using organic electrolyte instead of the aqueous. Despite having a low voltage window, they are nonetheless affordable and have a substantially higher conductivity than organic or ionic liquid (IL) electrolytes. Due to the aqueous electrolytes' excellent kinetic behavior of the electrolyte ions, charge and discharge rates are extremely efficient. As the conductivity is very high therefore the internal resistance of the supercapacitors using aqueous electrolytes is also very low and leads to significantly high-power density supercapacitors. Electrolyte-stable potential window (ESPW) values depend on the cations and anions of given conducting salts and therefore EPSW values can be increased by trying different aqueous electrolyte salts and optimizing the suitable electrolytes. It has also been found that electrodes of pseudocapacitive supercapacitors are provides higher energy densities in aqueous electrolytes and therefore efficiency of electrochemical capacitors can be increased by improving the specific surface area of the pseudocapacitive material. It is also very important for enhancing the efficiency of supercapacitor to use purified aqueous electrolyte as contaminated electrolyte can cause high self-discharge rates besides effecting the stability of the electrolyte(Ramachandran & Wang, 2018).

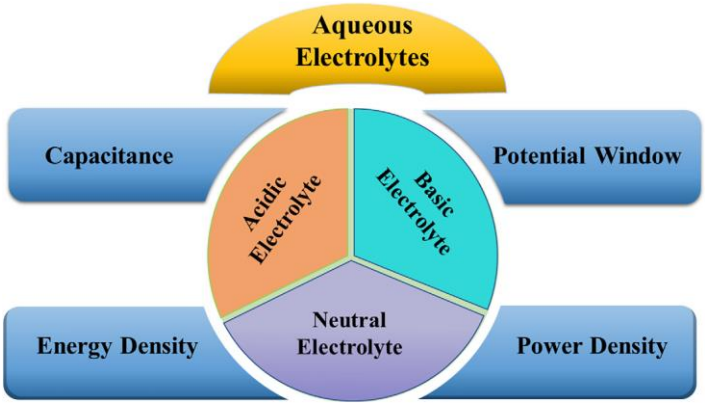

Figure 44 Aqueous electrolytes

3.2.2 Non-Aqueous Electrolytes

The electrolytes that are not soluble in water are quaternary ammonium salts that are dissolved in carbonates or acetonitrile. The supercapacitors that make use of a non-aqueous electrolyte are more electrochemically stable and are in a position to address the problem of current leakage that the system is experiencing. The use of non-aqueous electrolytes in supercapacitors results in higher energy output than the use of aqueous electrolytes because non-aqueous electrolytes have higher operating voltages and also contain larger internal resistances when

compared to aqueous electrolytes by a factor of 20-50 respectively. The non-aqueous electrolyte solutions are divided into inorganic and organic solutions. Lithium aluminium chloride ($LiACl_4$) dissolved in thionyl chloride is an example of inorganic non-aqueous electrolyte and is used in Li-$SOCL_2$ battery. Whereas, when an organic electrolyte is a solution of lithium salt and an organic solvent. Lithium salts like lithium perchorate ($LiClO_4$), lithium trifluoromethane sulfonate ($LiCF_3SO_3$) are examples of commonly used organic electrolyte solutions in energy storage devices(Soo-Keng Chang, 2019)(Nishio, 2009).

The lithium salts are used as lithium ions have very small effective diameter and move at high speeds under the influence of electric field.

The most common non-aqueous solvents used in supercapacitors electrolytes are propylene carbonate, dimethyl sulfoxide, ethylene carbonate, diethyl carbonate, acetonitrile etc (Sekhon, 2003).

3.2.2.1 Organic Electrolytes

As the organic electrolytes have a wide potential window so they can be very useful in attaining high energy supercapacitors. The most commonly used organic electrolytes are namely acetonitrile (ACN) and propylene carbonate (PC). As acetonitrile are not environmentally friendly therefore propylene carbonate (PC) as an electrolyte for supercapacitor devices is considered more acceptable choice. It is very important to consider the pore size and the size of ion for organic electrolyte. For example, the solvent ion is larger in carbon-based electrodes than the organic ion of the electrolyte thus results in low capacitance. The pores in carbon electrodes do provide large surface areas which can be accessible but at the same time suppress and limit the access of the organic electrolyte ions into small pores. So, for common organic ion the optimized pore size is considered between 0.7-0.8 nm. The following are the factors that can bound the performance of the organic electrolyte as:

1- Higher resistivity
2- Low salt solubility in organic solvents
3- Large size of organic molecules

Also, while selecting organic electrolyte, one must be aware of toxicity and flammability of the organic solvents being used and should be handled carefully. The binary salts or alternative solvents can be used to boost the operating temperature range and energy densities which increases the performance of the organic electrolyte (Heng Ivy, Lai WEi Chin, & Juan Joon Ching, 2019).

The high electrochemical stability window (ESW) for the organic electrolytes is a major reason for the commercial use in supercapacitors as this helps in enhancement of both energy and power densities as compared to the aqueous electrolytes. On the other hand, the use of organic electrolyte is costly, can result in lower specific capacitance, lower ionic conductivity and is hazardous to the humans and the environment. The low capacitance is due to larger solvent ion size and low dielectric constant of organic electrolytes. In (H. Zhou et al., 2016), A fluorine-rich carbon surface with a higher polarity provides a stronger affinity and wettability for the organic electrolyte, which results in higher electrochemical performance of the supercapacitor. This has been demonstrated experimentally and computationally. Additionally, highly mesoporous carbon flakes created by pre-carbonizing and activating tubular kapok fibers with KOH are regarded as an advantageous electrode material for EDCL in an organic electrolyte and have been known to produce some of the best results to date when using carbon electrodes made from biomass. These results include energy densities of 33.8 and 24 Wh kg^{-1} and power densities of 260 and 24,029 W kg^{-1}(Zou, Liu, & Jiang, 2019). The organic electrolytes that are used in supercapacitors can charge above the standard ranges of ESW (2.5-2.8V). This can produce redox reactions at the electrodes and in the electrolyte that are not what is wanted, which leads to electrolyte deterioration and carbon electrochemical oxidation. These processes cause supercapacitors to self-discharge and develop gases, and as a result, supercapacitors that use organic electrolytes are not regarded as being advantageous owing to performance and safety concerns.

3.2.2.2 Ionic Liquid Electrolytes

Ionic Liquids (ILs) are ionic salts composed of cations and anions that melt at temperatures below 100oC. These salts, which are also referred to as molten salts at room temperature, are made up of an inorganic/organic anion and asymmetric organic cations. These salts are utilized as environmentally friendly solvents and as electrolytes in various electrochemical devices, such as supercapacitors, due to their features such as non-flammability and minimal vapour pressure in addition to their excellent thermal and chemical stabilities(Brandt, Pohlmann, Varzi, Balducci, & Passerini, 2013). As these electrolytes do not contain volatile organic compounds but only salts (ILs) so they are also referred to as solvent free electrolytes. The ILs used for supercapacitors as electrolytes are mostly based on pyrrolidinium and imidazolium cations. As pyrrolidinium based possess higher electrochemical stability against oxidation and

are used to contribute strongly to the energy density of the device whereas imidazolium has low viscosities and higher conductivities which contribute to higher charge and discharge rates. Therefore, it is necessary to do select the right ILs and manipulate in order to get the desired results for supercapacitors rendering to diverse operating conditions and requirements based on different characteristics of the IL electrolytes. Also, it is important to note that the electrode structures do affect the arrangement of ILs at the interface like a layered structure is formed at the planner electrode, mono layer structure is formed on porous electrodes with a proper pore size and in porous electrodes with wider pores, a multilayer structure is formed. In case of nano porous electrodes when pores are matched well with the ion size of the ILs have the best performance under conditions(S. Pan et al., 2020) .

3.2.3 Solid or Quasi-Solid-State Electrolytes

The majority of supercapacitors, as will be shown in the following discussion, use electrodes made of activated carbon with liquid electrolytes such as aqueous, organic, or ionic liquids. However, the disadvantage of using these types of liquid electrolytes is that leakage can occur, despite the fact that separators are used to avoid electric contacts between electrodes and that heavy encapsulation materials are used to prevent these. Therefore, electrochemical devices that employ liquid electrolytes are not suitable for use in applications such as lightweight energy storage, microelectronics, or textiles (Khosrozadeh, Xing, & Wang, 2015). Since they may be utilized securely for quick power supplying in portable electronics, wearable electronics, microelectronics, printable electronics, and flexible electronic devices, there has been an increase in the need for storage devices that use solid electrolytes. This has caused the demand for storage devices that use solid electrolytes to rise. In comparison to liquid electrolytes, solid-state electrolytes provide a higher level of mechanical stability, and the fabrication process for these electrolytes is also less complicated, making them the superior option for usage in devices in terms of ensuring user safety. The polymer electrolyte is used in the electrochemical energy devices in the role of a solid-state electrolyte. Polymer electrolytes are solid ionic conductors and are generated by dissolving salts in appropriate high-molecular-weight polymers. This creates the polymer electrolyte. Get polymer electrolytes, also known as GPE, and solid polymer electrolytes, also known as SPE, are the two different kinds of polymer electrolytes. The gel type of polymers are combined polymer-solvent-salt systems. In these systems, the polymer is employed to act stiffer for the low molecular weight solvent,

which functions as a medium for the transportation of ions. The poly(vinyl alcohol, often known as PVA) lithium salt may be utilized to make GPE, and aqueous, organic, or il solvents can be employed in its production (Sequeira & Santos, 2010). Without the use of a solvent, the SPE is made up of polymers like poly ethylene oxide and PEO and inorganic salts like LiCl. Because there is liquid in the polymer matrix, the ionic conductivity of GPE is greater than the ionic conductivity of SPE. Despite having a lesser mechanical strength than SPE, GPE has a better conductivity. In (Qin et al., 2020), multifunctional supera-molecular GPE is prepared which has the properties of self-healing, stretchability and resistant to extreme cold temperatures. A supercapacitor using a high property PVA-TA-H_3PO_4 GPE as an electrolyte and separator simultaneously shows that it recovers its electrochemical properties with in 10 minutes without external treatment besides having properties such as flexibility to be repeatedly bent, twisted and even forced to take different geometric shapes without any change or deterioration of the supercapacitor properties. The supercapacitor attained specific capacitance of 68.3% at room temperature even at -20^{o}C.

CHAPTER 4

PERFORMANCE EVALUATION OF SUPERCAPACITORS

4.1 Techniques for structural studies

In this section we briefly discuss the techniques involved for structural and chemical studies of the supercapacitor.

In this dissertation, supercapacitor electrode material is created from the rind of a watermelon. Because of this, sophisticated characterisation methods are utilized in order to investigate the surface morphology, chemical characteristics, and physical properties of the material that has

been synthesized. Methods such as Scanning Electron Microscopy (SEM), X-Ray diffraction (XRD), Energy-dispersive X-ray (EDX), Raman Spectra, Fourier Transform Infrared (FTIR), and the BET (Brunauer- Emmett- Teller) were utilized for the aim of determining the surface area and pore size distribution.

4.1.1 Scanning Electron Microscopy (SEM)

A scanning electron microscope, often known as a SEM, is a specific kind of electron microscope that creates pictures by sweeping a sample along with a focused stream of electrons while it examines the sample. When electrons interact with the atoms in a sample, secondary and backscattered electrons are created. These electrons may be detected and include information on the topography and composition of the material's surface.

The use of Fourier transformation using a convex objective lens, followed by intermediate lenses and projection lenses for picture expansion, is the fundamental idea behind transmission electron microscopy imaging. In contrast, scanning electron microscopy (SEM) makes use of a unique imaging method that reveals surface details of specimens by employing a scanning electron probe in conjunction with secondary electrons that are released from the specimen's surface. The most important properties of SEM are as follows (National & Pillars, 2015):

1)Imaging with electrons emitted from specimen surfaces on the same side as the incidence of electrons.

2) Similar to facsimile and television technology, scanning methods use imaging.

3)Imaging uses electrons that are inelastically dispersed (secondary electrons) and have an energy of less than 50 eV.

4)Imaging a specimen by scanning from upper-left to lower-right pixels.

5)Due to a reflection mode, thick or bulk specimens can be seen.

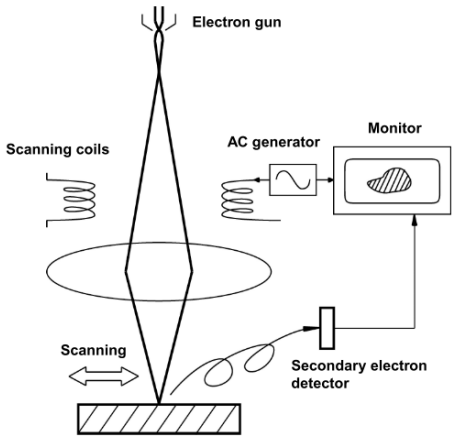

Figure 45 Basic ray diagram of SEM

4.1.2 Energy Dispersive X-Ray Spectroscopy (EDX)

In addition to that, energy dispersive X-ray spectroscopy, generally known as EDX, was utilized throughout this study. Quantitative data on the surface elements may be obtained by the EDX approach. The data for the EDX technique may be obtained using the scanning electron microscope (SEM) and associated equipment.

In a manner analogous to the scanning electron microscope (SEM), a high-energy beam of electrons impacts the sample on the specimen. The electrons that are contained within the electron shells of an atom are then energized and expelled, which results in the formation of an electron hole. After then, an electron coming from an outer shell with a higher energy level is used to fill the hole. The interaction between the high-energy electron beam and the sample creates a unique sort of X-ray, which may be detected by an energy-dispersive X-ray spectrometer that is built into the SEM equipment. This is because there is a difference in energy between the higher-energy shell and the lower-energy shell.

The application of X-ray diffraction as a method for locating flaws in crystal lattices is a powerful approach. The shrinkage of crystallite sizes in polycrystals and the appearance of crystal lattice distortions are the two main factors that contribute to the widening of diffraction lines. Because of this phenomena, it is now feasible to ascertain the sizes of particles in the nano-scale range. Additionally, EDX requires far less time to process, can be analyzed with greater ease, and offers a wider range of potential applications (Kämpfe, Luczak, & Michel, 2005).

4.1.3 X-Ray Diffraction (XRD)

X-ray diffraction (XRD) makes use of the coherent X-ray scattering by crystalline materials to get a wide range of crystallographic data. In reaction to the incoming beam, each scatterer reradiates a small portion of its intensity as a spherical wave. Only if scatterers are positioned symmetrically with a spacing of d will these spherical waves be in phase in directions where their path-length difference 2d sin equals an integer multiple of the wavelength. The incoming beam is deflected by an angle of 2θ in such case, causing a reflection spot to show up in the diffraction pattern.

Crystallographic information may be gleaned through the interpretation of various diffraction patterns, also known as scattered X-ray patterns. This information is based on the specific crystal orientation and structure of a certain material (Waseda, Matsubara, & Shinoda, 2011).Powder X-ray diffraction, in particular, is a helpful analytical tool for examining crystallographic structure and grain size of solid samples, and the following equation, known as Bragg's rule, can be used to get this information.

$$n\lambda = 2d \sin \theta \quad (4.1)$$

The functionality of the supercapacitor is mostly determined by the specific surface area of the porous electrodes, and the nitrogen adsorption-desorption measuring method is one that is frequently used by a lot of different researchers. However, despite its ease of use, the X-ray diffraction method is rarely employed to estimate the specific surface area of porous electrodes. This is despite the fact that it provides accurate results. In (Deraman et al., 2015), propose a novel equation in that expresses the specific surface area of electrodes as a function of electrode structural parameters derived from X-ray diffraction data and the duration of activation time used during electrode fabrication. This equation yields a reasonable result, and it is believed to be useful in the research of supercapacitor electrode materials. In our thesis we have used XRD method to characterize our samples.

4.1.4 BET and BJH Analysis

For a variety of materials, measuring surface properties is becoming more and more crucial, especially when choosing the suitable material for supercapacitor electrodes. One of the most fundamental of these qualities is the surface area available for gas molecule adsorption. The way a solid interacts with its surroundings, especially liquids and gases, depends on its surface area. Porous materials and particle size reduction techniques like grinding and milling can both be utilized to improve surface area.

Utilizing nitrogen multilayer adsorption and a fully automated analyzer, Brunauer-Emmett-Teller (BET) analysis calculates the specific surface area of materials as a function of relative pressure. Nitrogen is the gaseous adsorbate that is utilized for surface probing by BET methods almost all of the time. As a direct consequence of this, BET analysis is often carried out at the boiling point of nitrogen, which is 77 K (Bardestani, Patience, & Kaliaguine, 2019). In addition, other probing adsorbates are utilized, albeit at a lower frequency, to enable surface area measurements to be taken at a variety of temperatures and on a variety of scales. The approach utilizes external and pore area measurements to compute total specific surface area in m2/g. This method is valuable for exploring the influence of surface porosity and particle size in a number of applications since it allows for accurate calculations (Naderi, 2015). Barrett-Joyner-Halenda (BJH) analysis may also be used to assess pore area and specific pore volume using adsorption and desorption techniques. This method defines the pore size distribution regardless of the outside area because of the sample's particle size (Lucideon Materials Development and Commercialization, 2022).

One of the most significant textural characteristics of porous materials is the Pore Size Distribution (PSD), which defines the pore volumes for each pore size. Based on N2 adsorption-desorption experimental isotherm data at 77 K, which has been the subject of substantial research in order to apply various theories, the most popular techniques for calculating the PSD of nanoporous materials. The pore volume and pore size distribution may be calculated by progressively raising the gas pressure until all pores are filled with liquid. The condensed gas can then leave the system when the gas pressure is progressively reduced. By examining the adsorption and desorption isotherms, the pore volume and size distribution may be found. Pore volume and pore size distribution are calculated using the BJH (Barrett, Joyner, and Halenda) formula(EAG Laboratories, 2015).

There are two types of methodologies for evaluating the PSD: those that employ molecular theories i.e. microscopic methods and those that use the capillary condensation theory known as macroscopic methods(Villarroel-Rocha, Barrera, & Sapag, 2014).

In (Anton Paar GmbH, 2022), the article discusses the approach that may be used to describe the BET area of a microporous material. Materials are considered to be microporous if the diameter of the pores in the material is smaller than 2 nanometers. The surface area of porous materials is an essential property that is frequently computed using the BET equation. Accurately calculating the BET area of microporous materials requires a highly accurate understanding of the surface area of these materials. Because pore condensation is observed at pressures very close to the pressure range where mono layer-multilayer creation occurs on the

pore walls, using the BET method to estimate the specific surface area of mesoporous molecular sieves with pore widths less than 4 nm is problematic. Therefore, the surface area determined for microporous materials by using the BET equation should be referred to as "characteristic" or "equivalent" surface area, or simply BET area (Anton Paar GmbH, 2022).
The BET equation is:

$$1/w((Po/P)-1) = 1/WmC + (C-1)/(WmC)*(P/Po) \qquad (4.2)$$

Wm is the weight of the adsorbate constituting a monolayer of surface coverage, and W is the weight of gas adsorbed at a relative pressure of P/P0. The BET C constant, or C, is connected to the energy of adsorption in the first adsorbed layer, and hence its value indicates the scale of the adsorbent/adsorbate connections.

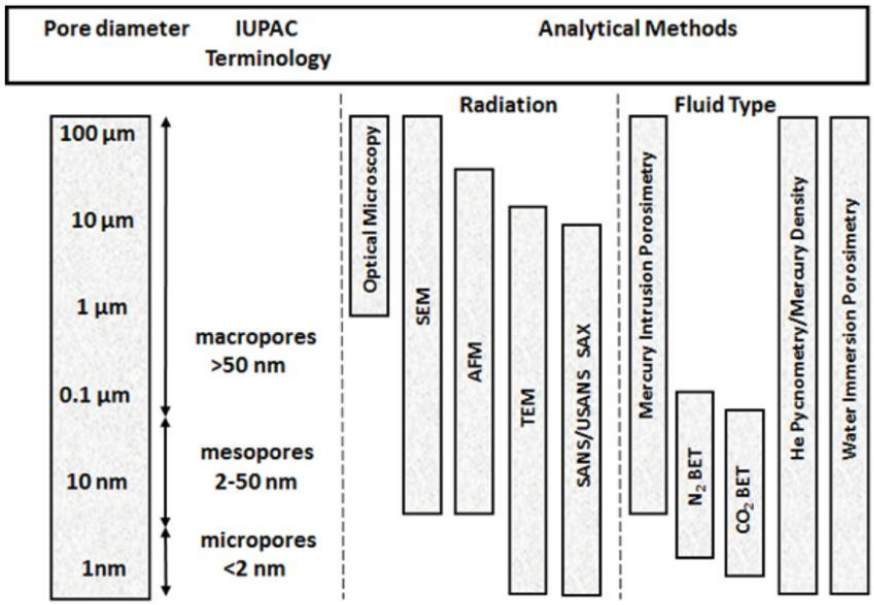

Figure 46 Methods used to determine porosity and pore size distribution(PSD) (Anovitz & Cole, 2015)

4.1.5 Roman Spectra

The observation of low-frequency vibrational, rotational, and other modes in a system can be accomplished by the use of a technique called Raman spectroscopy. Typically, a visible, near infrared, or near ultraviolet laser is used to do the Raman scattering, which is a process that involves the inelastic scattering of monochromatic light. When laser light interacts with phonons or any other excitations in the system, the energy of the photons emitted by the laser can either be increased or decreased. The change in energy yields information on the vibrational modes of the system. Therefore, when the laser light is concentrated on the test sample, and then reacts with the sample's vibrations or excitations on a molecular level, the outcome is shifted laser photons, which are promptly recorded on a Raman spectrum. The resolution of

the Raman spectra can be improved by the accumulation of scans that have a longer exposure duration. In (Shanmuga Priya, Divya, & Rajalakshmi, 2020), Raman spectroscopy evaluation of prepared carbon materials from various biomass is provided. As the graphitic phase of carbon conducts electricity, but the diamond phase does not therefore more graphitic phase (carbon's conducting phase) means less resistance when charging and discharging and this property of the material can be found using Raman Spectra.

4.1.6 FTIR

FT-IR stands for Fourier transform infrared, the preferred method of infrared spectroscopy. Light is known to be absorbed by chemical functional groups at certain frequencies. Thus, the chemical structure may be deduced from the observed frequencies. FT-IR spectrometer, measures the frequencies at which the sample absorbs the radiation as well as the intensities of the absorptions. The interaction of a single beam of un-dispersed infra-red radiation with a sample is recorded using an FT-IR spectrometer. Therefore, during an infrared spectroscopy experiment, when radiation is allowed to pass through a material. A portion of the infrared light is taken in by the sample, while the remaining portion is either reflected or transmitted. The spectrum that was produced as a consequence forms a molecular fingerprint by depicting the absorption and transmission of the sample's molecules. In the same way that no two fingerprints are exactly same, no two unique arrangements of molecules generate the same infrared spectrum. As a consequence of this, infrared spectroscopy may be applied to a wide number of different types of studies (Thermo, 2013). The FT-IR identifies the unknown materials in a sample, determines the quality and consistency along with the number of components in a mixture.

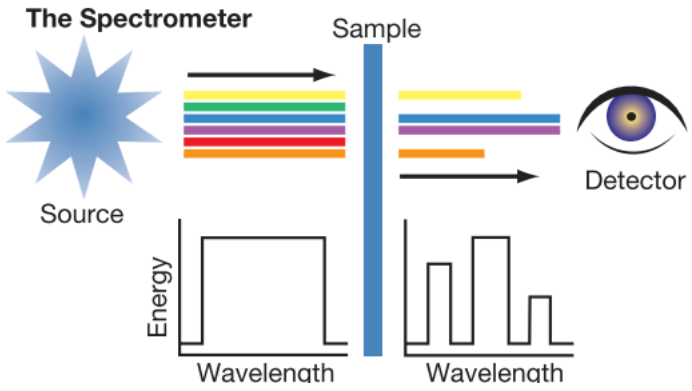

Figure 47 Spectroscopy

4.2 Techniques for Electrochemical Analysis

4.2.1 Cyclic Voltammetry (CV)

Cyclic voltammetry tests supercapacitor nanocomposites and is a rapid screening method for capacitor materials. This method studied electrode film materials (primarily carbons and CNT composites). CV involves cycling an electrode's voltage and measuring the resulting current. Working, reference, and counter electrodes make up the electrode system. To perform CV, electrolyte, reference, and three electrodes are added to an electrochemical cell. Then, a potentiostat linearly sweeps the potential between the working and reference electrodes until it hits a predefined limit. The changing current between the working and counter probes is measured in real time. Cyclic voltammograms are duck-shaped plots (Compton & Banks, 2007) .

During CV testing, the voltage is swept between two values at a fixed scanning rate (s = dV/dt), which measures the rate of change in voltage per unit of time.Throughout the course of this scan, time-varying current (I) is captured. The form of the current-voltage curve (CV) in a perfect EDLC is rectangular, which demonstrates that current is independent of potentialThe formula C = I/s provides the capacitance. Non-ideal EDLCs and pseudocapacitors have distorted CV shapes. I(t) is a function of time in these conditions, and C is defined by:

$$\boldsymbol{C_S} = \int \mathrm{IdV/SmV} \qquad (4.3)$$

Where I represents the average current, ΔV represents the voltage window, S represents the scan rate in mV/s, and m represents the total mass of active material in the electrode.

It is simple to calculate cycle life using CV, which is one reason why it is regarded as a major instrument for evaluating the performance of SCs. Another reason is that internal resistance effects and dissipative losses may be found using an analysis of the voltammogram morphologies as a function of s.

For a reversible electrochemical process, the CV of SCs should be rectangular, but the CV of faradaic capacitors is curved with anodic and cathodic peaks, as illustrated in the image below (Rajendran, Naushad, Raju, & Boukherroub, 2019):

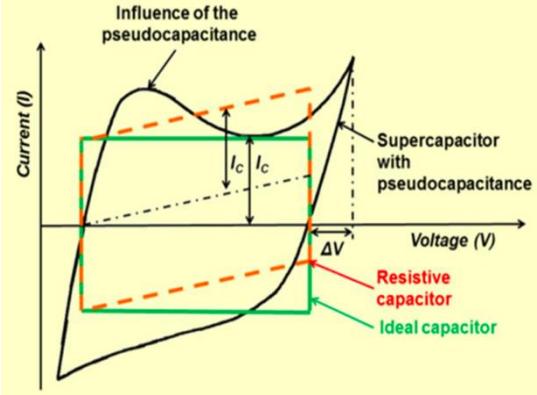

Figure 48 Diagram of typical electrochemical capacitor showing the difference between static capacitance (regular) and faradiac capacitance (curved)

4.2.2 Galvanostatic Charge-Discharge

Galvanostatic charge-discharge technique is used to examine a specific capacity under regulated current settings and to gauge the performance of materials and cells. In this approach, the potential response is calculated as a function of the applied current, which is constant in value and independent of time. In three electrode system the constant current is applied across working and counter electrodes in order to measure relative potential. The charge build-up (Δq) happens at the interface between a solid electrode film and a liquid electrolyte when a constant current (i) is supplied over a certain time period. This process leads in potential variations (ΔV) across interference during the time period.

$$C = \int i.dt / \Delta V \qquad (4.4)$$

$$C = \Delta q / \Delta V \qquad (4.5)$$

Where Δt is the given time to touch the particular potential and Δq = = ∫i.dt. As per above equation the capacitance value C should be determined by ΔV as other two values are fixed. It acts similarly to ideal double-layer ECs (EDLC), in which charge accumulation is driven by electrostatic attraction (non-faradaic) and perfect polarization. Therefore ΔV changes linearly for fixed current supply throughout the interval time Δt(Bard & Faulkner, 2001).

The specific gravimetric capacitance Csp using the discharge curves is calculated using

$$Csp = (I \times \Delta t) / (\Delta V \times m) \qquad (4.6)$$

where I is the applied current, t is the CD discharge time, V is the potential, and m is the active material mass (MOHD ABID et al., 2020).

4.2.3 AC Impedance Spectroscopy (EIS)

Alternating current electrode operations serve as the basis for the method known as electrochemical impedance spectroscopy (EIS). It is possible to cause a disruption in the electrochemical systems by providing an alternating signal with a tiny amplitude (between 5 and 10 millivolts) in order to get a linear response and then watching how the electrode recovers to its initial stationary condition(Negroiu, Svasta, Pirvu, Vasile, & Marghescu, 2017).Electrochemical impedance spectroscopy (EIS) is to understand the interfacial behaviour of electrochemical systems by performing diagnostics on processes like corrosion. Electrochemical interfacial behaviour in supercapacitors (including ohmic resistance, charge transfer resistance, interfacial charging, mass transfer, and diffusion control) may also be evaluated in this way. As supercapacitors consists of two porous electrodes, electrolyte and a separator therefore the functional groups on the electrode's surface do react with the electrolyte, resulting in reaction products that clog part of the electrode's pores as it ages. Gaseous reaction products may also raise the device's internal pressure, which can cause fractures in the electrodes and reduce the electrolyte's ability to reach those areas thus the capacitance is reduced and the equivalent series resistance is increased (ESR). Impedance spectroscopy (IS) in a broad frequency range is employed because it is non-destructive to the examined material and has a reasonably easy measurement approach(Oz, Hershkovitz, & Tsur, 2014).

In accordance with the Gouy-Chapman model, the Helmholtz double layer is more accurately described as a multiple layer (Fig. 49.). This multiple layer consists of a Helmholtz internal double layer (PHI) located at the interface between the electrode and the electrolyte solution, a Helmholtz external double layer (PHE) in which solvated but that is not absorbed, and a diffuse layer that is an area that extends to the mass of the solution. Each of these layers is located at the interface between the electrode and the electrolyte solution. At the contact between the electrode and the electrolyte solution is where you will find the ions that have been adsorbed.

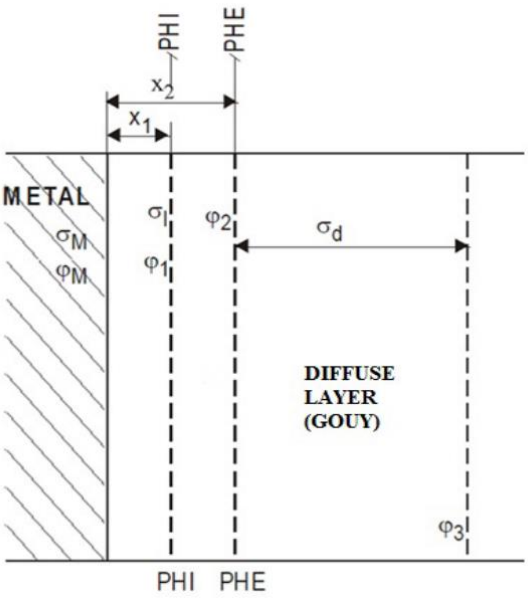

Figure 49 The model of Gouy-Chapman

Randles' equivalent circuit, shown in Fig. 2, may be used to represent a supercapacitor using the Gouy-Chapman model. The faradaic method and double-layer capacitance are combined in this circuit.

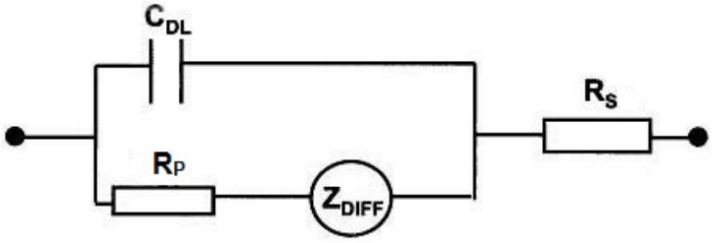

Figure 50 The equivalent circuit for modeling supercapacitor

In above circuit C_{DL} is the capacitance of double layer, R_p is the charge transfer resistance, Z_{DIFF} is the Warburg diffusion impedance and Rs is the resistance of electrolyte solution.

EIS is performed at the open circuit voltage (OCV) and implemented usually in a potentiostat and involves superimposing a low-amplitude (5-10 mV) sinusoidal signal over a direct current (DC) voltage and measuring the resultant alternating current's magnitude and phase angle. Thus, the resultant impedance is often shown as a complex quantity as shown below(Negroiu, Svasta, Ionescu, & Vasile, 2017):

$$Z(\omega) = Z'(\omega) + jZ''(\omega) \qquad (4.7)$$

The EIS data may be shown as a complicated Nyquist plot plane. Plotting the real component Z' and the imaginary component Z" of the impedance in the complex plane, with Z' on the x-axis and Z" on the y-axis, respectively, yields a route (hodograph) with the frequency as a parameter. A supercapacitor and an ideal capacitor linked in series with a resistance are shown in Fig. 49 as a typical Nyquist plot.

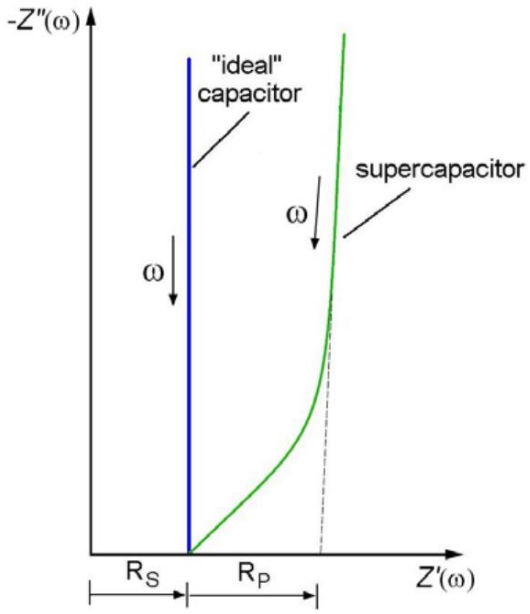

Figure 51 Nyquist impedance plot of an ideal capacitor in series with a resistance Rs and a typical supercapacitor. The Rp value results from the restricted motion of ions(Negroiu, Svasta, Ionescu, et al., 2017)

In (Vicentini et al., 2019), the equivalent series resistance (ESR) can also be obtained using galvanostatic charge discharge method as well. At frequencies over 10 kHz, the equivalent circuit model does not affect the values retrieved from EIS. The typical GCD technique, on the other hand, is more applicable since it more closely mimics the actual circumstances in which the device operates.

CHAPTER 5

BIOWASTES-DERIVED HIERARCHICAL POROUS CARBON AS A SUPERCAPACITOR ELECTRODE FOR ENERGY STORAGE

5.1 Experimental

Supercapacitors are still inappropriate for application in many electrical devices due to their low energy density of $0.5xCV^2$(S. Li et al., 2017). It is necessary to pay attention to both the operating potential window of the electrolyte and the capacitance of the electrode in order to increase the energy density of a supercapacitor. The materials that are used as electrodes need to have a high electrical conductivity so that electrons can be transferred, a large specific surface area so that charges can be stored, a high degree of wettability, and a hierarchical porosity so that electrostatic ions may move through and diffuse into the pores more easily (Z. Pan et al., 2022).

Carbon-based materials are frequently acknowledged as suitable materials for EDL capacitor electrodes due to their advantages of stable physico-chemical properties, variable pore structures, adequate electrical conductivity, abundance of polar functional groups, low production cost, tailorable structures, etc., and have been thoroughly researched. As compared to unsustainable and non-renewable fossil energy-based carbon, agrowaste-derived or biowaste carbonaceous materials are environmentally friendly, widely accessible, and affordable(Shah & Aziz, 2020). Many studies on the conversion of agricultural and biological waste into carbons have been published to far, and much effort has been put into adjusting the pore properties of these carbon-based electrode materials. A few examples of carbon-based agro-bio wastes electrode materials that have been shown to display adequate performance in electrochemical capacitors include coconut shell, soyabean, bamboo, egg shell, dead neem leaves, cow dung, banana peel and so forth(Sundriyal et al., 2021).

There aren't many articles on the use of watermelon peels as carbon-based supercapacitor electrode precursors, despite the fact that the amount of peels produced by watermelon during

Cyprus's yearly summer season much exceed any of the agro-wastes mentioned above. About 33–35% of watermelon fruit is peel, and this rind is often thrown away as untreated agricultural food waste. Not only does it include amino and carboxyl groups, but also the non-essential amino acid citrulline. It has been claimed that increasing the proportion of heteroatoms like N and O in a carbon network may greatly boost the material's specific capacitance, and hence these compounds include both N and O(Omar et al., 2022).

In (Pei Zhang et al., 2021), used a green chemical activation process to create porous carbon made from watermelon peel that is hetero-atom-doped. The symmetrical device has a specific capacitance of 226 F g^{-1} in a 1 M H2SO4 solution, and the doped electrode has a specific surface area of 1660 m^2 g^{-1}.

Watermelon peel is used in our research to create microwave-KOH activated hierarchical porous carbon. Then nitrogen and phosphorus are added to the carbon. The superior capacitance performance of carbon materials made from biomass is largely due to the integration of trace elements like nitrogen and phosphorus into carbon materials during the carbonization process. It is anticipated that nitrogen will improve the capacity of carbon-based materials to conduct electrons. Materials containing phosphorus may be able to raise the electronegativity of carbon, raising the hydrophilicity of carbon materials, by joining lone pair electron nitrogen with carbon (J. Zhou et al., 2020).

This method improved the electrochemical performance of the P-N dual doped porous carbon. The electrochemical performance of the electrode was investigated in electrolytes of 1 M H2SO4, 1 M Na_2SO_4, and 6 M KOH. The specific surface area of the related symmetrical supercapacitor was nearly 0.9 times that of (Pei Zhang et al., 2021), and its specific capacitance was noticeably higher.

In this research we made the discovery that co-doping the electrode with heteroatoms (N and P) not only changes the morphology and surface characteristics of the electrode, but it also creates pseudocapacitive, which boosts the performance of the electrode. The use of a circular economy strategy may result in the production of carbon-based electrode materials, which is a potential outcome of our study.

In this section the experimental details, material characterisation details and electrochemical performance of doped watermelon (WC)-based electrodes for supercapacitors are provided along with the results.

5.1.1 Materials and reagents

All reagents used in this research were analytic standards and purchased from Sigma-Aldrich in United Kingdom. Watermelon peels were gathered, chopped, and then dried in the sun for three days.

Diluted HCl (37%) in addition to acetone, ethanol, acetylene black, 98.8% sulfuric acid, melamine (an N dopant supplier), polyphosphoric acid (a 99.9% P dopant source and microwave absorber), a 60% polytetrafluoroethylene binder, and electrolytes (acidic: H2SO4, neutral: Na2SO4, and basic: KOH) was also used.

In this experiment, a typical two-step pre-carbonization and microwave-KOH activation procedure were used (Scheme 1). Various KOH concentrations (0.5–2.5 g), dopant doses (1-3 g), microwave powers (300–1000 W), and irradiation times (five to thirty minutes) were investigated in early testing; however, only the best outcomes are provided here in this thesis.

5.1.2 Preparation of watermelon peel-derived N, P-dual-doped porous carbon

These sun-dried watermelon peels were further dried for 12 hours, in an oven at 85^{o}C to eliminate all moisture before being crushed to a coarse powder in a laboratory grinder. The powdered peel was pre-carbonized for 120 minutes at 300^{o}C in a muffle furnace (5^{o}C min^{-1}). After that, doping and chemical activator reagents were added to the pre-carbonized sample and it was microwave irradiated. 25 mL of polyphosphoric acid (1 M), 5 g of pre-carbonized watermelon peel, and 0.85 g of KOH were combined in a 200 mL conical flask and stirred at 200 rpm for 1 hour at room temperature. After 1 hour of agitation, the aforesaid combination was added to 1.2 grams of melamine dissolved in 20ml of hot distilled water and again agitated for another 1 hour. The ingredients were then microwaved at 850 W for 25 minutes. It was estimated that the temperature at this point likely reached approximately 900 degrees Celsius. In order to remove any remaining contaminants, the resultant black slurry was washed with 0.5 M HCl, acetone, and an ethanol-distilled water combination until the pH of the filtrate was neutral, and then dried in an oven at 60^{o}C for 24 hours. Dual-doped watermelon-based porous carbon (NPW) is distinguished from single-doped N (no polyphosphoric acid) or P (no melamine) samples, which are denoted NW and PW.

Scheme 1 steps in the preparation of N,P-dual doped watermelon peel-derived porous carbon

5.1.3 Structural characteristics

The morphologies and elemental compositions of the samples were examined using a Zeiss Supra 35VP EDX-coupled scanning electron microscope from Germany. The 3Flex surface analyzer from Micromeritics Instrument Corp. was used to examine the surface area and pore structure. Using a Bruker X-ray diffractometer and a Thermo Fisher X-ray photoelectron spectrometer, respectively, crystal structure and elemental composition data were acquired.

5.1.4 Working electrode preparation

A 5 mm glassy carbon electrode was cleaned with deionized water and then polished with 0.05 mm alumina powder. It was swirled constantly in deionized water and ethanol for five minutes so that any traces of alumina that may have been left on the surface of the glassy carbon electrode could be removed.. 5 mg of active material (NPW or NW, PW) was disseminated in 10 ml of N- methylpyrrolidone with 5 wt.% acetylene carbon black and 5 wt.% PTFE binder, then sonicated for 1 hour to obtain a homogeneous slurry-like suspension. Before using the working electrode, a 10 µl slurry solution was applied to a glassy carbon and dried it for 12h under a vacuum at 80^{o}C.

5.1.5 Electrochemical measurements

The capacitance characteristics of the watermelon-based doped porous carbon samples that were used as supercapacitor electrodes were investigated with the use of a three-electrode setup so that the electrochemical performance of the samples could be evaluated, as well as their potential applications in the field (potentiostat/galvanostat-Sensit Smart, PalmSens BV, The Netherlands). A Pt foil was used as the counter electrode, a Hg/HgO was used as the reference electrode in KOH, and Hg/Hg2SO4 was used in the acidic and neutral electrolytes. The electrolyte solution was purged in nitrogen for 20 minutes before to each electrochemical test. The galvanostatic charge/discharge cycles (GCD, current density of 0.5–10 A g–1) and cyclic voltammetry (CV, scan rates of 50 – 200 mV s–1) tests were conducted with a potential window of –0.2 V to 0.75 V (a partial negative voltage was used to prevent the carbon electrode from oxidizing in the acidic electrolyte) and EIS tests was done at a frequency window of 0.1 Hz to 100 kHz with an amplitude of 0.005V and 0V DC bias. Finally, the electrochemical stability was evaluated by cycling 1–20 A g–1 over 10000 cycles under GCD. The current collector for the symmetric cell was a graphite-coated stainless steel (316 L) foil with a thickness of 20 mm and a mass loading of 5 mg WC-based material per active area manufactured by Redoxme Ab (Sweden). Coating the WC-based electrode material homogeneously mixed with PTFE binder onto the current collectors separated by porous cellulose film separator in presence of electrolytes to determine the commercial application and performance of the developed electrode materials in a 2-electrode STC20-split flat cell was used to assemble the symmetric solid-state device (MTI Corp., USA).

The specific capacitance of the 3-electrode system was calculated using Eq.1, taking into consideration the mass (m) of the electroactive materials, the response current (I), the discharge time (t), and the potential window (Vf –Vi) from the GCD curves.

$$C_{\text{sp,electrode}} = \frac{\Delta t \; X \; I}{(Vf - Vi) x \; m} \qquad (1)$$

Equations 1-4 were used to get the specific capacitance (F g-1, Csp), energy density (Wh kg-1, E), and specific power (W kg-1, P) of a symmetric supercapacitor for a two-electrode system.

$$C_{\text{sp,cell}} = \frac{4 \times (\Delta t \times I)}{(Vf - Vi) \times m\text{total}} \qquad (2)$$

$$E_{cell} = \frac{C_{sp,cell} \times V^2}{2 \times 3.6} \quad (3)$$

$$P = \frac{1}{\Delta t} \times E_{cell} \times 3600 \quad (4)$$

The symmetric device's columbic efficiency (%,η) was calculated using Eq.5, where c_t is the charging time

$$\eta = \Delta t/(c_t) \times 100\% \quad (5)$$

5.2 Results and discussion

5.2.1 Characterization results

As demonstrated in Fig. 52a–c, the SEM images exhibit a honeycomb-like structure with interconnecting disordered pores that contain dopant particles embedded in them as well as sharp uneven edges. PW has a rougher surface with fewer apparent pores than NW and NPW. The NPW, in contrast to the NW and PW, exhibits scale-like mesopores/micropores at the edges and more wide pores overall, which will facilitate the diffusion of electrolyte ions into the inner cavity of the electrodes and serve as locations for charge storage, resulting in a high specific capacitance and high-rate capability. According to EDX mapping, the oxygen, phosphorus, and nitrogen heteroatoms are evenly distributed throughout the carbon matrix. The elemental analysis' findings, which are shown in Table 1, demonstrate that NPW had nitrogen and phosphorus concentrations of 5.1 and 5.8 at%, respectively.

Fig. 52d displays the FTIR spectra of NPW, NW, and PW. In all of the materials, the acute peaks approximately found at 1676 cm^{-1} are related to the C=Y (where Y = O, N, or C) stretching vibration, whereas the wide band visible at 3355–3449 cm^{-1} relates to O–H stretching vibration due to physically absorbed water, including surface hydroxyls. N-H stretching vibration may be attributed to the shoulder peaks at 3218 cm^{-1}. Keep in mind that these peaks are easier to see in NW and NPW than in PW. In phenolic, lactone, and ether carboxyl structures, the bands at 1316-1163 cm^{-1} are responsible for the O-H bending and C-O stretching modes, while the tiny bands at 1070 cm^{-1} are responsible for the C-N bending. Both the PW

and NPW spectra's bands at 1065-962 cm^{-1} correspond to the stretching P-O/P=O/P=OOH vibration modes, whereas the doublet at 705-598 cm^{-1} corresponds to the bending O-P-O mode.

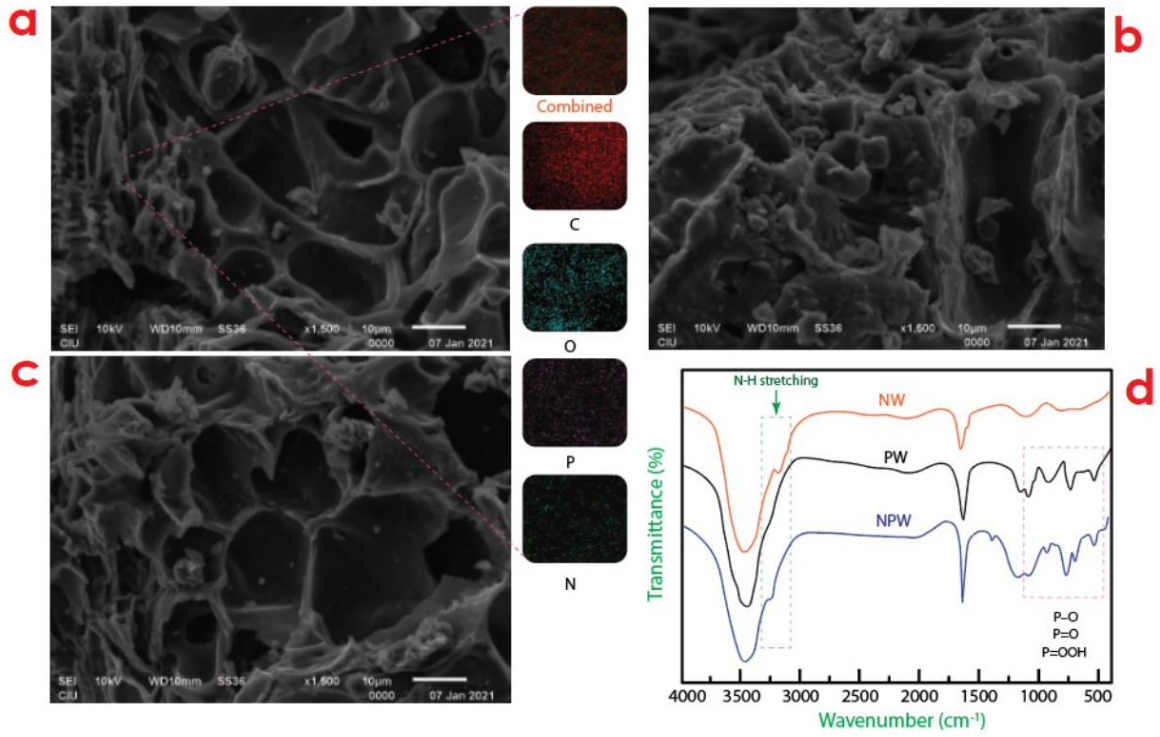

Figure 52

XPS was used to perform more study on the elemental compositions of NPW, and the spectrum reveals the coexistence of carbon, phosphorus, oxygen, and nitrogen elements, which is compatible with the results of the EDX. As shown in Figure. 53a, the complete scan spectra of all the samples displays two distinct peaks at around 285 eV and 531 eV, which are associated with the elements carbon and oxygen, respectively. The P2p (phosphorus) and N1s (nitrogen) peaks in NW and NPW at 133 and 400 eV, respectively, serve as evidence of the existence of heteroatoms. Four peaks with binding energies of 398.7, 400.4, 401.6, and 403.4 eV are produced by further deconvolution of the high-resolution N1s peak, and they correspond to pyridinic (N-6, 25.9%), pyrrolic (N-5, 56.8%), graphitic (N-Q, 13.2%), and oxidized nitrogen bonds (N-Y, 4.1%), respectively (Figure. 53b). Pyridinic and pyrrolic N may add additional capacitance by faradic redox reaction, and N-Q can speed up the rate of electron transport to the surface of porous carbon materials, increasing specific capacitance.

The P2p spectra of phosphorus, as shown in Figure. 53c, deconvoluted into two peaks at 132.5 and 133.7 eV, which are associated with the P-C/P-N and P-O bonds, respectively, and show

the formation of phosphorous species (Ramasahayam, Hicks, & Viswanathan, 2015). The NPW C 1s spectra shown in Fig. 2d has four peaks at 284.6, 285.7, 286.1, and 288.5 eV, which, respectively, correspond to the C-C, C-P/C-N, C-O, and C-O/C-N. The C-N/C-N/C-P has been proven in earlier investigations (Q. Zhang et al., 2022) to modify the carbon charge balance by increasing surface wettability and providing active sites for the pseudocapacitance characteristic. O-IV, chemisorbed oxygen of water or carboxylic groups, is represented by peaks with binding energies of 531.7 eV (P=O or C=O (quinone, O-I)), 532.9 eV (carbonyl, O-II; P-O-C or C-O-C/C-OH), 535.3 eV (ether), and 537.2 eV (O-IV, P-O-C or C-O-C/ The contact between the electrolyte and electrode may be made easier by these chemical linkages, which may also improve the surface-wetting capabilities of electrode materials. One of these oxygen roles is the induction of pseudocapacitance by quinone groups in the carbon matrix via redox processes (Gladvin, Sudhaakr, Swathi, & Santhisri, 2017)

In general, the presence of heteroatom groups may effectively boost the surface hydrophilicity of carbon materials. More importantly, the N and P enhance the electrochemical performances of the produced NPW by contributing pseudocapacitance during charge-discharging operations. It is noted that each atom's concentration in the electrode material fluctuates after peak deconvolution. PW showed lower amounts of both (0.9 at% quinone-based oxygen and 0.4 at% pyridinic nitrogen) than NW, which had greater quantities of quinone-based oxygen (1.9 at%) and pyridinic nitrogen (2.4 at%). Aside from having the greatest quantities of quinone-based oxygen (3.3 at%), ideal pyridinic nitrogen (2.1 at%), and high pyrrolic nitrogen (2.8at%), NPW also has the best ability for storing energy.

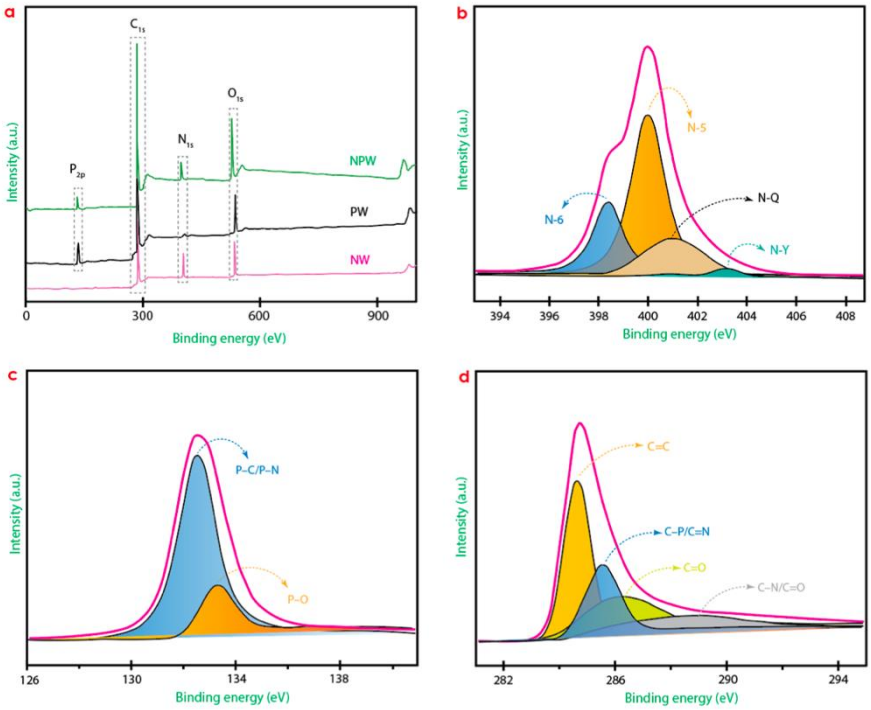

Figure 53

The XRD patterns of the electrode materials given in figure. 54a reveal two different wide peaks, the broad peaks centred at 28.3° (002) and comparatively low peaks at 2 = 47.9° (100) for all samples, which suggest disordered amorphous carbonized materials. The (002) peak for the NPW drifted to the right due to co-doping of P and N atoms, which may expand the interlayer spacing of the carbon lattice and indicate additional defects. Additionally, the lower intensity of the (100) peak in comparison to NW and PW illustrates the low degree of graphitization in NPW.

The Raman spectra may be fitted using the distinctive peaks D (1355 cm^{-1}) and G (1592 cm^{-1}) representing the disordered/defective carbon and graphitic phases, respectively as shown in figure 54b. The I_D/I_G ratio is the ratio of the intensity measurements of the two peaks, which is often used to determine the level of disordered or faulty carbon. The inclusion of P and N atoms in NPW resulted in further defects, according to the I_D/I_G values of the NW, PW, and NPW, which are 0.909, 0.842, and 0.917, respectively, which is consistent with the XRD result.

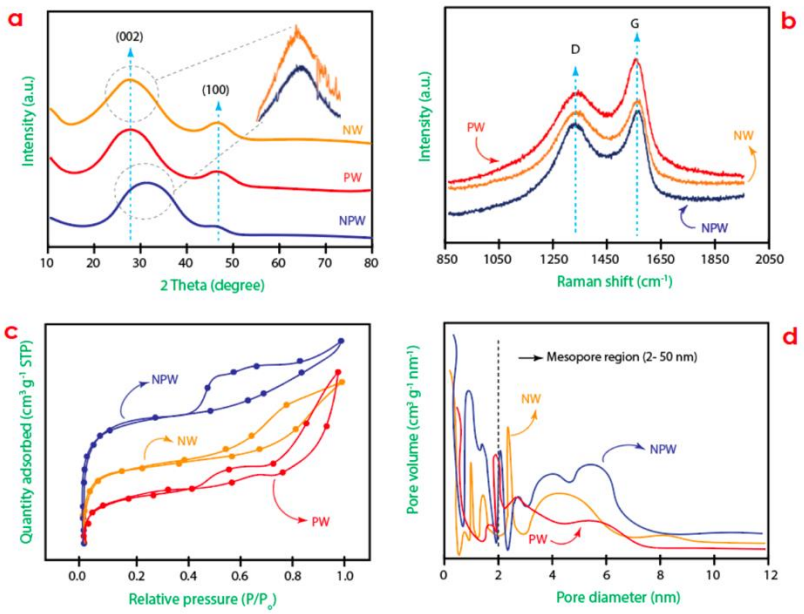

Figure 54

To learn more about the porous characteristics and specific surface area of the as-prepared WC, refer to Fig. 54c, which also displays the N_2 adsorption-desorption isotherms and pore size distributions. The existence of micropores (<2 nm) was observed at low pressure ($P/P_0 < 0.06$) in all of the samples. Additionally, a type IV isotherm with an apparent hysteresis loop ($0.5< P/P_0< 0.96$), which could point to the existence of mesopores, is realized at (2–50 nm). The specific surface area and pore volume of the samples are presented in Table 1. It is clear that mesoporous structures contributed the majority of the overall pore volume, with modest support from microporous structures. In contrast to micropores, which may often result in large specific surface area, mesopores enhance ions transfer from the bulk electrolyte by reducing the diffusion distance at the electrode and electrolyte interface (Ping Zhang, Liu, & Liu, 2020). The ratio of mesopore volume to micropore volume fell from 6.87 to 4.05 for NW and NPW, respectively. The mesopores are believed to have been produced by micropore widening during the KOH thermal activation procedure (C. Wang et al., 2013). Furthermore, Zhang et al.(Ping Zhang et al., 2020) determined that adding a dopant like phosphoric acid to the precursors might promote the emergence of micropores and enlarge the openings to create mesopores in the carbon materials produced as a consequence of the carbonization process. NPW has the greatest specific surface area (1809 m^2 g^{-1}) in comparison to NW and PW, which may be partially attributable to the occurrence of micropores. According to the pore size distribution curves, the three materials exhibit a hierarchical pore structure with micropores and substantially more mesopores (Fig. 54d).

5.2.2 Electrochemical performance of doped WC-based electrodes in the 3-electrode system

To test the capacitance performance of the electrode materials, several electrolytes were used. The CV curves of all samples had quasi-rectangular shapes with observable humps about 0.05–0.2 V when scanned at 50 mVs-1 in 1 M H2SO4 (figure. 55a). The presence of humps at the electrode interface is a characteristic of Faradaic redox reactions between the saturated electrolyte ions at the interface and electrochemically active functional groups (such as N, O, and P heteroatoms) in WCs [2,3, 20–26]. This proves that double-layer capacitance and pseudocapacitance both contribute to total capacitance. Due to the synergistic effects of the greatest specific surface area (1809 m2 g-1), an optimum amount of N, P-co-doped heteroatoms, and higher proportions of mesopores, the CV curve of NPW exhibited the largest loop in comparison, indicating the maximum capacitance of all the electrodes.

Further research reveals quasi-rectangular CV curves in aqueous solutions of 6 M KOH and 1 M Na_2SO_4 that are comparable to those in 1 M H_2SO_4. Compared to NW and PW, the basic and neutral electrolytes exhibit somewhat greater aberrations in the CV curves of NPW, but no noticeable humps.

The NPW material had the greatest specific capacitance in the H_2SO_4 medium, which was 498.8 F g–1 (Table 5). This is not only because of the faster mobility of solvated electrolyte ions (H+) in H_2SO_4 (size: 2.79 A°, conductivity at 25°C: 351 S cm^2 mol^{-1}) than in K+ (3.30 A°, 73.4 S cm^2 mol^{-1}) and Na+ (3.57A°, 56.3 S cm^2 mol^{-1}), but also because of its significantly higher ionic conductivity and acidic ions' stronger tendency to react with.

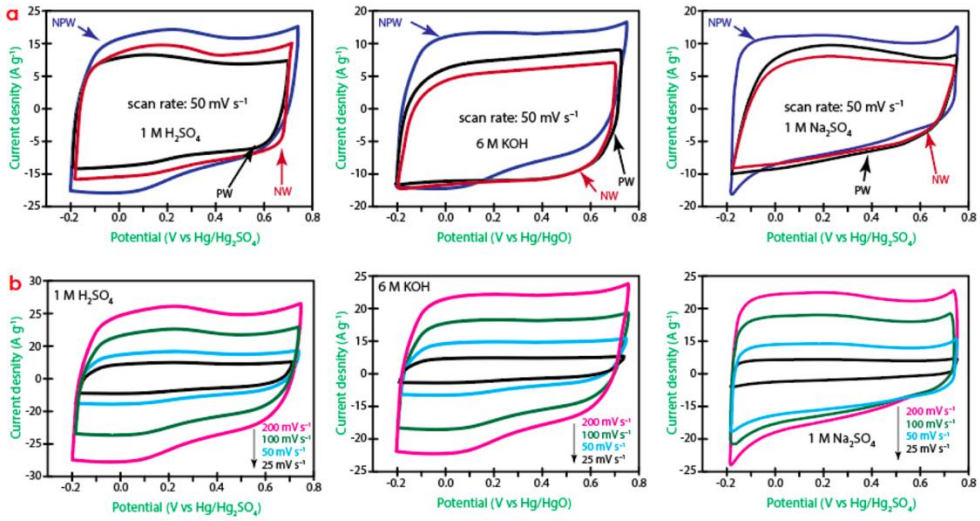

Figure 55 Electrochemical properties of NPW, NW and PW a) CV curves in different electrolytes b)CV curves of NPW at various scan rates (25-200 MVs^{-1}) using 3-electrode setup

In the acidic electrolyte, NW shows a higher current density compared to PW (0.9 at% quinone-based oxygen and 0.4 at% pyridinic nitrogen), suggesting a redox reaction associated to high quinone-O concentration (1.9 atom%) and pyridinic nitrogen (2.4 atom%). Higher nitrogen and oxygen functional groups in acidic electrolytes generate not only pseudocapacitance but also an increase in EDL capacitance. NW showed a lower specific capacitance in alkaline and neutral electrolytes as a result of less quinone-type reactions in the basic medium and its smaller pore size. The increased mesopore volume of PW made it simpler for solvated large-sized cationic electrolyte (K+/Na+) ions to penetrate the carbon pore structure or get adsorbed in the outer Helmholtz layer of the electrode surface.

The CV curves of NPW in different electrolytes are shown in figure.55b at scan rates ranging from 25 to 200 mV s^{-1}. Due to increased surface and physicochemical qualities, NPW retained a roughly quasi-rectangular shape even at a high scan rate of 200 mV s^{-1}. This resulted in excellent rate performance. Although the significant Faradaic reactions of the electrode's pyridinic nitrogen, quinone oxygen, and phosphonyl functional groups in acidic electrolytes are most likely to blame for the evident distortions in H_2SO_4. Similar findings were made by who reported a little distortion of the voltammograms in the acidic electrolyte at higher scan rates but no redox wave in the alkaline medium. They ascribed this to the presence of quinone oxygen, which is electrochemically inert.

Table 5 Specific capacitances and physiochemical properties of the WC-based electrodes

Electrodes	[a]Capacitance (Fg^{-1})			[b]N_2 physisorption textural properties				[h]Elemental composition (at%)			
	Electrolytes			[c]Pore volume ($cm^3\ g^{-1}$)		Pore size (nm)	Area ($m^2\ g^{-1}$)	C	N	P	O
	H_2SO_4	KOH	Na_2SO_4	[d]V_{micro}	[e]V_{meso}	[f]D_{BJH}	[g]SSA_{BET}				
NW	396.6	298.8	294.7	0.093	0.334	1.89	1659	80.9	9.7	2.3	5.6
PW	374.7	312.6	315.9	0.056	0.385	1.98	1583	82.1	1.4	10.7	4.9
NPW	498.8	412.3	398.6	0.078	0.397	2.56	1809	81.3	6.7	7.1	4.1

a: Current density is 1 Ag^{-1}.
b: Sample mass is 0.15 g, a direct non-linear fitting used based on at least 5 data points.
c: P/Po = 0.75 was used to compute the total pore volume of the sample.
d: The Dubinin–Radushkevich equation was used to calculate the micropore volume.
e: V_{micro} was subtracted from total volume to get the mesopore volume.
f: BJH equation was used to obtain the average pore size from the desorption data.
g: Brunauer–Emmett–Teller (BET) area.
h: Extracted from the Energy-dispersive X-ray (EDX) spectroscopy. At% of other elements not tabulated.

The remarkable electrochemical performance of the NPW electrode was confirmed by GCD measurements at 1 Ag^{-1} in a variety of electrolytes. The findings are shown in figure. 56a. Instead of a fully symmetrical triangle, the GCD curves in acidic and neutral electrolytes exhibit somewhat asymmetrical triangle-like shapes, which indicate the existence of pseudocapacitance **.**In 6 M KOH, NPW displayed normal EDL capacitor behaviour. According to the findings of the CV, NPW had the largest specific capacitance and the longest discharge

periods of any electrode in any of the electrolytes, which is consistent with those results. The NPW electrode, in particular, has a discharge duration of around 8 min, which is longer than that of the NW electrode (6.3 min) or the PW electrode (5.9 min) at 1 Ag^{-1}.

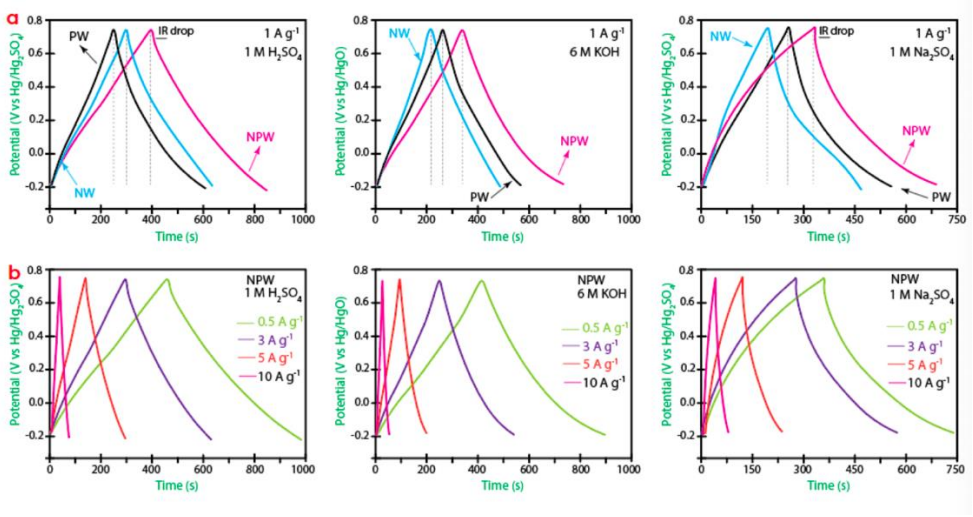

Figure 56 (a) GCD curves of NW,PW and NPW in different electrolytes at 1 Ag-1 (b) GCD curves of NPW in different electrolytes and current densities.

The specific capacitances of WCs were examined at different current densities (figure not shown), and it was discovered that they decreased as current density increased. As current density rises, the specific capacitance decreases because the electrolytes do not have enough time to fully diffuse into the electrode pores and carry out redox processes. Low total specific capacitance is the consequence of the EDL capacitance and pseudocapacitance being greatly lowered at high current density. Additionally, the GCD curves of NPW in different electrolytes at varying current densities were studied (0.5–10 A g^{-1}). Figure.56b demonstrates that NPW retained its quasi-triangle shape and had low internal resistance even at high current densities. This is probably because of the necessary amount of micro/mesopores and pseudocapacitance provided by enough N and P heteroatoms.

In comparison to the KOH electrolyte, the electrodes exhibited a greater internal resistance proportional to the electrode resistance (Rel), as shown by the minor IR decrease in acidic and neutral electrolytes, which is consistent with the EIS findings (see Nyquist plots).

In addition, IR drop was analyzed in 1 M H2SO4 at varying current densities for each electrode sample. NPW has less resistance than NW and PW, which is helpful for real-world applications, as seen in figure 57. In addition, the slope of the curve indicating the lowest internal direct current resistance reveals that NPW has a great capacity for ion diffusion in the electrolyte.

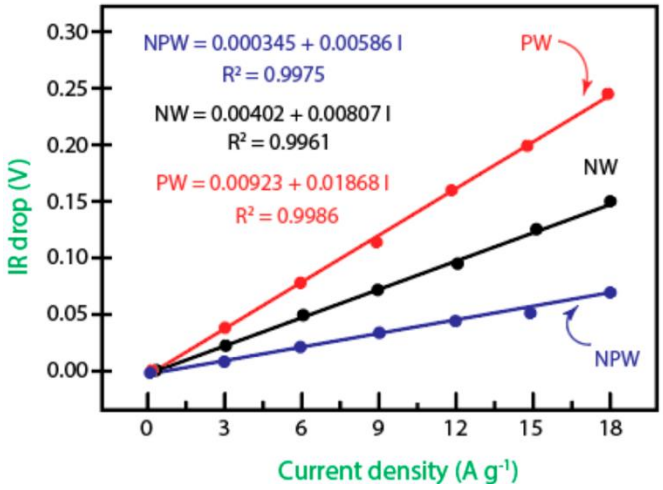

Figure 57

The NPW electrode's cyclic stability was evaluated. The results show that it has excellent cycle stability and strong specific retention. The NPW electrode maintained capacitance of 96.9%, 95.5%, and 94.9% during 10,000 GCD cycles in 1 M H_2SO_4, 6 M KOH, and 1 M Na_2SO_4 at a current density of 10 Ag^{-1}, respectively (figure.58a–c).

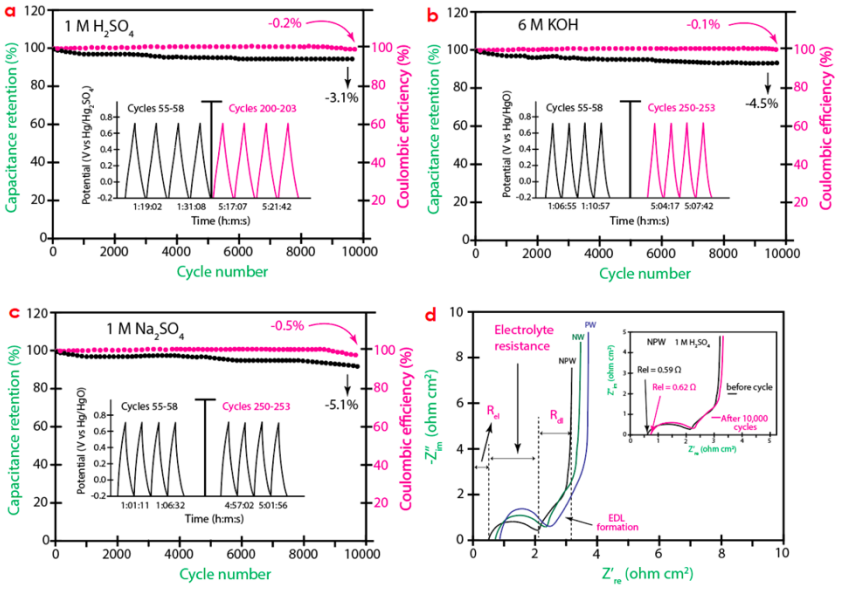

Figure 58 a-c) At a given current of 10 Ag^{-1}, cycling performance of the electrodes in different electrolytes (d) The electrode's Nyquist plots in 1 M H_2SO_4 (Inset: EIS plots of NPW before and after 10,000 cycles).

In addition to its high rate capacity, the NPW electrode offers a high average columbic efficiency of 99.7 percent. The size of the totally solvated electrolyte ions is related to the observed trend of capacitance retention. During discharging, the bigger hydrated ions, such as Na+ and K+, migrated quicker into the bulk electrolyte and returned to the electrode-electrolyte interface at a slower pace than the solvated H+ ion. After several cycle operations, the

micropores or mesopores of the electrode material may get clogged or collapse, resulting in a gradual reduction in capacitance retention. As a consequence, the kinetics of ion transit and adsorption may be retarded, and the capacitance may be diminished.

The EIS supported the GCD cycle results for the electrode materials. The electrolyte transportation process at and inside the electrode was examined using the Nyquist plot, which displays the electrode, bulk electrolyte, and diffuse layer resistances. The semicircles' width, which represented bulk electrolyte resistance (R_{∞}), non-vertical lines at intermediate frequencies, and almost vertical lines at low frequencies were all visible in the Nyquist plots (Figure. 58d), which are typical of porous carbon electrodes (provides information regarding the electrode capacitive behaviour). Real axis intercepts in the high- and intermediate-frequency regions were used to compute the resistances of the electrode (R_{el}) and diffuse layer (R_{dl}), respectively. The research showed that the electrode resistances (R_{el}) were negligible and did not substantially vary between the three electrodes in any of the electrolytes. The fact that the electrodes were created from the same precursor and were almost similar, but for the dopant, supports this. It's important to note that the basic medium had the lowest R_{el}, which may be related to KOH's inclusion of electrochemically inert quinone oxygen. This discovery is also consistent with KOH's GCD profile.

In addition, when all electrolytes are included, the R_{el} values are tiny compared to R, which was the most significant contributor to the internal resistance (R_{el} + R_{∞}). In addition, the R_{∞} value of NPW in the acidic medium (figure.58d) was much less than in the 6 M KOH and 1 M Na_2SO_4 media (Fig.59a). This is because 1 M H_2SO_4 has the highest ionic conductivity and the lowest solvated ion size. Also, the R_{dl} changes dramatically across the three electrodes in various electrolytes, which may be attributed to variances in pore structure and pore volume. Compared to PW (0.72Ω cm^2) and NW (0.68Ω cm^2) in 1 M H_2SO_4, NPW's electrode resistance of 0.59Ω cm^2 was the lowest (Table 6). NPW has a lower electrode resistance than nitrogen/sulfur-co-doped bamboo-based carbon (0.88Ω cm^2).animal bone-derived porous carbon (0.65Ω cm^2), agro-waste lemon peel-based carbon (LPC-700, 3.25Ω cm^2), and dead leaves-derived porous carbon (2.67Ω cm^2).

As seen in Table 6, the bulk electrolyte resistance reduces as the electrode conductivity rises. NPW has a R∞ of 2.26Ω cm^2, which is smaller than PW's (2.37Ω cm^2) and indicates that it is less conducting. The linked micro- and mesopores were appropriately concentrated in NPW, which is in accordance with (Mishra & Kant, 2020) **results**. NPW also had the lowest R_{dl}. The researchers found that mesopores have a low resistive ion transport channel while micropores

have a greater specific surface area, both of which are critical for high energy density and quick power delivery, respectively. The least amount of time is needed to discharge all the energy from the electrode with an efficiency greater than 50%, and this relaxation time constant for NPW τ_r was shown to be 0.83 s, which is much shorter than that for PW and NW electrodes. The findings indicate that NPW has excellent capacitive properties and is ideal for low-cost portable energy storage devices. In conclusion, NPW exhibited the lowest total resistance in 1 M M H2SO4 at 3.16Ω cm2, which was lower than 6 M KOH (3.68Ω cm2) and 1 M Na2SO4 (4.12 Ω cm2). It is believed that ionic conductivity and the size of solvated electrolyte ions are responsible for the observed trend. The Nyquist plot of NPW in 1 M H2SO4 in figure.58d (inset) demonstrates that after 10,000 GCD cycles, the electrode resistance declined by only 5.2% while the overall resistance decreased by around 4%, which is consistent with the study of capacity retention.

Table 6 Parameters from Nyquist plots in the 3-electrode and symmetric cells in 1 M H_2SO_4

Electrode/symmetric cell	[a]σ_{el}	[b]D_{el}	Resistance (Ω cm^2)			[c]C_{eqdiff}	[d]τ_r
	(S/cm) ×10^{-6}	(μm)	R_{el}	R_∞	R_{dl}	(μF/cm^2)	(s)
NW	1.76	0.012	0.68	2.31	0.39	66.9	1.48
PW	1.53	0.011	0.72	2.37	0.46	65.8	1.63
NPW	2.20	0.013	0.59	2.26	0.31	73.8	0.83
NPW//NPW cell	3.04	0.021	0.69	2.19	0.28	39.3	0.69
NPW//NW cell	2.72	0.022	0.81	2.11	0.31	41.8	0.78
NPW//PW cell	2.71	0.023	0.85	2.29	0.33	40.3	0.92

a: Electrode conductivity obtained from D_{el}/R_{el}
b: Measured using a digital micrometre.
c: Calculated using $-Z_{im} = -1/2\pi C_{eqdiff} \times f$, where f is the peak frequency in the low-frequency regime.
d: Calculated by $\tau_r = 1/f_r$, where f_r is the frequency that corresponds to the imaginary capacitance's maximum value.

To determine how well the produced electrode performs in practical applications, a symmetric supercapacitor cell (NPW/NPW) was built, and its EIS in 1 MH2SO4 was evaluated (figure.59b). The total contact and material resistance, or Rs, of the NPW/NPW cell was higher than that of the NPW electrode (including a current collector and electrolyte). The NPW/NPW cell's charge transfer resistance (Rct) is larger than that of the NPW electrode, which is in line with other results.

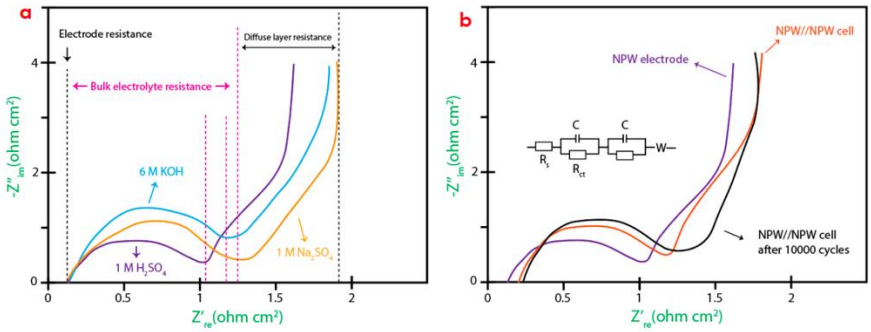

Figure 59 The Nyquist plots before and after 10,000 cycles

5.2.3 Electrochemical behaviour of NPW in a two-electrode system

A symmetric supercapacitor was made out of two NPW electrodes, and each electrode was put through its own set of tests using aqueous electrolytes consisting of 1 M H2SO4, 6 M KOH, and 1 M Na2SO4. The CV profile of the symmetric cell was investigated further by measuring it at 50 mV s–1 throughout a number of voltage windows ranging from 0.8 to 2.0 V. The CV profiles of the NPW supercapacitor cell stayed in the same rectangular shape regardless of the electrolyte. This suggests that the cell operates in a manner similar to that of a typical electrochemical capacitor (figure.60a-c). As shown in figure.9a, the anodic current in 1 M H2SO4 exhibits no detectable rise up to 1.4 V even if the potential difference has increased. In the meanwhile, when the potential was raised to 1.6 V, the anodic current rose considerably, with only a small bit of IR loss owing to electrolyte decomposition.

After increasing the potential window from 1.5 V to 2.0 V, there were no obvious anodic currents recorded in either 6 M KOH or 1 M Na2SO4, depending on the concentration. Both 1 M Na2SO4 and 6 M KOH were found to be capable of elevating the potential window of the NPW cell to about 2.0 V. These results are represented in figures 60b and 60c. When compared to the performance of certain carbons that have been co-doped with nitrogen and phosphorus, the performance of NPW cells is superior. For example, the voltage of the NPPC-700 device that (Ping Zhang et al., 2020)described couldn't be increased above 1.4 V when tested in 1 M Na2SO4. In an alkaline electrolyte consisting of 6 M KOH, (C. Wang et al., 2013) found a maximum working voltage of 1.4 V for nitrogen- and phosphorus-co-doped porous carbon. This value is comparable to the one obtained for nitrogen-doped porous carbon. Doping with nitrogen, oxygen, or phosphorus is responsible for the widening of the cell voltage produced by the heteroatoms doped carbon-based symmetric supercapacitor.

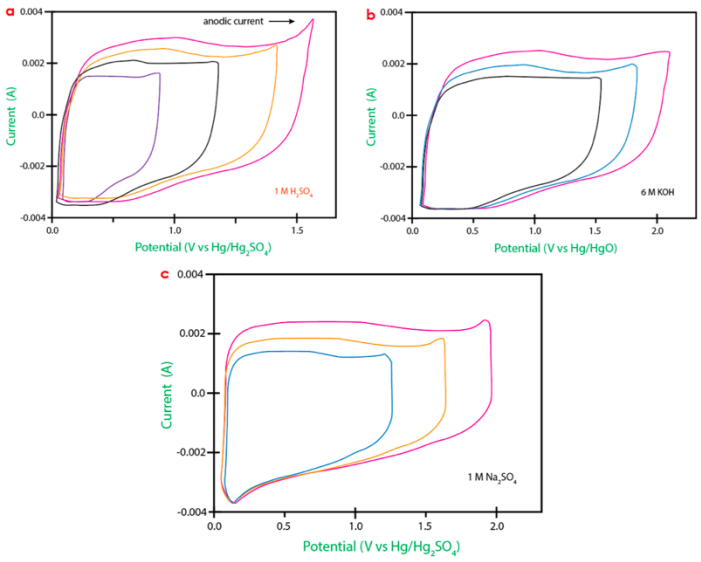

Figure 60 CV curves of NPW//NPW supercapacitor cell in different electrolytes at 50 m V S^{-1}

The results for the specific capacitance, energy, and power density of the symmetrical cell are shown in Table 7. It would seem that the cell has the highest possible specific capacitance when exposed to the acidic electrolyte. However, as a result of the broader operating voltage, the energy densities of the cell in the basic and neutral electrolytes are greater.

Table 7 Comparative performance of the as-prepared electrode materials for energy storage

Cell	Electrolyte	ΔV (V)	[a]Discharge time (s)	Csp (F g^{-1})	E (Wh kg^{-1})	P (W kg^{-1})	Ref.
NPW//NPW	1 M H_2SO_4/PVA	1.4	139.5	263.9	71.84	1853.9	
	1 M Na_2SO_4	2.0	108.9	174.8	97.11	3210.3	
	6 M KOH	1.8	117.7	189.3	85.19	2605.5	
NPW//NW	1 M H_2SO_4	1.3	124.9	239.6	56.24	1621.0	This study
NPW//PW	1 M H_2SO_4	1.3	119.8	211.8	49.71	1493.8	
PW//PW	1 M H_2SO_4	1.3	116.9	198.8	46.66	1436.9	
NW//NW	1 M H_2SO_4	1.3	109.8	178.9	41.99	1376.7	
PW//NW	1 M H_2SO_4	1.3	94.9	189.3	44.43	1685.4	
[b]$CB_{0.5}$–N,S//$CB_{0.5}$–N,S	1 M H_2SO_4	1.3	165.4	254.5	59.73	1300.0	[3]
	6 M KOH	1.8	132.4	147.1	66.20	1800.0	
[c]B_2–pC//B_2–pC	1 M H_2SO_4	1.3	155.1	238.5	55.99	1300.0	[2]
[d]PC600//PC600	BMIMBF$_4$	2.4	115.1	108.1	21.6	675.4	[55]
	1 M H_2SO_4	1.0	100.1	219.3	7.25	260.8	
[e]NPC-850// NPC-850	1 M TEABF$_4$/AN	2.6	58.7	193.0	21.2	1300.0	[56]
[f]$C_{-25\%}$ $CaCO_3$//$C_{-25\%}$ $CaCO_3$	6 M KOH	1.0	63.6	184.0	26.0	1470.9	[57]

[a] Current density is 1.0 A g^{-1}except C-25% $CaCO_3$ (0.05 A g^{-1}) and NPC-850 (0.1 A g^{-1}) from GCD.
[b] N, S co–doped chicken bone-derived biocarbon.
[c] Boron-doped sucrose-derived porous carbon.
[d] Nitrogen-doped waste pomelo peels-derived carbon.
[e] Fishbone-based nitrogen-doped porous carbon.
[f] Shrimp shell-based nitrogen-doped carbon.

CHAPTER 6

Conclusion

6.1 Conclusion

This research presents a straightforward, cost-effective, and ecologically friendly approach for synthesizing hierarchical porous carbon for use in energy storage applications. Through a KOH-microwave activation procedure, porous carbon compounds derived from watermelon peel were generated. Subsequently, the materials were doped with heteroatoms, resulting in nitrogen-, phosphorus-, and N, P-dual doped hierarchical porous carbon with outstanding supercapacitor performance (NW, PW, and NPW). NPW has the most interconnected micropores and mesopores and the largest specific surface area compared to NW and PW (1809 $m^2\ g^{-1}$). With 1 M H_2SO_4, 6 M KOH, and 1 M Na_2SO_4 electrolytes, the performance of both three- and two-electrode configurations of electrode materials was examined. In a three-electrode system, NPW exhibited an exceptional specific capacitance of 398.6 – 498.8 F g^{-1} at 1 A g^{-1} due to the optimal amount of dual active species doping, the larger specific surface area, the larger pore size, the higher conductivity, the lowest electrode resistance, and the interconnected porous structure. In addition to exhibiting extraordinary cyclic stability, the NPW-based symmetric cell produced an astounding 71.84 Wh kg^{-1} at 1854 W kg^{-1} in 1 M H_2SO_4. With a broader potential window of 2.0 V, the NPW/NPW device showed a much higher power density in 1 M Na_2SO_4 (3210,3 W kg^{-1}) than in 1 M H_2SO_4 and 6 M KOH (1 M H_2SO_4 and 6 M KOH)

REFERENCES

A.Amin Izazi, Chin-Wei Lai, Joon-Ching Juan, Siew-Moie Phang, G.-T. O. and T. C.-K. Y. (2019). Seperators for Supercapacitors. In M. I. A. and A. M. A. Inamuddin, Rajender Boddula (Ed.), *Supercapacitor Technology Materials, Processes and Architectures* (pp. 95–120). Millersville,PA 17551, USA: Materials Reserach Forum LLC.

Abbas, Q., Raza, R., Shabbir, I., & Olabi, A. G. (2019). Heteroatom doped high porosity carbon nanomaterials as electrodes for energy storage in electrochemical capacitors: A review. *Journal of Science: Advanced Materials and Devices*, *4*(3), 341–352. https://doi.org/10.1016/j.jsamd.2019.07.007

Aiping Yu, V. C. and J. Z. (2013). *ELECTROCHEMICAL SUPERCAPACITORS FOR ENERGY STORAGE AND DELIVERY FUNDAMENTALS AND APPLICATIONS*. https://doi.org/https://doi.org/10.1201/b14671

Anovitz, L. M., & Cole, D. R. (2015). Characterization and analysis of porosity and pore structures. *Pore Scale Geochemical Processes*, *80*, 61–164. https://doi.org/10.2138/rmg.2015.80.04

Anshupriya Si, Anup Kumar Misra. (2020). *Perspective on the transformation of carbohydrates under green and sustainable reaction conditions*, (R. A. Amélia Pilar Rauter, Bjørn E. Christensen, László Somsák, Paul Kosma, Ed.). https://doi.org/https://doi.org/10.1016/B978-0-12-817467-8.00001-3

Anton Paar GmbH. (2022). *How to Appropriately Characterize the BET Area of a Microporous Material*. Retrieved from https://www.anton-paar.com/corp-en/services-support/document-finder/application-reports/how-to-appropriately-characterize-the-bet-area-of-a-microporous-material/

Bard, A. J., & Faulkner, L. R. (2001). Double-Layer Structure and Adsorption. In *Electrochemical Methods - Fundamentals and Applications*.

Bardestani, R., Patience, G. S., & Kaliaguine, S. (2019). Experimental methods in chemical engineering: specific surface area and pore size distribution measurements—BET, BJH, and DFT. *Canadian Journal of Chemical Engineering*, Vol. 97, pp. 2781–2791. https://doi.org/10.1002/cjce.23632

Bello, A., Manyala, N., Barzegar, F., Khaleed, A. A., Momodu, D. Y., & Dangbegnon, J. K. (2016). Renewable pine cone biomass derived carbon materials for supercapacitor application. *RSC Advances*, *6*(3), 1800–1809. https://doi.org/10.1039/c5ra21708c

Benaouadj, M., Aboubou, A., Becherif, M., Ayad, M. Y., & Bahri, M. (2012). Recharging of

batteries/supercapacitors hybrid source for electric vehicles application using photovoltaic energy in a stand-alone point. *2012 1st International Conference on Renewable Energies and Vehicular Technology, REVET 2012*, 161–166. https://doi.org/10.1109/REVET.2012.6195264

Berrueta, A., Ursua, A., Martin, I. S., Eftekhari, A., & Sanchis, P. (2019). Supercapacitors: Electrical Characteristics, Modeling, Applications, and Future Trends. *IEEE Access*, *7*, 50869–50896. https://doi.org/10.1109/ACCESS.2019.2908558

Bokhari, S. W., Siddique, A. H., Sherrell, P. C., Yue, X., Karumbaiah, K. M., Wei, S., … Gao, W. (2020). Advances in graphene-based supercapacitor electrodes. *Energy Reports*, *6*, 2768–2784. https://doi.org/10.1016/j.egyr.2020.10.001

Borenstein, A., Hanna, O., Attias, R., Luski, S., Brousse, T., & Aurbach, D. (2017). Carbon-based composite materials for supercapacitor electrodes: A review. *Journal of Materials Chemistry A*, *5*(25), 12653–12672. https://doi.org/10.1039/c7ta00863e

Bostrom, A., Von Jouanne, A., Brekken, T. K. A., & Yokochi, A. (2013). Supercapacitor energy storage systems for voltage and power flow stabilization. *2013 1st IEEE Conference on Technologies for Sustainability, SusTech 2013*, 230–237. https://doi.org/10.1109/SusTech.2013.6617326

Brandt, A., Pohlmann, S., Varzi, A., Balducci, A., & Passerini, S. (2013). Ionic liquids in supercapacitors. *MRS Bulletin*, *38*(7), 554–559. https://doi.org/10.1557/mrs.2013.151

Breidenbach, N., Martin, C., Jockenhöfer, H., & Bauer, T. (2016). Thermal Energy Storage in Molten Salts: Overview of Novel Concepts and the DLR Test Facility TESIS. *Energy Procedia*, *99*(March), 120–129. https://doi.org/10.1016/j.egypro.2016.10.103

Burke, A., Liu, Z., & Zhao, H. (2014). Present and future applications of supercapacitors in electric and hybrid vehicles. *2014 IEEE International Electric Vehicle Conference, IEVC 2014*, 1–5. https://doi.org/10.1109/IEVC.2014.7056094

Castaings, A., Caron, H., Kharrat, H., Ovalle, A., & Vulturescu, B. (2019). Energy Storage System based on Supercapacitors for a 750 v DC railway power supply. *2018 IEEE International Conference on Electrical Systems for Aircraft, Railway, Ship Propulsion and Road Vehicles and International Transportation Electrification Conference, ESARS-ITEC 2018*. https://doi.org/10.1109/ESARS-ITEC.2018.8607725

Chae, J. S., Kwon, H. N., Yoon, W. S., & Roh, K. C. (2018). Non-aqueous quasi-solid electrolyte for use in supercapacitors. *Journal of Industrial and Engineering Chemistry*, *59*(October), 192–195. https://doi.org/10.1016/j.jiec.2017.10.023

Chandra, A., Roberts, A. J., Yee, E. L. H., & Slade, R. C. T. (2009). Nanostructured oxides

for energy storage applications in batteries and supercapacitors. *Pure and Applied Chemistry*, *81*(8), 1489–1498. https://doi.org/10.1351/PAC-CON-08-08-20

Chandrasekhar, P. (2018). Electro-Optic and Optical Devices. In *Conducting Polymers, Fundamentals and Applications*. https://doi.org/10.1007/978-3-319-69378-1_41

Chen, R., Kim, S., & Chang, Z. (2017). Redox Flow Batteries: Fundamentals and Applications. *Redox - Principles and Advanced Applications*. https://doi.org/10.5772/intechopen.68752

Chodankar, N. R., Pham, H. D., Nanjundan, A. K., Fernando, J. F. S., Jayaramulu, K., Golberg, D., … Dubal, D. P. (2020). True Meaning of Pseudocapacitors and Their Performance Metrics: Asymmetric versus Hybrid Supercapacitors. *Small*, *16*(37). https://doi.org/10.1002/smll.202002806

Choudhary, R. B., Ansari, S., & Majumder, M. (2021). Recent advances on redox active composites of metal-organic framework and conducting polymers as pseudocapacitor electrode material. *Renewable and Sustainable Energy Reviews*, *145*(July 2020), 110854. https://doi.org/10.1016/j.rser.2021.110854

Compton, R. G., & Banks, C. E. (2007). Voltammetry at Heterogeneous Surfaces. In *Understanding Voltammetry*. https://doi.org/10.1142/9789812779809_0006

Cui, G., Luo, L., Liang, C., Hu, S., Li, Y., Cao, Y., … Wang, T. (2019). Supercapacitor integrated railway static power conditioner for regenerative braking energy recycling and power quality improvement of high-speed railway system. *IEEE Transactions on Transportation Electrification*, *5*(3), 702–714. https://doi.org/10.1109/TTE.2019.2936686

Dasari, Y., Ronanki, D., & Williamson, S. S. (2020). Novel bank switching of supercapacitors with enhanced energy utilization for electric vehicular applications. *2020 IEEE Transportation Electrification Conference and Expo, ITEC 2020*, 484–488. https://doi.org/10.1109/ITEC48692.2020.9161745

Deng, D. (2015). Li-ion batteries: Basics, progress, and challenges. *Energy Science and Engineering*, *3*(5), 385–418. https://doi.org/10.1002/ese3.95

Denge, N. (2016). *Study of Hybrid Super-capacitor*. 1012–1016.

Deraman, M., Daik, R., Soltaninejad, S., Nor, N. S. M., Awitdrus, Farma, R., … Othman, M. A. R. (2015). A New Empirical Equation for Estimating Specific Surface Area of Supercapacitor Carbon Electrode from X-Ray Diffraction. *Advanced Materials Research*, *1108*, 1–7. https://doi.org/10.4028/www.scientific.net/amr.1108.1

Dixon, J. (2010). Energy storage for electric vehicles. *Proceedings of the IEEE International*

Conference on Industrial Technology, 20–25. https://doi.org/10.1109/ICIT.2010.5472647

Donnellan, B. J., Vowles, D. J., & Soong, W. L. (2015). A review of energy storage and its application in power systems. *2015 Australasian Universities Power Engineering Conference: Challenges for Future Grids, AUPEC 2015*. https://doi.org/10.1109/AUPEC.2015.7324839

Dutta, A., Mahanta, J., & Banerjee, T. (2020). Supercapacitors in the Light of Solid Waste and Energy Management: A Review. *Advanced Sustainable Systems*, *2000182*, 1–32. https://doi.org/10.1002/adsu.202000182

EAG Laboratories. (2015). Surface Area | Pore Size | BET and BJH | EAG Laboratories. Retrieved April 26, 2022, from https://www.eag.com/techniques/phys-chem/bet-bjh/

El-Kady, M. F., Ihns, M., Li, M., Hwang, J. Y., Mousavi, M. F., Chaney, L., … Kaner, R. B. (2015). Engineering three-dimensional hybrid supercapacitors and microsupercapacitors for high-performance integrated energy storage. *Proceedings of the National Academy of Sciences of the United States of America*, *112*(14), 4233–4238. https://doi.org/10.1073/pnas.1420398112

Ellenbogen, J. C. (2006). *Supercapacitors : A Brief Overview*. (March).

Equilibria, J. P. (2006). *Open Archive Toulouse Archive Ouverte (OATAO). 508*, 621–628. https://doi.org/10.4028/www.scientific.net/MSF.508.621

European Commission. (2014). *Frequently Asked Questions on Directive 2012 / 19 / EU on Waste Electrical and Electronic Equipment (WEEE)*. (April), 1–30.

Fallah, A., Oladipo, A. A., & Gazi, M. (2020). Boron-doped sucrose carbons for supercapacitor electrode: artificial neural network-based modelling approach. *Journal of Materials Science: Materials in Electronics*, *31*(17), 14563–14576. https://doi.org/10.1007/s10854-020-04017-y

Forouzandeh, P., Kumaravel, V., & Pillai, S. C. (2020). Electrode materials for supercapacitors: A review of recent advances. *Catalysts*, *10*(9), 1–73. https://doi.org/10.3390/catal10090969

Forti, V., Baldé, C. P., Kuehr, R., & Bel, G. (2020). The Global E-waste Monitor 2020: Quantities, Flows, and the Circular Economy Potential. In *United Nations University (UNU)/United Nations Institute for Training and Research (UNITAR) – co-hosted SCYCLE Programme, International Telecommunication Union (ITU) & International Solid Waste Association (ISWA), Bonn/Geneva/Rotterdam*.

Freeborn, T. J., Maundy, B., & Elwakil, A. S. (2015). Fractional-order models of

supercapacitors, batteries and fuel cells: A survey. *Materials for Renewable and Sustainable Energy*, *4*(3), 1–7. https://doi.org/10.1007/s40243-015-0052-y

Gao, M., Wang, W. K., Zheng, Y. M., Zhao, Q. B., & Yu, H. Q. (2020). Hierarchically porous biochar for supercapacitor and electrochemical H2O2 production. *Chemical Engineering Journal*, *402*(July), 126171. https://doi.org/10.1016/j.cej.2020.126171

Gautham Prasad, G., Shetty, N., Thakur, S., Rakshitha, & Bommegowda, K. B. (2019). Supercapacitor technology and its applications: A review. *IOP Conference Series: Materials Science and Engineering*, *561*(1). https://doi.org/10.1088/1757-899X/561/1/012105

Gianfranco Pistoia. (2005). *Batteries for Portable Devices* (Vol. 1; G. Pistoia, Ed.). https://doi.org/https://doi.org/10.1016/B978-044451672-5/50009-0

Gladvin, G., Sudhaakr, G., Swathi, V., & Santhisri, K. V. (2017). Mineral and Vitamin Compositions Contents in Watermelon Peel (Rind). *International Journal of Current Microbiology and Applied Sciences*, *5*(5), 129. Retrieved from http://www.ijcmas.com

Goia, C., Popa, L., Popescu, C., & Popescu, M. O. (2011). Supercapacitors used as an energy source to drive the short urban electric vehicles. *2011 7th International Symposium on Advanced Topics in Electrical Engineering, ATEE 2011*.

Guerrero, M. A., Romero, E., Barrero, F., Milanes, M. I., & Gonzalez, E. (2009). Supercapacitors: Alternative energy storage systems. *Przeglad Elektrotechniczny*, *85*(10), 188–195.

Hamilton, P. J., & Pollet, B. G. (2010). Polymer electrolyte membrane fuel cell (PEMFC) flow field plate: Design, materials and characterisation. *Fuel Cells*, *10*(4), 489–509. https://doi.org/10.1002/fuce.201000033

Hans, B., Melin, E., & Storage, C. E. (2019). *Analysis of the climate impact of lithium-ion batteries and how to measure it*. (July), 1–17.

Hartono, A., Sanjaya, E., & Ramli, R. (2018). Glucose sensing using capacitive biosensor based on polyvinylidene fluoride thin film. *Biosensors*, *8*(1), 10. https://doi.org/10.3390/bios8010012

Hemmati, R., & Saboori, H. (2016). Emergence of hybrid energy storage systems in renewable energy and transport applications – A review. *Renewable and Sustainable Energy Reviews*, *65*, 11–23. https://doi.org/10.1016/j.rser.2016.06.029

Heng Ivy, Lai WEi Chin, & Juan Joon Ching. (2019). Organic Electrolyte for Supercapacitors. In Inamuddin, Boddula Rajender, Ahmed Mohd Imran, & Asiri Abdullah (Eds.), *Supercapacitor Technology: Materials, Processes and Architectures*

(Vol. 61, pp. 1–10). Retrieved from https://books.google.com.cy/books?hl=en&lr=&id=WHG9DwAAQBAJ&oi=fnd&pg=PA1&dq=Organic+Electrolytes+for+supercapacitors+review&ots=s0W2ZeQ9Pj&sig=sntyXYl4sEPd5VdL1PFpcvLQkoE&redir_esc=y#v=onepage&q=Organic Electrolytes for supercapacitors review&f=false

Herrmann, U., Kelly, B., & Price, H. (2004). Two-tank molten salt storage for parabolic trough solar power plants. *Energy*, *29*(5–6), 883–893. https://doi.org/10.1016/S0360-5442(03)00193-2

Ho, J., Jow, T. R., & Boggs, S. (2010). Historical introduction to capacitor technology. *IEEE Electrical Insulation Magazine*, *26*(1), 20–25. https://doi.org/10.1109/MEI.2010.5383924

Holze, R. (2012). Gianfranco Pistoia: Battery Operated Devices and Systems. *Journal of Solid State Electrochemistry*, *16*(1), 415–415. https://doi.org/10.1007/s10008-011-1302-2

Huang, Y., Liang, J., & Chen, Y. (2012). *An Overview of the Applications of Graphene-Based Materials in Supercapacitors*. *8*(12), 1805–1834. https://doi.org/10.1002/smll.201102635

Ingram, W. J. (1998). *New Technology Batteries Guide*. 1–63. Retrieved from http://www.southernsafetysupply.com/industrial/MS/documents/Battery_Guide.pdf%5Cnpapers2://publication/uuid/BBDE7FF1-483D-4D92-9CED-790FF959DE8B%5Cnpapers2://publication/uuid/C4AF06D1-15E2-4309-B94E-565A9A51471D%5Cnpapers2://publication/uuid/3FA5BA58-B607

Iqbal, M. Z., Zakar, S., & Haider, S. S. (2020). Role of aqueous electrolytes on the performance of electrochemical energy storage device. *Journal of Electroanalytical Chemistry*, *858*, 113793. https://doi.org/10.1016/j.jelechem.2019.113793

Irimia-Vladu, M. (2014). “Green” electronics: Biodegradable and biocompatible materials and devices for sustainable future. *Chemical Society Reviews*, *43*(2), 588–610. https://doi.org/10.1039/c3cs60235d

Iro, Z. S., Subramani, C., & Dash, S. S. (2016). A brief review on electrode materials for supercapacitor. *International Journal of Electrochemical Science*, *11*(12), 10628–10643. https://doi.org/10.20964/2016.12.50

Ishii, K. (2013). *Hitachi Chemical Technical Report*. (55), 50–53. Retrieved from http://www.hitachi-chem.co.jp/english/report/055/55.pdf

Jayalakshmi, M., & Balasubramanian, K. (2008). Simple capacitors to supercapacitors - An

overview. *International Journal of Electrochemical Science*, *3*(11), 1196–1217.

Jiya, I. N., Gurusinghe, N., & Gouws, R. (2018). Hybridization of Battery, Supercapacitor and Hybrid Capacitor for Electric Vehicles. *2018 IEEE PES/IAS PowerAfrica, PowerAfrica 2018*, 19–24. https://doi.org/10.1109/PowerAfrica.2018.8520991

Kämpfe, B., Luczak, F., & Michel, B. (2005). *Energy Dispersive X-Ray Diffraction 1 Principle of the Method*. https://doi.org/10.1002/ppsc.200501007

Kang, D. H. P., Chen, M., & Ogunseitan, O. A. (2013). Potential environmental and human health impacts of rechargeable lithium batteries in electronic waste. *Environmental Science and Technology*, *47*(10), 5495–5503. https://doi.org/10.1021/es400614y

Kasian, P., Nilmoung, S., & Pukird, S. (2019). Biomass derived carbon materials for electrochemical energy storage devices. *Journal of Physics: Conference Series*, *1259*(1). https://doi.org/10.1088/1742-6596/1259/1/012013

Kaushal, A., & Prakash, S. (2019). Solar energy harvesting in wireless sensor networks: A survey. *Proceedings of the 2019 6th International Conference on Computing for Sustainable Global Development, INDIACom 2019*, 224–229.

Ke, Q., & Wang, J. (2016). Graphene-based materials for supercapacitor electrodes – A review. *Journal of Materiomics*, *2*(1), 37–54. https://doi.org/10.1016/j.jmat.2016.01.001

Khan, Y., Ostfeld, A. E., Lochner, C. M., Pierre, A., & Arias, A. C. (2016). Monitoring of Vital Signs with Flexible and Wearable Medical Devices. *Advanced Materials*, *28*(22), 4373–4395. https://doi.org/10.1002/adma.201504366

Khosrozadeh, A., Xing, M., & Wang, Q. (2015). A high-capacitance solid-state supercapacitor based on free-standing film of polyaniline and carbon particles. *Applied Energy*, *153*, 87–93. https://doi.org/10.1016/J.APENERGY.2014.08.046

Kou, L., Huang, T., Zheng, B., Han, Y., Zhao, X., Gopalsamy, K., … Gao, C. (2014). Coaxial wet-spun yarn supercapacitors for high-energy density and safe wearable electronics. *Nature Communications*, *5*(May), 1–10. https://doi.org/10.1038/ncomms4754

Lan, T., Cao, S., Cheng, Z., Huang, Q., Yang, Z., & Xie, L. (2019). The Wireless Electric Vehicle System Based on Super-capacitor Power Supply. *Proceedings of 2019 IEEE International Conference on Mechatronics and Automation, ICMA 2019*, 1818–1822. https://doi.org/10.1109/ICMA.2019.8816408

LeiZhou, ChunyangLi, XiangLiu, YusongZhu, YupingWu, T. R. (2018). Metal oxides in supercapacitors. In Y. Wu (Ed.), *Metal Oxides in Energy Technologies A volume in Metal Oxides* (2019th ed., pp. 169–203). https://doi.org/https://doi.org/10.1016/B978-0-

12-811167-3.00007-9

Lemofouet, S., & Rufer, A. (2006). A hybrid energy storage system based on compressed air and supercapacitors with maximum efficiency point tracking (MEPT). *IEEE Transactions on Industrial Electronics*, *53*(4), 1105–1115. https://doi.org/10.1109/TIE.2006.878323

Li, J., Cornelusse, B., Vanderbemden, P., & Ernst, D. (2017). A SC/battery Hybrid Energy Storage System in the Microgrid. *Energy Procedia*, *142*, 3697–3702. https://doi.org/10.1016/j.egypro.2017.12.264

Li, S., Cheng, P., Luo, J., Zhou, D., Xu, W., Li, J., … Yuan, D. (2017). High-performance flexible asymmetric supercapacitor based on CoAl-LDH and rGO electrodes. *Nano-Micro Letters*, *9*(3), 1–10. https://doi.org/10.1007/s40820-017-0134-8

Liang, R., Du, Y., Xiao, P., Cheng, J., Yuan, S., Chen, Y., … Chen, J. (2021). Transition metal oxide electrode materials for supercapacitors: A review of recent developments. *Nanomaterials*, *11*(5). https://doi.org/10.3390/nano11051248

Liang, Y., Zhao, C., Yuan, H., Chen, Y., Zhang, W., Huang, J., … Zhang, Q. (2019). A review of rechargeable batteries for portable electronic devices. *InfoMat*, *1*(1), 6–32. https://doi.org/10.1002/inf2.12000

Lithium South Development Corp. and Emerging Markets Consulting, L. (2021). Emerging Markets Report: Lithium Could Run out by 2025. Retrieved August 10, 2021, from https://www.globenewswire.com/news-release/2021/04/14/2209842/0/en/Emerging-Markets-Report-Lithium-Could-Run-out-by-2025.html

Lucideon Materials Development and Commercialization. (2022). BET Surface Area Analysis & BJH Pore Size & Volume Analysis Technique | Lucideon. Retrieved April 22, 2022, from https://www.lucideon.com/testing-characterization/techniques/bet-surface-area-analysis-bjh-pore-size-volume-analysis

Mastragostino, M., Soavi, F., & Arbizzani, C. (2002). Electrochemical Supercapacitors. *Advances in Lithium-Ion Batteries*, pp. 481–505. https://doi.org/10.1007/0-306-47508-1_17

Melaina, M., & Eichman, J. (2015). Hydrogen Energy Storage: Grid and Transportation Services (Technical Report). *Related Information: NREL (National Renewable Energy Laboratory)*, (February), Medium: ED; Size: 66 pp. Retrieved from http://www.osti.gov/scitech//servlets/purl/1170355/

Mishra, G. K., & Kant, R. (2020). Modular theory for DC-biased electrochemical impedance response of supercapacitor. *Journal of Power Sources*, *473*(July), 228467.

https://doi.org/10.1016/j.jpowsour.2020.228467

Mohd Abdah, M. A. A., Azman, N. H. N., Kulandaivalu, S., & Sulaiman, Y. (2020). Review of the use of transition-metal-oxide and conducting polymer-based fibres for high-performance supercapacitors. *Materials and Design*, *186*, 108199. https://doi.org/10.1016/j.matdes.2019.108199

MOHD ABID, M. A. 'AZAM, Radzi, M. I., Mupit, M., Osman, H., Munawar, R. F., Samat, K. F., … Islam, M. R. (2020). Cyclic Voltammetry and Galvanostatic Charge-Discharge Analyses of Polyaniline/Graphene Oxide Nanocomposite based Supercapacitor. *Malaysian Journal on Composites Science and Manufacturing*, *3*(1), 14–26. https://doi.org/10.37934/mjcsm.3.1.1426

Naderi, M. (2015). Surface Area: Brunauer-Emmett-Teller (BET). *Progress in Filtration and Separation*, 585–608. https://doi.org/10.1016/B978-0-12-384746-1.00014-8

Naswali, E., Alexander, C., Han, H. Y., Naviaux, D., Bistrika, A., Von Jouanne, A., … Brekken, T. K. A. (2011). Supercapacitor energy storage for wind energy integration. *IEEE Energy Conversion Congress and Exposition: Energy Conversion Innovation for a Clean Energy Future, ECCE 2011, Proceedings*, 298–305. https://doi.org/10.1109/ECCE.2011.6063783

National, G., & Pillars, H. (2015). *SCANNING TRANSMISSION ELECTRON MICROSCOPY OF NANOMATERIALS Basics of Imaging and Analysis* (J. Nobuo Tanaka Nagoya University, Ed.). Imperial College Press.

Negroiu, R., Svasta, P., Ionescu, C., & Vasile, A. (2017). Investigation of Supercapacitor's Impedance Based on Spectroscopic Measurements. *1st PCNS Passive Components Networking Days*, *1*(3.2), 56–62.

Negroiu, R., Svasta, P., Pirvu, C., Vasile, A., & Marghescu, C. (2017). Electrochemical impedance spectroscopy for different types of supercapacitors. *Proceedings of the International Spring Seminar on Electronics Technology*, 1–4. https://doi.org/10.1109/ISSE.2017.8000889

Nikolaidis, P., & Poullikkas, A. (2011). Journal of power technologies. *Journal of Power Technologies*, *97*(3), 220–245. Retrieved from http://papers.itc.pw.edu.pl/index.php/JPT/article/view/1096/776

Nishio, K. (2009). Primary Batteries - Nonaqueous Systems | Lithium Primary: Overview. In *Encyclopedia of Electrochemical Power Sources* (pp. 68–75). https://doi.org/10.1016/B978-044452745-5.00105-2

Niu, B., & Xu, Z. (2019). Innovating e-waste recycling: From waste multi-layer ceramic

capacitors to Nb–Pb codoped and ag-Pd-Sn-Ni loaded BaTiO 3 nano-photocatalyst through one-step ball milling process. *Sustainable Materials and Technologies*, *21*, e00101. https://doi.org/10.1016/j.susmat.2019.e00101

Oladipo, A. A. (2021). N , S co – doped biocarbon for supercapacitor application : Effect of electrolytes concentration and modelling with artificial neural network. *Materials Chemistry and Physics*, *260*(August 2020), 124129. https://doi.org/10.1016/j.matchemphys.2020.124129

Omar, N., Abdullah, E. C., Numan, A., Mubarak, N. M., Khalid, M., Aid, S. R., & Agudosi, E. S. (2022). Facile synthesis of a binary composite from watermelon rind using response surface methodology for supercapacitor electrode material. *Journal of Energy Storage*, *49*(October 2021), 104147. https://doi.org/10.1016/j.est.2022.104147

Oz, A., Hershkovitz, S., & Tsur, Y. (2014). *Electrochemical impedance spectroscopy of supercapacitors: A novel analysis approach using evolutionary programming*. *1627*(February 2015), 76–80. https://doi.org/10.1063/1.4901661

Pan, S., Yao, M., Zhang, J., Li, B., Xing, C., Song, X., … Zhang, H. (2020). Recognition of Ionic Liquids as High-Voltage Electrolytes for Supercapacitors. *Frontiers in Chemistry*, *8*(May), 1–18. https://doi.org/10.3389/fchem.2020.00261

Pan, Z., Yang, J., Kong, J., Loh, X. J., Wang, J., & Liu, Z. (2022). "Porous and Yet Dense" Electrodes for High-Volumetric-Performance Electrochemical Capacitors: Principles, Advances, and Challenges. *Advanced Science*, *9*(4). https://doi.org/10.1002/advs.202103953

Panda, P. K., Grigoriev, A., Mishra, Y. K., & Ahuja, R. (2020). Progress in supercapacitors: Roles of two dimensional nanotubular materials. *Nanoscale Advances*, *2*(1), 70–108. https://doi.org/10.1039/c9na00307j

Patel, H. (2018). Charcoal as an adsorbent for textile wastewater treatment. *Separation Science and Technology (Philadelphia)*, *53*(17), 2797–2812. https://doi.org/10.1080/01496395.2018.1473880

Pay, S., & Baghzouz, Y. (2003). Effectiveness of battery-supercapacitor combination in electric vehicles. *2003 IEEE Bologna PowerTech - Conference Proceedings*, *3*, 728–733. https://doi.org/10.1109/PTC.2003.1304472

Perdana, Y. S., Muyeen, S. M., Al-Durra, A., Morales-Paredes, H. K., & Simoes, M. G. (2019). Direct connection of supercapacitor-battery hybrid storage system to the grid-tied photovoltaic system. *IEEE Transactions on Sustainable Energy*, *10*(3), 1370–1379. https://doi.org/10.1109/TSTE.2018.2868073

Perez, F., Hoffmann, B. V., Dos S Pereira, G. M., Küster, K. K., & Durce, C. C. (2019). The use of Supercapacitors in Microgrids as Hybrid Energy Storage Systems - A review. *2019 IEEE PES Conference on Innovative Smart Grid Technologies, ISGT Latin America 2019*. https://doi.org/10.1109/ISGT-LA.2019.8895484

Primavesi, G. (1997). Aluminium Electrolytic Capacitors - A brief history The basic theory of capacitors is quite old and goes back. *"Aluminium Electrolytic Capacitors," IEE Half-Day Colloquium on Power Electronics in Traction (Digest No. 1997/324), 1745*, 4/1-446. https://doi.org/doi: 10.1049/ic:19971089.

Pullanchiyodan, A., Manjakkal, L., & Dahiya, R. (2021). Metal Coated Fabric Based Asymmetric Supercapacitor for Wearable Applications. *IEEE Sensors Journal*, *XX*(XX). https://doi.org/10.1109/JSEN.2021.3058894

Qin, G., Wang, M., Fan, L., Fang, X., Zhang, D., Liu, J., … Chen, Q. (2020). Multifunctional supramolecular gel polymer electrolyte for self-healable and cold-resistant supercapacitor. *Journal of Power Sources*, *474*, 228602. https://doi.org/10.1016/J.JPOWSOUR.2020.228602

Qu, W. H., Xu, Y. Y., Lu, A. H., Zhang, X. Q., & Li, W. C. (2015). Converting biowaste corncob residue into high value added porous carbon for supercapacitor electrodes. *Bioresource Technology*, *189*, 285–291. https://doi.org/10.1016/j.biortech.2015.04.005

Rabbani, M. A. (2018). Smart grids and photovoltaic integration-analysis of residential grid connected system in north Cyprus. *ANNALS OF THE UNIVERSITY OF ORADEA. Fascicle of Management and Technological Engineering*, *XXVII*(03). https://doi.org/10.15660/AUOFMTE.2018-3.3305

Rabbani, M. A. (2021). Smart Grids and Hybrid Energy Storage Systems: Optimization Techniques Applied in Control Strategies for Hybrid Energy Storage Systems Muhammad. In A. Abdelmadjid Recioui Université M'hamed Bougara de Boumerdes & A. Hamid Bentarzi Université M'hamed Bougara de Boumerdes (Eds.), *Optimizing and Measuring Smart Grid Operation and Control*: *Vol. A volume i* (pp. 170–196). Retrieved from https://books.google.com.cy/books?id=4rgIEAAAQBAJ&pg=PA170&lpg=PA170&dq=170+Chapter+8+Smart+Grids+and+Hybrid+Energy+Storage+Systems:+Optimization+Techniques+Applied+in+Control+Strategies+for+Hybrid+Energy+Storage+Systems&source=bl&ots=LAMLYvKkMT&sig=ACfU3

Railanmaa, A., Soltani, A., Lehtimäki, S., Pournoori, N., Keskinen, J., Hokka, M., & Lupo, D. (2020). Skin-conformable printed supercapacitors and their performance in wear.

Scientific Reports, *10*(1), 1–10. https://doi.org/10.1038/s41598-020-72244-8

Rajendran, S., & Balakumar, S. (2019). *Nanostructured materials for energy related applications.pdf* (M. N. and S. B. Rajendran, Saravanan, Ed.). Retrieved from http://www.springer.com/series/11480

Rajendran, S., Naushad, M., Raju, K., & Boukherroub, R. (2019). *Emerging nanostructured materials for energy and environmental science*.

Ramachandran, R., & Wang, F. (2018). Electrochemical Capacitor Performance: Influence of Aqueous Electrolytes. In *Supercapacitors - Theoretical and Practical Solutions*. https://doi.org/10.5772/intechopen.70694

Ramasahayam, S. K., Hicks, Z., & Viswanathan, T. (2015). Thiamine-Based Nitrogen, Phosphorus, and Silicon Tri-doped Carbon for Supercapacitor Applications. *ACS Sustainable Chemistry and Engineering*, *3*(9), 2194–2202. https://doi.org/10.1021/ACSSUSCHEMENG.5B00453/SUPPL_FILE/SC5B00453_SI_001.PDF

Reddy, T. N., Mishra, M. K., & Srinivas, S. (2015). Grid interactive combined supercapacitor/battery energy storage system with power quality features. *Proceedings of the IEEE International Conference on Industrial Technology*, *2015-June*(June), 2600–2605. https://doi.org/10.1109/ICIT.2015.7125481

Rout, S. R. C. V. and C. S. (2008). Graphene-based electrochemical supercapacitors. *Journal of Chemical Sciences*, *Vol. 120*(No. 1,), 9–13.

Salanne, M., Rotenberg, B., Naoi, K., Kaneko, K., Taberna, P. L., Grey, C. P., … Simon, P. (2016). Efficient storage mechanisms for building better supercapacitors. *Nature Energy*, *1*(6), 1–10. https://doi.org/10.1038/nenergy.2016.70

Salleh, N. A., Kheawhom, S., & Mohamad, A. A. (2020). Characterizations of nickel mesh and nickel foam current collectors for supercapacitor application. *Arabian Journal of Chemistry*, *13*(8), 6838–6846. https://doi.org/10.1016/j.arabjc.2020.06.036

Sedlakova, V., Sikula, J., Majzner, J., Sedlak, P., Kuparowitz, T., Buergler, B., & Vasina, P. (2015). Supercapacitor equivalent electrical circuit model based on charges redistribution by diffusion. *Journal of Power Sources*, *286*, 58–65. https://doi.org/10.1016/j.jpowsour.2015.03.122

Sekhon, S. S. (2003). Conductivity behaviour of polymer gel electrolytes: Role of polymer. *Bulletin of Materials Science*, *26*(3), 321–328. https://doi.org/10.1007/BF02707454

Sequeira, C. A. C., & Santos, D. M. F. (2010). Polymer Electrolytes: Fundamentals and Applications. *Polymer Electrolytes: Fundamentals and Applications*, 1–623.

https://doi.org/10.1533/9781845699772

Shah, S. S., & Aziz, M. A. (2020). Agricultural product-derived carbon for energy, sensing, and environmental applications: A mini-review. *Bangladesh Journal of Plant Taxonomy*, *27*(2), 467–478. https://doi.org/10.3329/bjpt.v27i2.50686

Shanmuga Priya, M., Divya, P., & Rajalakshmi, R. (2020). A review status on characterization and electrochemical behaviour of biomass derived carbon materials for energy storage supercapacitors. *Sustainable Chemistry and Pharmacy*, *16*(November 2019), 100243. https://doi.org/10.1016/j.scp.2020.100243

Shen, C., Xu, S., Xie, Y., Sanghadasa, M., Wang, X., & Lin, L. (2017). A Review of On-Chip Micro Supercapacitors for Integrated Self-Powering Systems. *Journal of Microelectromechanical Systems*, *26*(5), 949–965. https://doi.org/10.1109/JMEMS.2017.2723018

Sinnaduraiand, N., & Charles, H. K. (2009). Electronics and its impact on energy and the environment. *ISSE 2009: 32nd International Spring Seminar on Electronics Technology: Hetero System Integration, the Path to New Solutions in the Modern Electronics - Conference Proceedings*, 1–10. https://doi.org/10.1109/ISSE.2009.5206941

Soo-Keng Chang, Z. Z. (2019). Activated Carbon for Supercapacitors. In R. N. I. R. O. and M. Z. H. Suraya Abdul Rashid (Ed.), *Synthesis, Technology and Applications of Carbon Nanomaterials* (pp. 309–334). https://doi.org/https://doi.org/10.1016/B978-0-12-815757-2.00012-7

Stevens, J. L., Shaffer, J. S., & Vandenham, J. T. (2002). The service life of large aluminum electrolytic capacitors: Effects of construction and application. *IEEE Transactions on Industry Applications*, *38*(5), 1441–1446. https://doi.org/10.1109/TIA.2002.802922

Sundriyal, S., Shrivastav, V., Pham, H. D., Mishra, S., Deep, A., & Dubal, D. P. (2021). Advances in bio-waste derived activated carbon for supercapacitors: Trends, challenges and prospective. *Resources, Conservation and Recycling*, *169*(March), 105548. https://doi.org/10.1016/j.resconrec.2021.105548

Supercapacitors can take market share from lithium batteries | IDTechEx Research Article. (2012). Retrieved May 24, 2021, from https://www.idtechex.com/en/research-article/supercapacitors-can-take-market-share-from-lithium-batteries/4808

Szewczyk, A., Sikula, J., Sedlakova, V., Majzner, J., Sedlak, P., & Kuparowitz, T. (2016). Voltage dependence of supercapacitor capacitance. *Metrology and Measurement Systems*, *23*(3), 403–411. https://doi.org/10.1515/mms-2016-0031

Thermo, S. (2013). *Introduction to Fourier Transform Infrared Spectroscopy*. 1–8. Retrieved from www.thermoscientific.com

Tony Pandolfo, Vanessa Ruiz, Seepalakottai Sivakkumar, and J. N. (2013). *Supercapacitors Materials, Systems, and Applications* (E. F. Francois Beguin, Ed.). Wiley-VCH Verlag GmbH & Co. KGaA, Boschstr. 12, 69469 Weinheim, Ger- many All.

Vicentini, R., Da Silva, L. M., Cecilio, E. P., Alves, T. A., Nunes, W. G., & Zanin, H. (2019). How to measure and calculate equivalent series resistance of electric double-layer capacitors. *Molecules*, *24*(8). https://doi.org/10.3390/molecules24081452

Villarroel-Rocha, J., Barrera, D., & Sapag, K. (2014). Introducing a self-consistent test and the corresponding modification in the Barrett, Joyner and Halenda method for pore-size determination. *Microporous and Mesoporous Materials*, *200*, 68–78. https://doi.org/10.1016/j.micromeso.2014.08.017

W. J. Sarjeant. (1990). *Transactions, Ieee Insulation, Electrical Engineering, Electrical*. *25*(5).

Wagih, M., Hillier, N., Yong, S., Weddell, A. S., & Beeby, S. (2021). RF-Powered Wearable Energy Harvesting and Storage Module Based on E-Textile Coplanar Waveguide Rectenna and Supercapacitor. *IEEE Open Journal of Antennas and Propagation*, *2*(January), 302–314. https://doi.org/10.1109/ojap.2021.3059501

Wang, C., Zhou, Y., Sun, L., Wan, P., Zhang, X., & Qiu, J. (2013). Sustainable synthesis of phosphorus- and nitrogen-co-doped porous carbons with tunable surface properties for supercapacitors. *Journal of Power Sources*, *239*, 81–88. https://doi.org/10.1016/j.jpowsour.2013.03.126

Wang, D., Liu, S., Fang, G., Geng, G., & Ma, J. (2016). From Trash to Treasure: Direct Transformation of Onion Husks into Three-Dimensional Interconnected Porous Carbon Frameworks for High-Performance Supercapacitors in Organic Electrolyte. *Electrochimica Acta*, *216*, 405–411. https://doi.org/10.1016/j.electacta.2016.09.053

Wang, J., Li, X., Zi, Y., Wang, S., Li, Z., Zheng, L., … Wang, Z. L. (2015). A Flexible Fiber-Based Supercapacitor-Triboelectric-Nanogenerator Power System for Wearable Electronics. *Advanced Materials*, *27*(33), 4830–4836. https://doi.org/10.1002/adma.201501934

Wang, L., Ye, X., Zhao, P., Jiang, H., Zhu, Y., Wan, Z., … Jia, C. (2019). Toward high capacitance and rate capability supercapacitor: Three dimensional graphene network fabricated by electric field-assisted assembly method. *Applied Surface Science*, *467–468*(September 2018), 949–953. https://doi.org/10.1016/j.apsusc.2018.10.169

Wang, R., Yao, M., & Niu, Z. (2020). Smart supercapacitors from materials to devices. *InfoMat*, *2*(1), 113–125. https://doi.org/10.1002/inf2.12037

Wang, Y., Shi, Z., Huang, Y., Ma, Y., Wang, C., Chen, M., & Chen, Y. (2009). Supercapacitor devices based on graphene materials. *Journal of Physical Chemistry C*, *113*(30), 13103–13107. https://doi.org/10.1021/jp902214f

Waseda, Y., Matsubara, E., & Shinoda, K. (2011). *X-RayDiffractionCrystallography*. Springer Heidelberg Dordrecht London New York Library.

Waterproof supercapacitor fabrics to be laser printed in minutes. (2019). Retrieved May 25, 2021, from https://www.eenewseurope.com/news/waterproof-supercapacitor-fabrics-be-laser-printed-minutes

Weinstein, L., & Dash, R. (2013). Supercapacitor carbons: Have exotic carbons failed? *Materials Today*, *16*(10), 356–357. https://doi.org/10.1016/j.mattod.2013.09.005

World Energy Council. (2020). *Five Steps to Energy Storage. Innovation Insights Brief 2020*. 62. Retrieved from www.worldenergy.org

Xia, H., Shirley Meng, Y., Yuan, G., Cui, C., & Lu, L. (2012). A symmetric RuO 2RuO 2 supercapacitor operating at 1.6 v by using a neutral aqueous electrolyte. *Electrochemical and Solid-State Letters*, *15*(4), 1–5. https://doi.org/10.1149/2.023204esl

Xu, Y., Ren, B., Wang, S., Zhang, L., & Liu, Z. (2018). Carbon aerogel-based supercapacitors modified by hummers oxidation method. *Journal of Colloid and Interface Science*, *527*, 25–32. https://doi.org/10.1016/j.jcis.2018.04.108

Yaici, W., Kouchachvili, L., Entchev, E., & Longo, M. (2019). Dynamic simulation of battery/supercapacitor hybrid energy storage system for the electric vehicles. *8th International Conference on Renewable Energy Research and Applications, ICRERA 2019*, 460–465. https://doi.org/10.1109/ICRERA47325.2019.8996509

Yang, G., & Park, S. J. (2018). MnO2 and biomass-derived 3D porous carbon composites electrodes for high performance supercapacitor applications. *Journal of Alloys and Compounds*, *741*, 360–367. https://doi.org/10.1016/j.jallcom.2018.01.108

Yong, H., Park, H., & Jung, C. (2020). Quasi-solid-state gel polymer electrolyte for a wide temperature range application of acetonitrile-based supercapacitors. *Journal of Power Sources*, *447*(July 2019), 227390. https://doi.org/10.1016/j.jpowsour.2019.227390

Zhang, H., Wang, K., Zhang, X., Lin, H., Sun, X., Li, C., & Ma, Y. (2015). Self-generating graphene and porous nanocarbon composites for capacitive energy storage. *Journal of Materials Chemistry A*, *3*(21), 11277–11286. https://doi.org/10.1039/c5ta01783a

Zhang, L., Hu, X., Wang, Z., Sun, F., & Dorrell, D. G. (2018). A review of supercapacitor

modeling, estimation, and applications: A control/management perspective. *Renewable and Sustainable Energy Reviews*, *81*(June 2017), 1868–1878. https://doi.org/10.1016/j.rser.2017.05.283

Zhang, Pei, Mu, J., Guo, Z., Wong, S. I., Sunarso, J., Zhao, Y., … Zhuo, S. (2021). Watermelon Peel-Derived Heteroatom-Doped Hierarchical Porous Carbon as a High-Performance Electrode Material for Supercapacitors. *ChemElectroChem*, *8*(6), 1196–1203. https://doi.org/10.1002/celc.202100267

Zhang, Ping, Liu, M., & Liu, S. (2020). N-doped honeycomb-like hierarchical porous carbon foams for supercapacitor applications with different PC/RF mass ratios. *Journal of Materials Science: Materials in Electronics*, *31*(4), 3519–3528. https://doi.org/10.1007/s10854-020-02900-2

Zhang, Q., Yan, B., Feng, L., Zheng, J., You, B., Chen, J., … He, S. (2022). Progress in the use of organic potassium salts for the synthesis of porous carbon nanomaterials: microstructure engineering for advanced supercapacitors. *Nanoscale*, *14*(23), 8216–8244. https://doi.org/10.1039/D2NR01986H

Zhang, Y., Feng, H., Wu, X., Wang, L., Zhang, A., Xia, T., … Zhang, L. (2009). Progress of electrochemical capacitor electrode materials: A review. *International Journal of Hydrogen Energy*, *34*(11), 4889–4899. https://doi.org/10.1016/j.ijhydene.2009.04.005

Zheng, Y., Yang, Y., Chen, S., & Yuan, Q. (2016). Smart, stretchable and wearable supercapacitors: Prospects and challenges. *CrystEngComm*, *18*(23), 4218–4235. https://doi.org/10.1039/c5ce02510a

Zhong, C., Deng, Y., Hu, W., Qiao, J., Zhang, L., & Zhang, J. (2015a). A review of electrolyte materials and compositions for electrochemical supercapacitors. *Chemical Society Reviews*, *44*(21), 7484–7539. https://doi.org/10.1039/C5CS00303B

Zhong, C., Deng, Y., Hu, W., Qiao, J., Zhang, L., & Zhang, J. (2015b). A review of electrolyte materials and compositions for electrochemical supercapacitors. *Chemical Society Reviews*, *44*(21), 7484–7539. https://doi.org/10.1039/c5cs00303b

Zhong, C., Deng, Y., Hu, W., Sun, D., Han, X., Qiao, J., & Zhang, J. (2016). Electrolytes for electrochemical supercapacitors. In *Electrolytes for Electrochemical Supercapacitors*. https://doi.org/10.1201/b21497-6

Zhou, H., Peng, Y., Wu, H. Bin, Sun, F., Yu, H., Liu, F., … Lu, Y. (2016). Fluorine-rich nanoporous carbon with enhanced surface affinity in organic electrolyte for high-performance supercapacitors. *Nano Energy*, *21*, 80–89. https://doi.org/10.1016/j.nanoen.2015.12.016

Zhou, J., Ye, S., Zeng, Q., Yang, H., Chen, J., Guo, Z., … Rajan, K. (2020). Nitrogen and Phosphorus Co-doped Porous Carbon for High-Performance Supercapacitors. *Frontiers in Chemistry*, *8*(February), 1–8. https://doi.org/10.3389/fchem.2020.00105

Zhou, Y., & Li, X. (2015). Vehicle to grid technology: A review. *Chinese Control Conference, CCC*, *2015-Septe*, 9031–9036. https://doi.org/10.1109/ChiCC.2015.7261068

Zou, Z., Liu, T., & Jiang, C. (2019). Highly mesoporous carbon flakes derived from a tubular biomass for high power electrochemical energy storage in organic electrolyte. *Materials Chemistry and Physics*, *223*(September 2018), 16–23. https://doi.org/10.1016/j.matchemphys.2018.10.036

APPENDICES